Bio-composites Materials from Engineered Natural Fibres for Structural Applications

A thesis

submitted in fulfilment

of the requirements for the degree

of

Doctor of Philosophy in Engineering

at

The University of Waikato

by

Aruan Efendy Mohd Ghazali

THE UNIVERSITY OF
WAIKATO
Te Whare Wānanga o Waikato

2016

Abstract

The large environmental footprint caused by conventional synthetic fibre reinforced petrochemical-derived polymer composites along with potential improvement in mechanical properties for natural fibre reinforced bio-derived polymer composites, have long been a motivation for further research and innovation in natural fibre composites. Harakeke and hemp fibres, amongst other natural fibres, possess respectable mechanical properties along with other advantages such as low cost, low production energy requirements and abundant availability. Polylactic acid (PLA), a sustainable alternative to petrochemical-derived polymers, is produced on a mass scale from 100% renewable resources and can be degraded at end of life by simple hydrolysis under the appropriate conditions. It has high stiffness, strength, thermal and UV stability, but is low in toughness. Limited applications of natural fibre reinforced PLA composites so far is mainly due to low mechanical properties of discontinuous fibre composites made using injection moulding or compression moulding using randomly oriented fibre mats attributed to poor fibre orientation and fibre-matrix incompatibility. Presented in this study are experimental investigations of the properties of PLA reinforced aligned discontinuous harakeke and hemp fibre mats produced using a dynamic sheet former (DSF) to provide improved performance of discontinuous fibre composites.

Harakeke and hemp fibres were treated using either a solution of 5 wt% or 10 wt% NaOH or combination of 5 wt% NaOH with 2 wt% Na_2SO_3 at elevated

temperatures in a small pressure vessel. Treated fibres were assessed using single fibre tensile testing, X-ray diffraction (XRD), scanning electron microscopy (SEM) and thermogravimetric analysis (TGA). It was found that 5 wt% NaOH/2 wt% Na_2SO_3 and 5 wt% NaOH effectively removed non-cellulosic materials from harakeke and hemp fibre surfaces, respectively, giving good fibre separation without greatly reducing the tensile strength of the fibres. It was also found that these treatments lead to a higher crystallinity index and improved thermal stability of fibres.

Fibre alignment in fibre mats produced using a DSF was observed using light microscopy. Visual observation supported that the fibre alignment had occurred. Fibre orientation factors (K_o) determined for harakeke and hemp composites using the Bowyer-Bader model were found higher compared to K_o values obtained for other natural composites prepared using injection and compression moulding. Improved fibre orientation resulted in improved reinforcement giving large increases for tensile strengths up to approximately 90 and 60% for harakeke and hemp composites reinforced with inclusion of 30 and 25 wt% fibre respectively.

The effect of silane and peroxide as additional fibre treatments and MA-g-PLA as a coupling agent was evaluated by scanning electron microscopy (SEM), composite swelling analysis, tensile testing, dynamic mechanical analysis (DMA) and thermogravimetric analysis (TGA). Scanning electron micrographs of fractured composite surfaces revealed that the gaps between fibres and matrix for composites with fibres treated using silane and peroxide and composites coupled with MA-g-PLA were smaller compared to the surfaces for composites with fibres

treated using just alkali. Improved interfacial strength was also supported by lower swelling indices, lower peaks on tan δ and higher residual composites weights, compared to those values obtained for composites with fibres treated using just alkali, which was found to lead to higher composite tensile strengths.

Harakeke and hemp fibre composites were plasticised using hyper-branched polymer (HBP) and assessed using SEM, tensile and impact testing. SEM micrographs for plasticised composites revealed longer pultruding fibres than un-plasticised composites, with gaps between the fibre and matrix appearing to be slightly larger, indicating a weaker interface between fibres and matrix compared to those composites without plasticiser. Improved composite ductility and impact strength were demonstrated for plasticised composites without dramatic reduction of composite tensile strength.

Acknowledgements

I would like to express my deepest gratitude, respect and appreciation to my honourable supervisor, Professor Kim Pickering for her constant supervision, guidance, priceless advices and patience throughout the entire period of my study. I would like to thanks my co-supervisor, Dr. Johan Verbeek for his direct and indirect support and help.

I am very thankful for the help from all the laboratory technicians who provided the technical assistance especially Chris Wang, Yuanzi Zhang, Helen Turner, Stephen Hardy, Martin Gore, Michael Hoogeveen, Brett Nichols, Alan Smith and Stewart Finlay. Special thanks to Mary Dalbeth for the administrative assistance and Cheryl Ward for the help during the writing of this thesis. Thanks also to all friends, composite group members for the help, suggestions and friendship.

I deeply thank my parents, my mother in-law, brothers and sisters and all family members for their encouragement, unconditional trust and endless prayers. The most special thank with love goes to my dear wife Rina Norlina for endless patience, comforting and encouraging me during this challenging period of my life. Without your support and sacrifice, I would not have been able to do this. Also thanks to my son Akil, for being such a good boy.

I would also like to acknowledge Universiti Teknologi Mara and the Ministry of Education Malaysia for the financial supports.

Publications

Journal

Title: Comparison of harakeke with hemp fibre as a potential reinforcement in composites
Authors: M.G. Aruan Efendy and K.L. Pickering
Parent Document: Elsevier, Composites Part A: Applied Science and Manufacturing
Date Published: September 2014

Title: A review of recent developments in natural fibre composites and their mechanical performance
Authors: K.L. Pickering, M.G. Aruan Efendy and T.M. Le
Parent Document: Elsevier, Composites Part A: Applied Science and Manufacturing
Date Published: September 2015

Title: Preparation and mechanical properties of novel bio-composite made of dynamically sheet formed discontinuous harakeke and hemp fibre mat reinforced pla composites for structural applications
Authors: K.L. Pickering and M.G. Aruan Efendy
Parent Document: Elsevier, Industrial Crops and Products
Date Published: February 2016

Title: Fibre Orientation of Novel Dynamically Sheet Formed Discontinuous Natural Fibre PLA Composites
Authors: M.G. Aruan Efendy and K.L. Pickering
Parent Document: Elsevier, Composites Part A: Applied Science and Manufacturing
Date Published: July 2016

Table of Contents

List of Figures

List of Tables

Symbols and Abbreviations

Symbols

K_o	Fibre orientation factor
σ_f	Fibre tensile strength
L_c	Critical fibre length
L	Average fibre length
D	Fibre diameter
τ_i	Interfacial shear strength
$P_{f(L)}$	Probability of failure of fibre at particular length
σ_0	Characteristic stress
w	Shape parameter
n	Number of data point
i	Rank of data point
I_c	Crystallinity index
σ	Tensile strength
E	Young's modulus
V	Volume fraction
V_f	Fibre volume fraction
V_m	Matrix volume fraction
W_f	Fibre weight fraction
ρ_f	Density of fibre
ρ_m	Density of matrix
x	Fitting parameter
ζ	Shape fitting parameter
d	Fibre diameter
l	Length of fibre in direction of load
$\text{ø}_{\max}$	Maximum fibre packing
r	Radius of fibre
G_m	Shear modulus of matrix
K_{st}	Fibre stress transfer factor
L_ε	Fibre length at particular strain
σ_ε	Composite stress at a particular strain
σ_c	Composite strength
V_i	Volume fractions of subcritical fibre
V_j	Volume fractions of supercritical fibre
L_i	Subcritical fibre length
L_j	Supercritical fibre length
ε_{c1}	Strain of composite at point 1
σ_{c1}	Composite stress at strain of composite at point 1
ε_{c2}	Strain of composite at point 2
σ_{c2}	Composite stress at strain of composite at point 2
X	Strength contributions of fibres with subcritical fibre length

Y	Strength contributions of fibres with supercritical fibre length
$V_{f,min}$	Minimum fibre volume fraction
$V_{f,crit}$	Critical fibre volume fraction
$V_{f,max}$	Maximum fibre volume fraction
ε_f	Strain of fibre
ε_m	Strain of matrix
σ'_m	Matrix stress at fibre failure strain
θ_n	Orientation angle
τ_m	Shear strength of matrix
E'	Storage modulus
E''	Loss modulus
A_s	Amount of solvent absorbed by sample
W	Initial weight of sample before swelling
T_g	Glass transition temperature
T_m	Melting temperature

Abbreviations

PLA	Polylactic acid
PHB	Polyhydroxybutyrate
DSF	Dynamic sheet former
WPC	Wood-plastic composite
OH	Hydroxyl groups
PUR	Polyurethane
PE	Polyethylene
PP	Polypropylene
PVC	Poly (vinyl chloride)
PS	Polystyrene
PET	Poly (ethylene terephthalate)
UV	Ultra-violet
ILSS	Inter-laminar shear strength
NaOH	Sodium hydroxide
Na_2SO_3	Sodium sulphite
CH_3CO	Acetyl group
OH	Hydroxyl group
IFSS	Interfacial shear strength
Si-OH	Silanols
MPS	Methacryl silane
GPS	Glycidoxy silane
HDS	Alkyl silane
BP	Benzoyl peroxide
DCP	Dicumyl peroxide
PF	Phenol formaldehyde
MA	Maleic anhydride
MAPP	MA grafted polypropylene
MAPE	MA grafted polyethylene
MAPLA	MA grafted poly lactic acid

HBP	Hyper branched polymer
XRD	X-ray diffraction
SEM	Scanning electron microscopy
TGA	Thermogravimetric Analysis
ASTM	American Society for Testing and Materials
PVA	Poly(vinyl acetate)
TS	Tensile strength
YM	Young's modulus
DTA	Differential thermal analysis
HR	Harakeke
HM	Hemp
MROM	Modified Rule of Mixtures
APS	3-aminopropyl triethoxy silane
ISO	International Organization for Standardization

CHAPTER 1

Research Direction

1.1 Introduction

Increased environmental awareness has led to growing interest in the use of materials that are more sustainable. Typical construction materials have large ecological footprints; synthetic composites are generally energy intensive to produce [1]. Natural-fibre-reinforced bio-derived polymer matrix composites, commonly referred to as bio-composites, have gained renewed interest over the past few decades because of their low material costs, low densities, high specific moduli and environmentally friendly appeal, as well as their low production energy requirements [2]. The natural fibres used are renewable, nonabrasive, can be incinerated for energy recovery and they give less concern regarding health and safety during handling than synthetic fibres. Their excellent price-performance ratios at low weight in combination with their low environmental impact has resulted in increasing uptake by engineering markets such as the automotive and construction industries [3].

Many studies have been carried out internationally to assess the possibility of using natural fibre-composites for non-structural and structural applications [4-8]. However, development of such low cost material with high durability and high mechanical performance is still a real challenge faced by engineers of the 21st century to enable natural fibre composites to be put on a par with synthetic fibre

composites. Natural fibres can generally be classified into two major categories; plant based and animal based [9]. Of those that are readily available, plant based fibres tend to have better mechanical performance. Plant based fibres can be classified further into two broad categories (as shown in Figure 1.1**)**: non-wood fibres and wood fibres. Non-wood fibres such as flax, hemp, jute and kenaf tend to be stronger than wood, some fibres have specific strengths and specific moduli that are comparable or even superior to E-glass. In a composite, generally, the fibre provides stiffness and strength to support load, while the matrix holds the fibres together, transfers applied loads via the interface to the fibres and protects them from mechanical damage and other environmental factors.

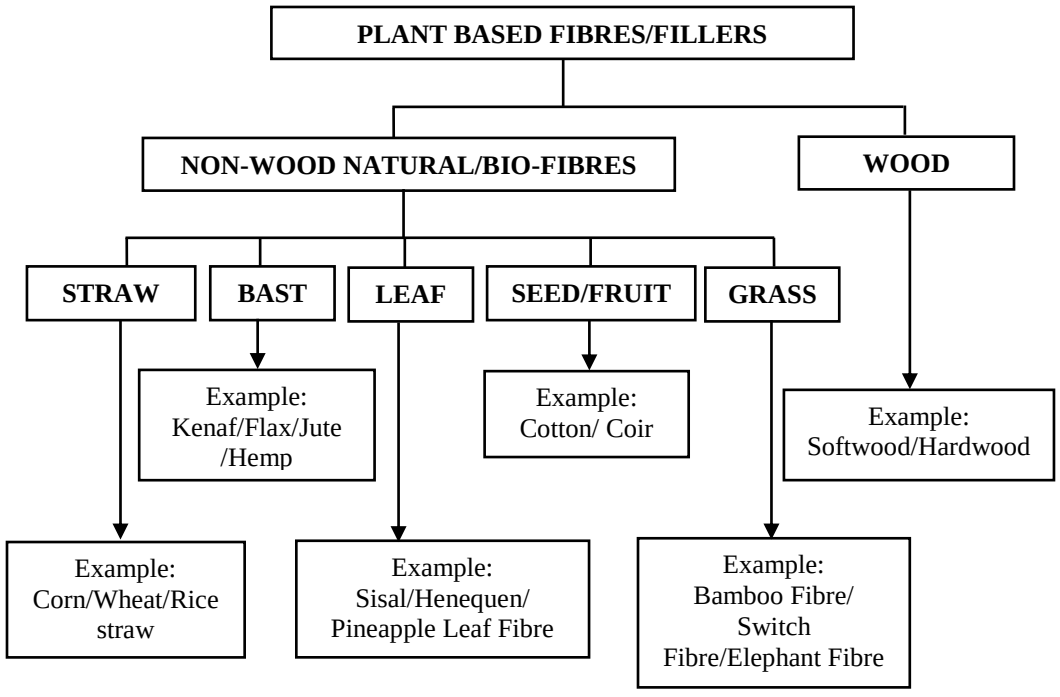

Figure 1.1: Classification of plant reinforcing fibres [10].

In respect to obtaining a good quality and environmentally harmless composite, the selection of the best matrix remains a major issue. Matrix choice largely affects the potential for biodegradability or recyclability. The matrix in common

traditional composites is either a thermoplastic or thermoset polymer. The essential difference between these is that thermoplastics remain permanently fusible so that they will soften when heat is applied, whereas cured thermoset polymers do not soften. This allows thermoplastic materials to be reclaimed and recycled and makes the composites made from thermoplastics more desirable. First generation partially biodegradable thermoplastic polymer matrices made from blends of non-biodegradable with biodegradable polymers are being replaced by thermoplastic polymers that are fully biodegradable such as: polylactic acid (PLA), polyhydroxybutyrate (PHB), cellulose esters, polyhydroxyalkanoates, and soy-resin [11]. However, these polymer matrices have had limitations including poor commercial availability, poor process ability, low toughness and low moisture stability. Amongst these polymer matrices, PLA is the front-runner in terms of mechanical properties as well as availability and is used commercially in its non-reinforced form. Although natural fibre reinforced PLA is an active research area, its commercial application is still limited. Therefore, research aimed at overcoming the limitations of natural fibre reinforced PLA would be expected to encourage commercial success for these materials.

1.2 Research Rationale

The mechanical properties of composites, including natural fibre composites, depend not only on the properties of the constituents, but on fibre alignment and interfacial bonding.

Composites with fibres aligned parallel to the loading direction are found to have the best composite strengths and stiffnesses [12]. Natural fibre composites with a

high degree of fibre alignment can be produced using carding, where long fibres are carded and combined with polymer prior to compression moulding. A high degree of fibre alignment can also be obtained using continuous fibre yarn, which is normally produced by fibre spinning or wrapping fibres together. Fibre yarns can be made from the same type of fibre, a mixture of different fibres, or can be a mixture of fibres and thermoplastic filaments [13]. Production of these forms of fibres, however, are often time consuming and limited to certain types of fibres. Some degree of fibre alignment can be obtained during injection moulding, dependent on matrix viscosity, mould design and size, length and fibre concentration [14-16]. In this method, discontinuous fibres are generally added to the matrix in a loose form during extrusion prior to injection moulding. The mechanical properties of composites produced are much lower compared to composites produced using aligned fibre yarn and carded long fibres, but fabrication is easier and would be applicable to almost all types of fibres. One aim of this work was to assess the potential for aligning discontinuous fibres to give composites with acceptable strengths and stiffnesses that can be used in broader applications.

A strong interface provides composites that display good strength and stiffness but tend to be brittle. A weaker interface on the other hand, may reduce the stress transfer from matrix to the fibre, hence display lower strength and stiffness but in contrast may increase composite toughness. Cellulose based natural fibre, however, due to its hydrophilic nature has limited interaction with hydrophobic matrices commonly resulting in limited interfacial strength. Depending on the application, increased interfacial strength can be achieved by modifying the fibre

surface using physical and chemical treatments and modifying the matrix by addition of a coupling agent. Previous studies show that these methods increase the compatibility/bondability between fibres and matrix and hence improve the interface strength between the fibre and matrix [17].

Natural fibre reinforced PLA composites have received widespread attention in the past decade because of their good strength and stiffness. However, the shortcomings of PLA composites such as their brittleness and low impact resistance limit their applications [18]. Substantial research has been conducted to address these shortcomings, such as blending with various polymers or plasticisation using plasticiser is likely to increase the environmental impact of PLA. The use of plasticisers has been shown to provide modest improvement of impact strength and failure strain; however, this is generally at the expense of strength and stiffness. Ideally, development of natural fibre reinforced PLA composites with higher failure strain and impact strength, without dramatically reduced strength and Young's modulus could be achieved.

In this work, research efforts to address the issues identified above were undertaken. Systematic approaches to produce novel short aligned fibre mats using a dynamic sheet former (DSF) were introduced. Efforts were made to increase the interfacial strength between fibre and matrix using fibre treatments and coupling agents in addition to alkali treatment. Hyper-branced polymer (HBP) was used as a plasticiser to improve failure strain and impact strength of PLA. These methods for improving the overall mechanical properties of the composite were carried out without greatly increasing environmental impact.

1.3 Research Objectives

The present work looks ahead to the next generation of bio-composites made with natural fibres and bio-derived matrices. This study proposes to significantly add to the value of such bio-composites by improving their strength, stiffness and failure strain. This work utilised New Zealand hemp and harakeke fibres as reinforcements and PLA as a matrix. The specific objectives of the study are summarised as follows:

1. To study the influence of different alkali fibre treatments on harakeke and hemp fibre properties.
2. To assess the tensile properties of aligned harakeke and hemp fibre composites using optimum alkali treated fibre mats produced using a dynamic sheet former (DSF).
3. To evaluate the fibre orientation and performance of aligned harakeke and hemp fibre composites produced in this study by comparing experimentally obtained composite strengths with theoretical composite strengths and stiffness obtained using mathematical modelling.
4. To assess the effect of coupling agent and fibre treatments (silane and peroxide) on the mechanical properties of aligned harakeke and hemp fibre composites.
5. To assess the influence of plasticiser on tensile properties and impact strength of aligned fibre composites.

1.4 Thesis Outlines

This thesis is divided into 7 chapters. Chapter 1 gives general information about the study including an introduction, research rationale, research goals and an outline of the thesis. Chapter 2 presents general knowledge and relevant literature related to natural fibres, matrices and natural fibre thermoplastic composites. It also includes factors affecting composite performance, composite treatments, composite processing and other issues related to natural fibre composites. Chapter 3 covers alkali treatment for optimal fibre properties. Chapter 4 discusses the effect of fibre orientation on tensile properties of composites. This chapter also contains mathematical modelling to determine fibre orientation, assess interfacial strength and compare with experimental composite strength and stiffness. Chapter 5 covers the effect of coupling agent, fibre treatments and plasticiser on mechanical properties of the composites. Chapter 6 draws the main conclusions of the study. Finally, Chapter 7 suggests some recommendations and future work based on the findings of the study.

CHAPTER 2

Background and Literature Review

2.1 Introduction

Composites are materials engineered from two or more constituents with different physical or chemical properties, which remain separate and distinct within the finished structure. Composites of various kinds, natural and synthetic, surround us in everyday life. Humans have used composite materials for ages in various applications such as building blocks from straw and clay, concrete reinforced with steel and polymers reinforced by various kinds of fibres [19]. Polymer matrix composites are the most commonly used due to their high strength to weight ratio coupled with availability of relatively simple fabrication methods. Traditional engineered fibre reinforced polymer composites are generally composed of glass or carbon fibres, reinforcing unsaturated polyester or epoxy [20]. Composites made of these materials are shown to have good mechanical properties and are used in many applications, but their production generally relies on unsustainable materials, involving a high carbon footprint and their disposal generally involves landfill. Bearing this in mind, development of more environmentally friendly composites utilising natural fibre as reinforcement with more sustainable polymer matrix becomes desirable. Indeed, natural fibres have been used by humankind in the absence of a matrix for centuries to make clothes, ship sails and ropes due to their availability and structural performance. Composites containing natural fibre are known worldwide as being more sustainable and ecologically friendly in terms

of their life cycle, are also gaining increasing attention due to economic reasons [21].

Over the past few decades, a number of car models, first in Europe and then in North America, have featured natural fibre-reinforced polymers in door panels, package trays, seat backs and trunk liners. In the construction industry, natural fibre reinforced composites are gaining popularity as materials in non-structural construction applications and have been used for doors and window frames, wall insulation and floor lamination [22-25]. They have also been used in different fields of application such as toys, funeral articles, packaging and cases for electronic devices as a replacement for synthetic fibre

In relatively recent times, development of natural fibre composite materials has resulted in improved mechanical performance giving potential to extend application of these materials. Phillips and Lessard [26] have found that flax fibre reinforced epoxy composites can have similar specific moduli to glass fibre epoxy composites and could therefore be employed in stiffness-driven applications. Alvarez *et al*.[27] have evaluated the flexural behaviour of extruded hollow cross-section wood-plastic composites (WPCs) for light weight sheet piles. Results highlighted significant promise for these materials to replace conventional sheet piles made from concrete and steel. There has also been suggestion of similar materials to be used for beams and slabs [10]. R. Burgueno *et al*. [28] has suggested that improvements of natural fibre composites addressing fibre-matrix interaction, thermal stability, manufacturing and experimental characterization are needed in order for natural fibre reinforced composite structural components to

become reliable in broader applications. Addressing these challenges in research will encourage application of low cost materials based on green resources in structural applications.

2.2 Natural Fibres

Natural fibres can be categorised based on their origin: plants and animals. The major component of plant fibres is of cellulose, whereas animal fibres mainly consist of protein [29]. Although mineral-based natural fibres exist within the asbestos group of minerals and were once used extensively in composites, these are now avoided due to associated health issues (carcinogenic through inhalation/ingestion) and are banned in many countries. Plant fibres are generally stronger than animal fibres, which makes them more suitable for use in composites. Plant fibres can generally be grown in many countries and can be harvested after a short period [30].

2.2.1 Advantages and Disadvantages of Natural Plant Fibres

An overview of advantages and disadvantages of natural plant fibres in current applications is tabulated in Table 2.1. It can be seen that they are low in cost with high specific strength stiffness and are normally non-abrasive to composite processing equipment which can contribute to significant equipment maintenance cost reductions.

Table 2.1: Advantages and disadvantages of natural fibre [31-34]

Advantages	Disadvantages
• Low density and high specific strength and stiffness • non-abrasive to composite processing equipment • Producible at lower cost than synthetic fibre • A renewable resource, for which production requires little energy, involves CO_2 absorption, while returning oxygen to the environment • Low hazard manufacturing processes • Low emission of toxic fumes when subjected to heat and during incineration at end of life	• Lower durability than synthetic fibre, but can be improved considerably with proper treatment • High moisture absorption, which results in swelling • Lower strength, in particular impact strength compared to synthetic fibre • High level of variability in fibre properties • Limited to lower processing temperature compared to synthetic fibres

2.2.2 Mechanical Properties of Natural fibre

Applications of natural fibre obviously depend on its mechanical properties. The properties of natural fibre vary considerably depending on chemical composition and structure, fibre type and also growing conditions. Strength and stiffness of natural fibres are relatively low compared to glass fibre. However, due to their low density, the specific properties are comparable to glass fibre. Table 2.2 shows some of properties of natural fibres and the main type of glass fibre (E-glass). From the information provided in Table 2.2, it can be seen that hemp fibre is amongst those having the highest specific moduli and tensile strengths. Harakeke fibre, (known as phormium tenax or New Zealand flax) is also being considered to be used in structural applications due to good mechanical properties and its local availability which makes harakeke slightly cheaper than other natural fibres.

Table 2.2: Mechanical properties of natural and synthetic fibre [2, 9, 35]

Fibre	Density (g/cm3)	Length (mm)	Elongation (%)	Young's Modulus (GPa)	Tensile Strength (MPa)	Specific Tensile Strength	Specific Modulus
Flax	1.5	5 – 900	1.2 – 3.2	27 – 80	345 – 1500	230 – 1000	45
Cotton	1.5 – 1.6	10 – 60	3.0 – 10	5.5 – 12.6	287 – 800	190 – 530	6
Jute	1.3 – 1.5	1.5 – 120	1.5 – 1.8	10 – 55	393 – 800	300 – 610	30
Hemp	1.5	5 – 55	1.6	70	550 – 900	370 – 600	40
Sisal	1.3 – 1.5	900	2.0 – 2.5	9.4 – 28	511 – 635	390 – 490	17
Ramie	1.5	900 – 1200	2.0 – 3.8	44 – 128	400 – 938	270 – 620	60
Coir	1.2	20 – 150	15 – 30	4 – 6	131 – 220	110 – 180	4
Harakeke	-	-	4.2 – 5.8	14 – 33	440 – 990	-	-
E-glass	2.5	-	2.5	70	2000 – 3000	800 - 1400	29

2.2.3 Industrial Hemp Fibre

Hemp, originating from central Asia, is one of the most utilised fibres historically and currently one of the most ecologically friendly due to no requirement for herbicides and pesticides [36]. Hemp is an herbaceous annual plant, abundantly available in many moderately hot countries. It is dioecious, which means it has separate male (staminate) and female (pistillate) plants (shown in Figure 2.1) having different growth characteristics. Male plants tend to be taller and more slender with few leaves surrounding the flowers, while female plants are shorter and stockier with many leaves meeting at each inflorescence [37]. Generally, the hemp plant has a single woody stem which grows 1 to 5 m high with stem diameters ranging between 6 to 60 mm. This generally consists of a woody core and surrounded by a bast layer, which is covered by epidermis. The main constituents of hemp fibre are cellulose, hemi-cellulose, lignin, and pectin; cellulose is the stiffest component found in the fibre. The relative amount of these

components may vary from one fibre to another which thus may result in variability in its physical and mechanical properties mainly depending on the source, age and geographic origin. Table 2.3 shows the chemical compositions of hemp fibre extracted from various sources [36]. It can be seen that hemp fibres consist mainly cellulose, followed by hemicellulose and small amount of other extractives. Physical and mechanical properties of fibre can also significantly differ depending on retting, separation techniques and treatment used [38].

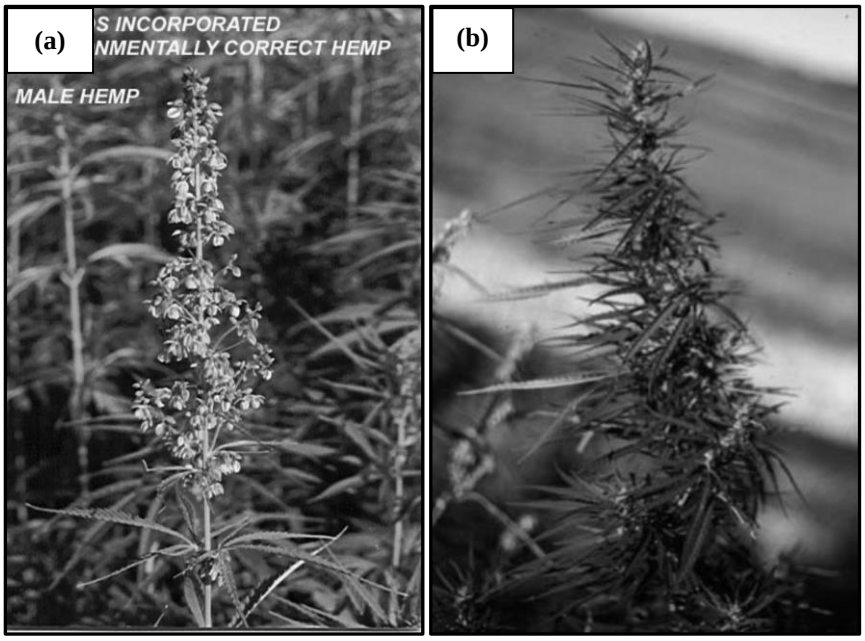

Figure 2.1: Hemp plant: (a) male hemp, (b) female hemp [39].

Hemp fibres have been used by humans for thousands of years for food, textiles, paper, fabric and fuel oil. Hemp fibre was the world's largest agricultural crop in the early 19th century, but demand for the material declined with advances of synthetic fibres [6]. Hemp fibre is currently found to be used in a wide range of products, including spun fibre for textiles, carpeting and paper and in many cases used in composites for automotive, construction and insulation materials. Hemp

seed which is high in protein is used in a range of foods and beverages which allows increased potential for economic feasibility of hemp; oil from the crushed hemp seed is used as an ingredient in a range of body-care products and nutritional supplements.

Table 2.3: Chemical composition of hemp fibre

Cellulose (%)	Hemicellulose (%)	Lignin (%)	Extractives (%)
67	16.1	3.3	3.6
74.4	17.9	3.7	1.7
74	18	4	1
55	16	4	35
76	11.5	3.2	1.3
57-77	-	9-13	-
75.1	<2	8	-
70-74	17.9-22.4	3.7-5.7	1.5
75.6	10.7	6.6	-
78.3	-	2.9	-
76.1	12.3	5.7	4.9

The bast fibre of interest for composite materials is located between the hurd and epidermis as mentioned previously, shown schematically in Figure 2.2. The bast fibre provides the tensile and flexural strength, resistance against mildew and microbial and determines the length of the plant stalk [37]. Bast fibre is found in fibre bundles within the plant stalks. Fibres are connected within bundle by lignified pectin. This fibre bundle is commonly treated to separate it into single fibres. The length a single fibre is from 35 to 40 mm [40].

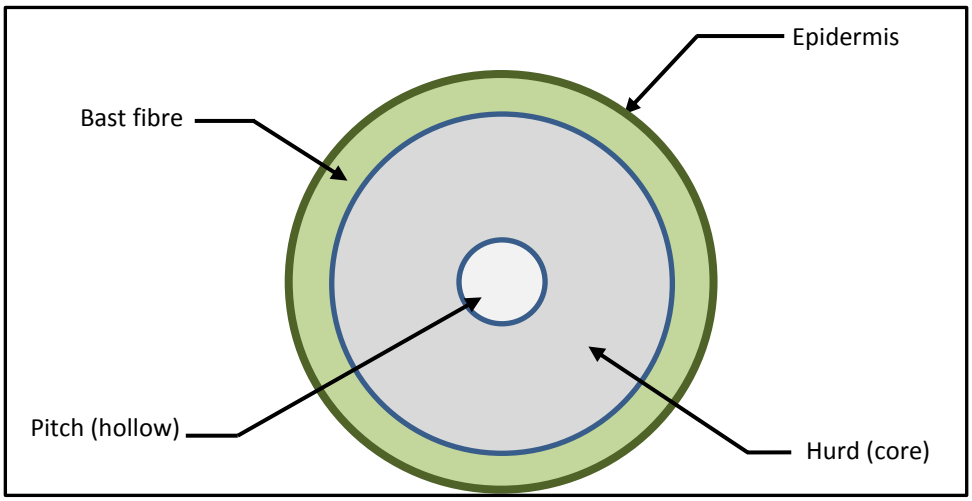

Figure 2.2: Schematic of plant stem cross section (not to scale) [41].

There are two types of bast fibre: primary bast fibre and secondary bast fibre. Primary bast fibre makes up approximately 70 percent of the mass of the bast fibre while secondary bast fibre makes up the remaining 30 percent [17]. Primary bast fibre is usually longer and coarser than secondary bast fibre, and comprises of 10 to 40% of the mass of the stem depending on the species of plant. Widely used bast fibre includes that from flax, hemp, kenaf, sunn-hemp and jute. Bast fibre is commonly separated from hurd and epidermis by retting and/or mechanical decortication [42].

2.2.4 Harakeke Fibre

Harakeke or phormium tenax, shown in Figure 2.3, is a monocotyledonous plant, endemic to New Zealand used traditionally by Maori and by early European settlers in New Zealand as a replacement for European flax and hence is commonly called ‘native flax’; they were originally used for cordage, textiles, art, and clothing. Fibre from harakeke plants is extracted from the upper and lower

sides of its leaves, which are stiff and tough and can grow up to 3 m long and 125 mm wide [35].

Figure 2.3: Harakeke or phormium tenax abundantly available in New Zealand.

The chemical composition of harakeke fibre is tabulated in Table 2.4 [43]. In comparison to hemp fibre, the cellulose content of harakeke fibre is slightly lower, but hemicellulose and lignin contents are higher. The favourable strength and stiffness of the fibre and mechanisation of extraction around the 1920s resulted in an expansion of the harakeke fibre industry with the fibres becoming an important export commodity and used in a variety of applications such as clothing, mats, baskets, ropes, fishing lines and nets [44].

Table 2.4: Chemical composition of harakeke fibre

Composition	Content (%)
Cellulose	60.9 ± 4.4
Hemicellulose	27.3 ± 4.1
Lignin	7.8 ± 1.3
Extractives	4.0 ± 0.3

Similar to other plant fibres, the physical and mechanical properties of harakeke fibre are dependent on a numbers of factors including the age of the plant, growth condition and the part of the leaf where the fibre is extracted. Further factors include the fibre extraction process, treatment and testing procedures [45]. Similar to hemp fibres, harakeke fibres are present in bundles (also called technical fibres) within harakeke leaves [46]. The cross-sectional shapes of fibre in bundles can be classified into two main types: horseshoe and keyhole, as shown in Figure 2.4 [35]. Fibre bundles have been treated to separate them into single fibres to increase the contact area between fibre and the matrix in a composite [47].

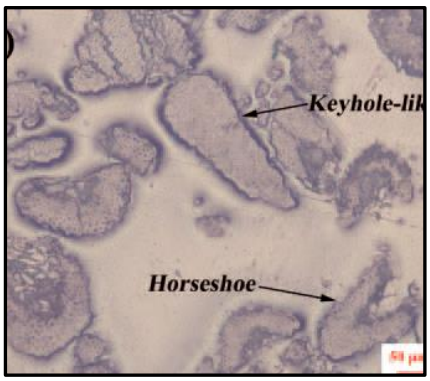

Figure 2.4: Cross-section of typical harakeke fibre showing keyhole-like and horseshoe-like shapes [35].

Previous research has shown that the pectin which cements single fibres together in the fibre bundles, surface wax and hemicellulose present in the primary cell wall of the fibres can be removed under optimum treatment giving good fibre separation (see Figure 2.5). As for other natural fibres, removing unwanted low stiffness components such as hemicellulose, lignin and other extractives from natural fibre through chemical and physical treatments can also improve the fibre properties

[47, 48]. Treated fibres generally appear clean and slightly browner than the raw fibres [49].

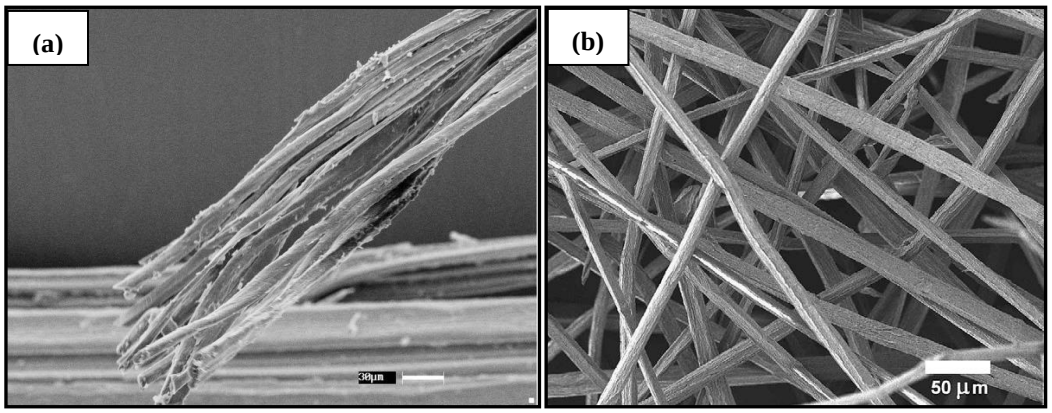

Figure 2.5: SEM of harakeke fibres: (a) fibres in bundle form, (b) treated fibres in single fibre form [47, 48].

Similar to bast fibre, it is very important to ensure that a fibre bundle is treated to separate it into single fibres prior to composites processing. Using fibres in bundle form instead of single form is expected to reduce tensile strength of composites due to smaller contact area between the reinforcement and matrix; smaller diameter of reinforcement expose larger proportion of bonding area with the matrix, helping to account for better mechanical properties of the composites [47].

2.2.5 Structure and Composition of Natural Fibre

Although the chemical composition of plant fibres varies between plant species, the chemical components present are similar. Plant fibre is made up of three major chemical constituents: cellulose, hemicellulose and lignin. These chemical constituents make up a total of 80-90% of the dry materials. Other minor constituents include pectin, waxes and water-soluble components. The major constituents of plant fibre are briefly described in the following sections.

2.2.5.1 Cellulose

Cellulose is the main structural component of plant fibre and as such is the most abundant organic compound on Earth. The cellulose molecule is a long, straight linear homo-polymer chain consisting D-anhydroglucose (glucose unit) which are connected by ß-1, 4-glycosidic linkages through hydrogen bonding and Van Der Waals force to produce a strong crystalline structure [50]. The general arrangement and chemical structure of cellulose is illustrated in Figure 2.6. Cellulose is generally composed of two regions namely: crystalline and amorphous and is typically 60-90% crystalline by weight [51]. In crystalline regions, very limited numbers of hydroxyl groups (OH) are available due to the closely packed inter-chain bonds that make it less hydrophilic. In amorphous regions, fewer inter-chain hydrogen bonds are formed, exposing more hydroxyl groups (OH) to bond with water molecules, thus making it more hydrophilic.

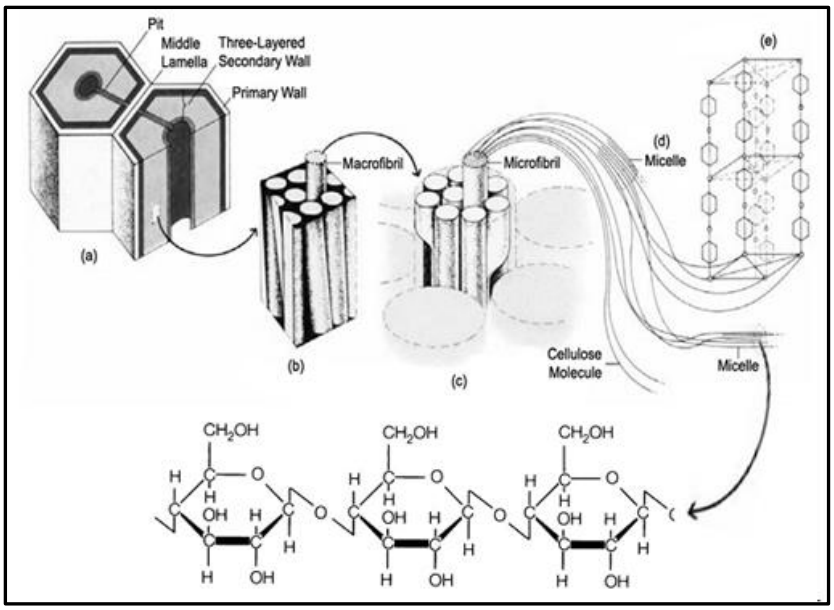

Figure 2.6: The arrangement and molecular structure of cellulose [52-54].

2.2.5.2 Hemicellulose

Hemicellulose has a lower molecular weight than cellulose and is present in almost all plant cell walls as a wrapping material filling cavities between the micro fibrils in cellulose. The main difference to cellulose is that hemicellulose has branches with short lateral chains (as shown in Figure 2.7) consisting of different sugars such as xylose, mannose and galactose, whereas cellulose as previously mentioned contains only 1, 4-β-D-glucopyranose units. It comprises a group of polysaccharides composed of a combination of 5- and 6-carbon ring sugars. Hemicellulose is bonded to cellulose by hydrogen bonding to form a cellulose-hemicellulose network creating the structural component of the fibre cell [55]. Due to its amorphous structure, its hydroxyl groups are much more accessible to water than those of cellulose [56]. Therefore, hemicellulose is more easily hydrolysed by dilute acids or bases.

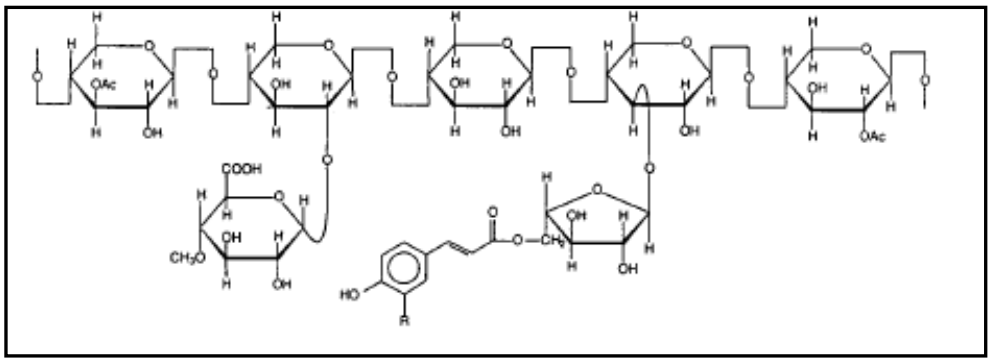

Figure 2.7: Typical chemical structure of hemicellulose [57].

2.2.5.3 Lignin

Lignin is the second most abundant polymer on Earth and by itself is very weak. However, natural fibres could not attain great heights or rigidity without support from lignin. Lignin is a complex hydrocarbon polymer comprised of carbon, hydrogen and oxygen (see Figure 2.8), insoluble in most solvents and cannot

easily be broken down to monomeric units as it is held together with strong chemical and many hydrogen bonds. It comes generally in amorphous and hydrophobic form in nature. It is found in all vascular plants, mostly between the cells and also within the cells to effectively acting as the plant matrix [55]. Lignin confers not only structural support to plants, but resistance against microbial attack and oxidative stress. Elimination of lignin from the cell wall at cellulosic level increases the stiffness of the fibre and allows the effective stress transfer between fibres and matrix in natural fibre composites.

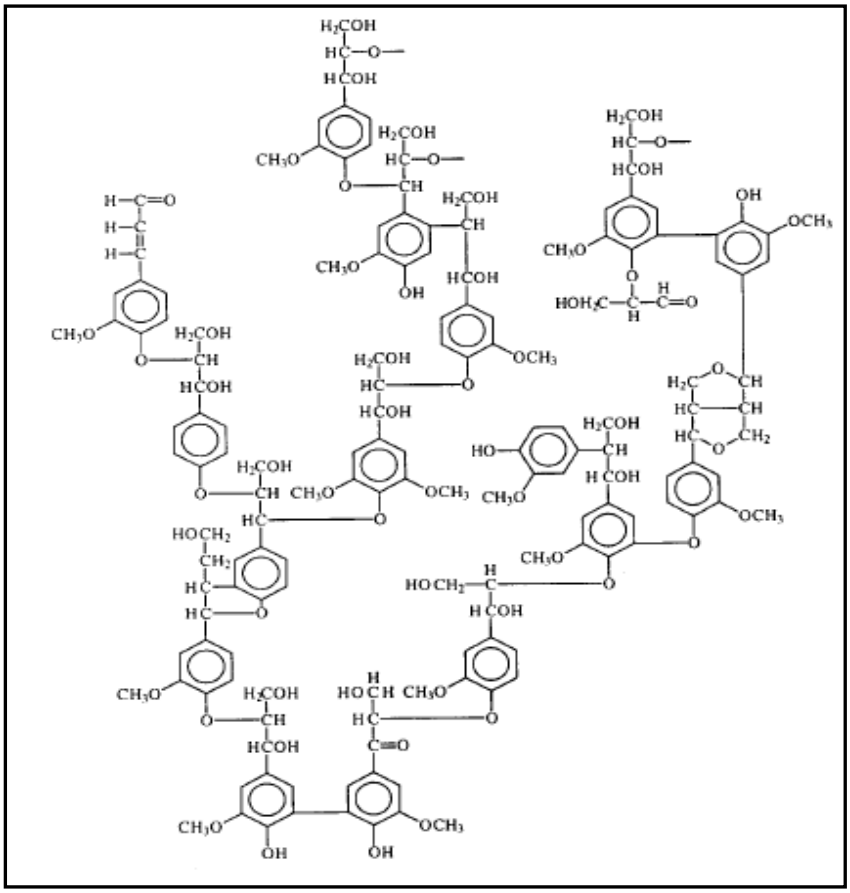

Figure 2.8: Typical structure of lignin [54].

2.2.6 Fibre Factors Influencing Performance of Natural Fibres Composites

The fibre, in most cases is a major controlling constituent towards composite performance. A fibre's thermal stability, ability to disperse, wettability and low moisture absorption along with mechanical performance will influence composite properties.

2.2.6.1 Thermal Stability

Degradation during processing has been a limiting factor in promoting natural fibre composites in wider applications [58]. Natural fibres are normally not viable to be processed at high temperature due to the possibility of degradation and emissions of volatile materials that could adversely affect the composite properties. Most of the natural fibres used as a reinforcing agent are thermally stable below 200^{o}C, although at some circumstances it is possible to be processed at higher temperature for a short period of time [59]. Due to this limitation, only thermoplastics that soften below this temperature such as polyethylene, polypropylene, polyolefin, polyvinyl chloride, polystyrene and PLA are useable as a matrix [60]. However, it should be noted that these thermoplastics constitute most of the total thermoplastics consumed by the plastics industry and far outweigh the use of any other matrices.

2.2.6.2 Fibre Dispersion

Good fibre dispersion within a matrix promotes better interfacial strength in composites. Natural fibre, however, is often associated with poor fibre dispersion due to differences in polarity between the fibres and matrix, and strong intermolecular hydrogen bonds between the fibres [61] and use of longer fibres

can further increase its tendency to agglomerate. Poor fibre dispersion leads to inhomogeneous matrix-rich and fibre-rich areas and increases the porosity within the matrix [62]. The matrix-rich areas are weak and the fibre-rich areas are vulnerable to premature composite cracking, which results in inferior composite mechanical properties. In order to improve fibre dispersion, different methods have been employed. Chemical treatment has led to improvement in fibre dispersion to an acceptable level [33, 63]. Chemical treatments are discussed in Section 2.5.2.

Intensive mixing using a twin-screw extruder rather than a single screw extruder also leads to better fibre dispersion, but this method can cause fibre damage and reduction in fibre lengths depending on temperature and time of processing, screw configuration and viscosity of melt mixture [61, 64].

2.2.6.3 Wettability

Most thermoplastics are generally hydrophobic (non-polar) in nature, which makes them incompatible with hydrophilic (polar) materials such as natural fibres which results in low fibre wettability. The fibre wetting is of great importance as a precursor in achieving of a strong bond as it allows intimate molecular contact at the interface. Insufficient fibre wetting causes interfacial defects and reduces the interfacial strength by flaw-induced stress concentration [65]. Fibre wetting can generally be assessed from the contact angle between fibre and matrix (shown in Figure 2.9) [66, 67].

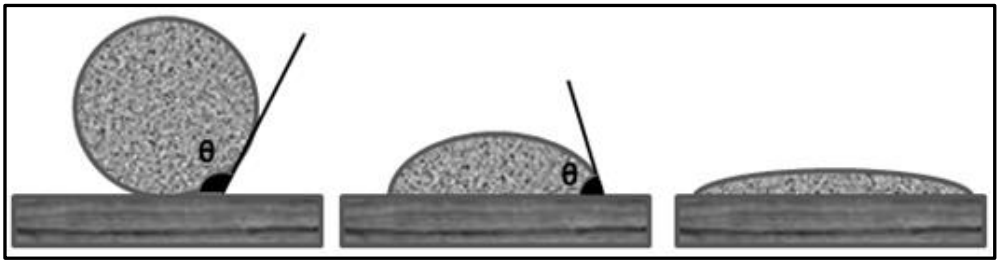

Figure 2.9: Different configurations of the fibre-matrix interfaces, from left to right; non-wetting, partial wetting and nearly complete wetting [68].

A small contact angle between fibre and matrix indicates that the fibre is well wetted, while a big contact angle indicates that fibre wetting is poor [65]. It has been found that physical [69, 70] and chemical treatments [71] improve the wettability of the fibre and hence improve interfacial bonding between fibre and the matrix. However, it should be kept in mind that there can be a compromise between obtaining good fibre wetting using chemical treatment and avoiding extensive fibre degradation to enable good properties of natural fibre composites.

2.2.6.4 Moisture Absorption

Plant fibres generally contain large amounts of hydroxyl groups, which make them a polar and hydrophilic in nature. This polar nature results in high moisture sorption increasing fibre swelling and increase the potential of voids formation within composites. Insufficient fibre drying prior to composites production increases the tendency of fibres to release moisture in the composite during high temperature processing, leading to the formation of highly porous composites. These pores can act as stress concentration points, induce premature cracking and can lead to premature failure of the composites during loading. At higher fibre contents, void contents would be higher and hence could dramatically decrease the composite strength [72]. Another problem associated with moisture is a

reduction in the adhesion between the fibre and the matrix, leading to a reduction in the mechanical properties and loss in dimension stability of the composites [73]. It has been reported that the interfacial strength of bamboo vinyl ester composites was reduced significantly with increasing moisture content. Interfacial shear strength was found to decrease from 11 to 66 MPa when moisture content increased from 0 to 10% [73]. Along with fibre drying, the use of fibre treatments and coupling agents were also found to reduce moisture absorption [74-77].

2.3 Matrices

The matrix is a very important element in a fibre-reinforced composite. As described earlier, it provides a barrier against adverse environments; it protects the surface of the fibres from mechanical abrasion along with transferring load to fibres. There are four (4) major types of matrices that have been used for composites namely: polymeric, metallic, carbon and ceramic [78]. The most common matrices currently used in natural fibre composites are polymeric, which are light weight and process-able at low temperatures. There are two main types of polymer matrix: thermoset and thermoplastic [79].

Thermoset polymers are cured into an irreversibly hardened material, which is accomplished by cross-linking or a network of covalent bonds (see Figure 2.10). The covalent bonds anchor the molecules together to resist vibrational and rotational chain motions at high temperatures and give the material a stable structure. As a consequence, mechanical strength and stiffness are not highly temperature dependent and they cannot be recycled through simple re-shaping, as for thermoplastics.

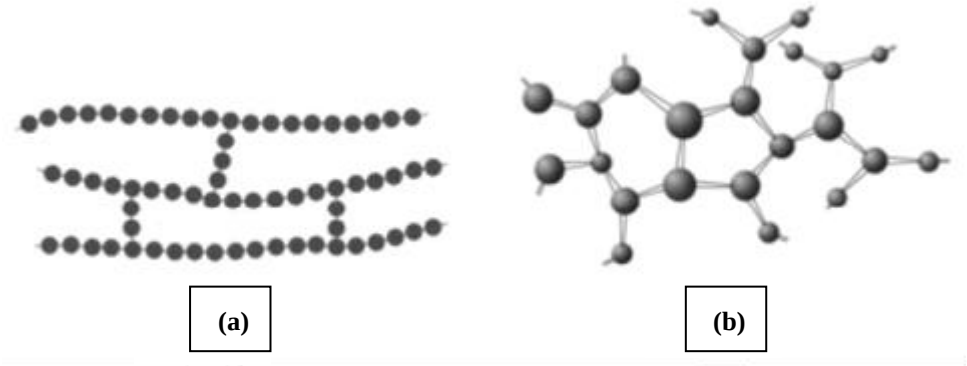

Figure 2.10: Schematic representative of thermosetting polymer structure: (a) cross-linked, (b) network molecular structures. Circles designate individual mer units [80].

Examples of some common thermoset polymers are:

- Epoxy
- Polyester
- Polyurethane (PUR)
- Phenol-formaldehyde
- Vulcanized rubber.

Thermoplastic polymers consist of linear or branched chain molecules with strong intra-molecular bonds but weak intermolecular bonds [81] (see Figure 2.11). As a consequence, thermoplastic polymers soften upon heating and can be reshaped upon reheating on application of pressure. They are capable of being repeatedly softened by the application of heat and hardened by cooling and are therefore recyclable. Modern thermoplastic polymers soften anywhere between 65 ºC and 200 ºC.

Figure 2.11: Schematic representative of thermoplastic polymer structure: (a) linear, (b) branched molecular structures. Circles designate individual mer units [80].

Examples of some common thermoplastic polymers are:

- Poly lactic acid (PLA)
- Polyethylene (PE)
- Polypropylene (PP)
- Poly (vinyl chloride) (PVC)
- Polystyrene (PS)
- Poly (ethylene terephthalate) (PET)
- Nylon (polyamide).

Considering good mechanical properties and biodegradability of PLA and resulting composites, PLA was selected as a matrix for this study.

2.3.1 Poly (lactic acid) (PLA)

Poly (lactic acid) (PLA) was amongst the first polymers to be commercially produced from renewable resources. PLA has been the most popular due to its high mechanical strength, which can be potentially used for structural materials [21]. PLA is colourless, glossy and rigid and its properties are largely dependent

on the component isomers, processing temperature, annealing time and molecular weight [82]. PLA is an aliphatic polyester thermoplastic that can be derived using fermentation, followed by either ring-opening polymerization or by condensation polymerization of lactic acid (Figure 2.12). The molecular structure of PLA is shown in Figure 2.13.

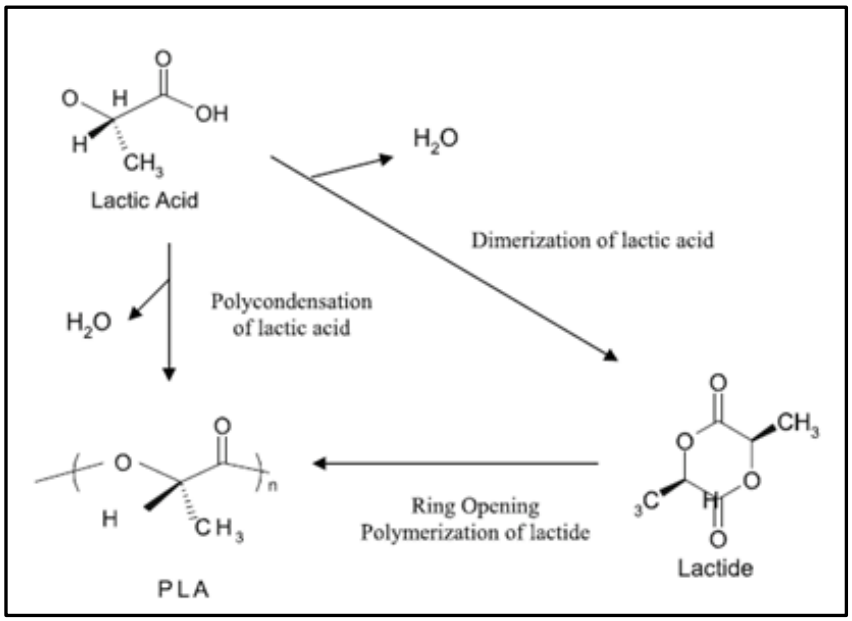

Figure 2.12: Polymerization routes of PLA [83].

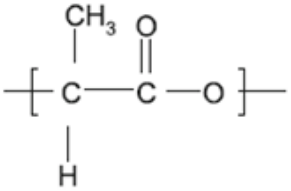

Figure 2.13: Molecular structure of PLA.

Lactic acid has two isomers L-lactic acid and D-lactic acid (as shown in Figure 2.14). Both isomers can be produced by chemical synthesis, whilst L-lactic acid

can also be produced by fermentation [17]. It should be noted that the majority of lactic acid used in PLA production is L-lactic acid from agricultural products [82].

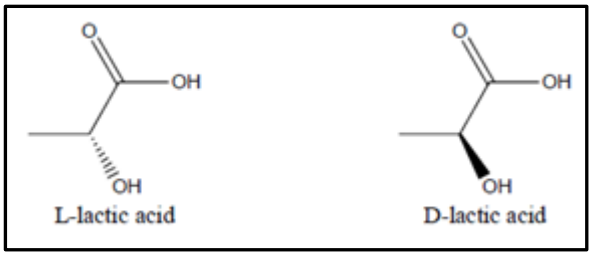

Figure 2.14: Chemical structures of lactic acid [83].

PLA can be either amorphous or semi crystalline, depending on the stereochemistry and thermal history. For amorphous PLA, the glass transition temperature (T_g) determines the temperature limit for most commercial applications and there is not a sharp melting point. For semi crystalline PLA, both T_g (around 58°C) relating to the amorphous phase and melting point (T_m) (130°–230°C) relating to crystalline phase, are important for determining the use temperatures across various applications and processing [84]. Both T_g and T_m of PLAs are commonly influenced by their primary structure, thermal history and molecular weight. Upon heating, the PLA goes through a transition from brittle glassy solid to an elastic rubber (viscoelastic).

PLA is a polymer that in many ways can behave like polyethylene terephthalate (PET) and polypropylene (PP), as it has high strength to weight ratio, relatively low cost and easy recycling [85]. PLA has a broad range of applications because of its ability to be stress crystallized, thermally crystallized, impact modified, filled, copolymerised, and processed in most polymer processing equipment. It can be formed into transparent films, fibres, or injection moulded into blow

mouldable preforms for bottles [84]. It also possesses other good properties such as high stiffness and UV stability [86].

PLA is compostable, and easily degrades by simple hydrolysis without requiring the presence of enzymes to catalyse it [83]. PLA is also found to be harmless to the human body and can be used for food contact products and related packaging applications and is also currently being used in biomedical applications.

2.4 Factors affecting natural fibre composite properties

In ensuring the potential of fibre and matrix properties are fully utilised to produce good performance natural fibre composites, further factors such as fibre orientation, fibre length and fibre–matrix interface should be taken into consideration. Details of the influence of these factors on the mechanical properties of composites form the basis for the rest of this section.

2.4.1 Fibre Orientation

Fibre orientation has an important influence on properties of natural fibre composites. Fibre aligned parallel to the loading direction is found to give the best composite tensile properties [87-89]. High levels of fibre alignment also allow high fibre volume fractions to be attained. The fibre orientation factor (K_o) is often used to represent the degree to which fibres are aligned parallel to the loading direction. Composites with high fibre alignment ($K_o \rightarrow 1$) can be obtained when carded long fibres or continuous fibre yarns (produced by fibre spinning or fibre wrapping) are placed manually with polymer sheets or powder prior to

impregnation by compression moulding [13, 90, 91]. Some degree of fibre alignment ($0.3 < K_o < 0.4$) can be obtained during injection moulding [14-16]; however, fibre alignment for composites using this method cannot be greatly improved, but given the convenience in injection moulding overall mechanical performance of composites may be acceptable for some applications.

Loose short fibres can also be used to produce fibre mats for use in compression moulding. Generally, the fibre alignment obtained from this method is found to be the lowest ($K_o = 0.2$) [92]. However, fibre alignment of fibre mats can be increased depending on the processing used to prepare the fibre mats. Yu *et al.*[12] in a study found that high fibre alignment (K_o up to 0.91) could be obtained by feeding fibre through multiple narrow channels. Lower fibre alignment (K_o up to 0.6) has been seen to be obtained for nonwoven mats using drawing method [93]. It should be acknowledged that these methods require additional processing stages to bring about alignment. Other than these methods, there is limited work reported on the efforts to improve fibre alignment in short fibre mats to date.

2.4.2 Fibre Length

Length of fibre is an important factor influencing the mechanical properties of composites. Tensile load is transferred into a discontinuous fibre from the matrix through shear at the interface. At the ends of the fibre, the tensile stress is zero and increases along the fibre length until the stress in the fibre (if it is long enough) reaches the fibre fracture tensile stress (σ_f) [94]. The effectiveness of load transferred depends largely on the critical fibre length (L_c), which is defined as the

length at which the fibre can be fully loaded at its centre point as if it were continuous. If fibre length (L) > L_c, the fibre reinforcement becomes more effective and the fibre can be fully loaded over a greater length of fibre prior to fibre fracture. However, if $L<L_c$ debonding would occur [16]. L_c can be expressed as follows:

$$\frac{L_c}{d} = \frac{\sigma_f}{2\tau_i} \tag{2.1}$$

where d is fibre diameter, σ_f is tensile strength of fibre and τ_i is the interfacial strength. The critical fibre length has been found to vary depending on fibre [95, 96], matrix [97] and fibre content [98]. It should be kept in mind that, if the fibre is too long, the fibres may get entangled during composite processing, resulting in poor fibre dispersion.

2.4.3 Fibre-Matrix Interfacial Bonding

Interfacial bonding between the fibres and matrix can generally be explained by means of various mechanisms, namely mechanical interlocking, electrostatic bonding, chemical bonding and inter-diffusion bonding. Mechanical interlocking at the fibre-matrix interface occurs when the fibre surface is rough, thus increasing the interfacial shear strength. Electrostatic bonding occurs due to negative and positive charges which are only noticeable at metal interfaces and hardly occurs in polymer matrix-fibre systems. Chemical bonding occurs when fibre surface chemical groups react with chemical groups in the matrix to form chemical bonds. The strength of the bond depends on the type and density of the bond. Inter-diffusion bonding occurs when atoms and molecules of the fibre and matrix interact at the interface. For interfaces involving polymers, bonding may take place when polymer chains from each component entangle together and this

bonding depends on the distance over which the chains are intertwined, the degree of entanglement and number of chains per unit area. It should be noted that multiple bonds can occur at the same interface at the same time [41]. However, for natural fibre composites there is usually limited interfacial bonding between the hydrophilic fibres and matrices which are commonly hydrophobic leading to limited mechanical performance. It is shown that, interfacial bonding of natural fibre composites can be improved using physical treatment and chemical treatments [69-71].

2.4.4 Fibre volume fraction

The properties of natural fibre composites are also strongly influenced by the proportions of the matrix and the fibre, which commonly are expressed using volume or weight fraction. In most cases, improvement in mechanical properties of composites including strength and stiffness can be obtained by increasing the fibre volume fraction up to a point where fibre wetting becomes poor [99-102]. However, composite strength lower than the strength of the matrix on its own is sometimes observed at low fibre volume fractions; this is detailed in Section 4.3.2.

2.5 Fibre and Matrix Treatments

In polymer matrix composites, improvement in interfacial strength can be achieved by modifying the surface characteristics of fibres by means of mechanical, physical and chemical treatments and by modification of the matrix properties using coupling agent. Increased interfacial strength can occur through

improved wettability to give more contact and increased bonding between fibre and matrix.

2.5.1 Physical Treatment

Corona, plasma and heat treatment are the three most common physical treatments. These treatments commonly require highly specialised equipment.

2.5.1.1 Corona Treatment

Corona treatment is a surface modification technique used to change the properties of fibre surfaces using low temperature corona discharge plasma. The corona plasma is generated by the application of a high voltage to sharp electrode tips at low temperature and atmospheric pressure. A typical corona treatment uses electrodes made from aluminium and electric spacers which are normally made from quartz [81]. In many cases, prolonged treatment time will result in significant fibre surface roughening. Gassan, J and Gutauski, V.S. [103] used corona discharge and ultraviolet (UV) to treat jute fibres and found the treatment improved flexural strength of composites to about 30%. Ragoubi *et al*. [104] also found that corona treatment greatly improved the surface roughness of the fibres and wetting between the fibres and the matrix, which was believed would improve the composite strength and stiffness. Ragoubi et al. [105] in a later study found that this treatment also improved storage modulus and thermal stability of composites which was attributed to better interfacial bonding between fibres and matrix.

2.5.1.2 Plasma Treatment

Plasma treatment is another physical treatment that exploits charge to alter the surface of the fibres. Plasma treatment has been shown to result in the development of hydrophobicity and roughen surfaces thus improving the adhesion between the fibres and matrix [70]. Unlike corona treatment, plasma treatment must be performed using a vacuum chamber and gas continuously supplied to maintain the appropriate pressure and gas composition [81]. This method is proven to be one of the most effective ways amongst the physical treatments to enhance the properties of composites. Seki *et al*. [106] found that inter-laminar shear strength (ILSS) and flexural strength of composites increased up to 35% and 30% compared to composites with untreated fibres.

2.5.1.3 Heat Treatment

Heat treatment involves heating fibres at temperatures close to those that bring about fibre degradation. Heat treatment can affect physical and chemical properties of the fibres; changes can occur in weight, strength, colour and crystallinity of cellulose. Chemical changes involve reduction of degree of polymerisation, formation of carbonyl, peroxide groups, carbon dioxide and evolution of water [81]. Similar to the corona and plasma treatment, heat treatment relies on time, temperature and composition of the gases involved during the treatment. Cao *et al*. [107] found that tensile strength of heat treated kenaf fibre using temperature of 140°C improved by approximately 70% compared to untreated fibre, which attributed to increased fibre crystallinity. Further increase in temperature, however, reduced tensile strength and crystallinity of the fibre greatly due to cellulose degradation.

2.5.2 Chemical Treatment

Hydrophilic cellulose is generally not compatible with matrices which are hydrophobic. This, however, can be overcome by treating the fibres with suitable chemical agents to improve interfacial strength between the fibres and matrix. It has been found that chemical treatments increase the wettability and bonding potential of fibres and matrix by a number of mechanisms including removing non-cellulosic components to expose more hydroxyl groups on fibre surface for bonding with the matrix and addition of chemical group for improved wettability or for chemical reactions [108]. Treatment of fibres is generally conducted prior to composite processing. Chemical treatments include those using alkali, acetyl, silane and peroxide.

2.5.2.1 Alkali Treatment

Alkali treatment is one of the most commonly used chemical treatments to improve interfacial bonding in natural fibre composites. Alkali fibre treatments using sodium hydroxide (NaOH) and sodium sulphite (Na_2SO_3) or combinations of these solutions have been used extensively for treating natural fibre [63, 109, 110]. Alkali is applied to remove hemicellulose, lignin, pectin, fat, wax and water soluble substances which results in fibre separation, exposure of cellulose at the fibre surface as well as fibre surface roughness, leading to a better mechanical interlocking and increased number of possible reaction sites for bonding with the matrix. As a consequence, increased interfacial strength, tensile strength and Young's modulus of composites can be obtained. Removal of these non-cellulosic materials has also shown to increase fibre crystallinity and thermal stability of

fibre [38, 63, 111] and allows microfibrils to be better aligned during tensile testing, which results in higher fibre tensile strength and failure strain [112].

Islam *et al*. [109] in a study using hemp fibre with PLA have found that treating fibre at 120 °C for 60 minutes using 5 wt% of NaOH and 2 wt% of Na_2SO_3 relative to fibre weight resulted in higher interfacial shear strength compared to untreated fibre. Ibrahim *et al*. [113] found that alkali (4 wt% NaOH) treatment conducted at room temperature improved tensile strength of kenaf fibre composites by 52% (16.48 MPa) compared to untreated composites (10.8 MPa), but tensile strength of composites decreased with higher concentration of alkali solution due to fibre degradation. A later study conducted by Kabir *et al*. [114] verified that the alkali treatment not only improve strength, stiffness and flexural strength, but also thermal stability of the composites.

Pickering *et al.*[38] has found that, tensile strength of hemp fibre treated with 10 wt% NaOH (relative to fibre weight) at 160 °C for 45 minutes improved by approximately 12% compared to untreated fibre. Crystallinity index of treated fibres also found increased to 93.9% from 83.7% (for untreated fibre). Dramatic reductions of tensile strength of fibres, however, have been observed as alkali concentration increased to 15 wt% for the same treatment duration, which was thought to be due to cellulose degradation. Higher improvement for tensile strength of hemp fibre was obtained in a later study [64] using a combination of NaOH (5 wt%) and Na_2SO_3 (2 wt%). It has been reported that tensile strength and Young's modulus of treated hemp fibres improved by 20 and 22% respectively compared to untreated fibres. However, using this treatment, fibre crystallinity

was not greatly increased. Similar improvement in tensile strength for alkali treated kenaf fibres has also obtained by Goda *et al.* [112]. Along with improvement in fibre strength, it was also found that failure strain of treated fibre improved by nearly three times compared to untreated fibre.

2.5.2.2 Acetyl Treatment

Acetylation, results in the introduction of acetyl groups (CH_3CO-) through esterification with hydroxyl group (-OH) on fibre surfaces resulting in increased hydrophobicity of the fibre. The esterification process is demonstrated in Figure 2.15. Alkali treatment is generally applied prior to this treatment to expose cellulose hydroxyl groups. It has been shown that acetylation improves interfacial bonding, tensile strength, stiffness and flexural strength, as well as dimensional and thermal stability of composites [115-117].

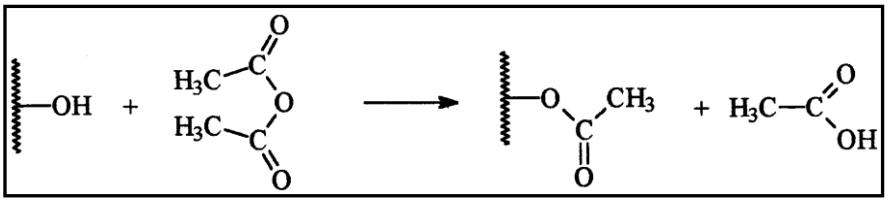

Figure 2.15: Reaction of acetic anhydride with cell wall polymers [118].

Khalid *et al*. [116] found that acetylation treatment improved interfacial shear strength (IFSS) between palm oil fibres and the polystyrene resin by up to 71% (increased from 1.4 to 2.4 MPa). Bledzki *et al.* [115] in a later study on flax fibre composite have found that tensile strength of composites improved by 22% with 3.6% degree of acetylation (measured by saponification methods) compared to untreated fibre. Steady improvements in composite strengths were obtained with

acetylation degree up to 18%, before reduction in strengths was observed; which was believed to be due to the degradation of cellulose. Acetylation was found to reduce the impact strength of composites [115]. This is not surprising giving that good interfacial bonding can increase ease of crack propagation.

2.5.2.3 Silane Treatment

Silane is a hydrophobic compound having different functional groups at either end, which interact at one end with hydrophilic groups of cellulose through a siloxane bridge, while the organic end interacts with the hydrophobic groups of the matrix [63]. In the presence of water under acid catalysed conditions, hydrolysable alkoxy groups of silane are hydrolysed to form silanols (Si-OH), which then reacts with hydroxyl groups of the fibre through an ether linkages and with subsequent drying, condenses the silanol groups to form a macromolecular network [119-121]. The effectiveness of silane treatment is strongly dependent on the amount of silanol coupled with hydroxyl group in the fibre surfaces; at low levels of silane, insufficient amount of silanol is formed and results in less optimal bonding. As the silane content increases, more silanol is formed thus interfacial strength increases as a result of increased interfacial bonding, but as silane content is further increased, even more silanol is formed with some of it not coupled with hydroxyl group of fibre and becomes free silanol. This free silanol can react with each other on the fibre surfaces thereby forming a rigid polysiloxane structures as an alternative to reacting with matrix and limits interfacial bonding [120, 122]. The most commonly reported silanes used in natural composites are amino (APS), methacryl (MPS), glycidoxy (GPS) and alkyl (HDS). Silane treatment has been

found to increase not only tensile strength, stiffness, flexural strength [123-126], but also thermal stability of the composites [122, 127].

2.5.2.4 Peroxide treatment

Peroxide is an organic compound with the functional group ROOR containing the divalent ion O-O [33]. Organic peroxides tend to decompose to form free radicals (RO) and react with the hydroxyl groups of the fibre during fibre treatment, and with the matrix during composite processing [120]. Benzoyl peroxide (BP) and dicumyl peroxide (DCP) are most commonly used in natural fibre treatment [128-130]. In peroxide treatment, fibres are commonly immersed in acetone solution containing BP or DCP after alkali pre-treatment. Although no significant improvement in tensile strength has been reported, this treatment has been seen to improve flexural strength of oil palm fibre phenol formaldehyde (PF) composites by 45% [130] and decreased moisture absorption of flax fibre HDPE composites by 18% [131].

2.5.3 Coupling Agents

Maleic anhydride (MA) grafted polymers are widely used as coupling agent to improve the mechanical properties of natural fibre composites due to their good chemical reactivity under free radical grafting conditions induced by initiator. MA is commonly grafted to the same polymer as that used as the matrix to ensure compatibility between the matrix and the coupling agent. MA grafted polymer can react with the hydroxyl groups on fibre surfaces through the MA groups leading to covalent or hydrogen bonding. MA grafted polymer can be used as an additive during processing or grafted to the fibre prior to processing. It has been shown

that using MA grafted with polypropylene (MAPP) [63], polyethylene (MAPE) [132] and poly lactic acid (MAPLA) [133] as coupling agents improves mechanical properties of composites considerably. Improvement in tensile strength by up to 60% [64], 17% [132] and 23% [133] has been obtained using MAPP, MAPE and MAPLA as coupling agents in natural fibre reinforced PP, PE and PLA composites respectively.

Slight improvement of composite properties has been seen with the application of hyper-branched polymer (HBP) as a coupling agent, with tensile and impact strength of optimized ultrasound-alkali treated oil palm empty fruit bunch fibre PLA composites seen to improve by 6 and 5% respectively, considered to be due to increased compatibility between fibres and PLA through bonding of hydroxyl groups. It has also been reported in a number of publications that failure strain as well as impact strength of PLA has been improved significantly without improvement of tensile strength and stiffness with addition of HBP, such that it is acting more as a plasticiser than a coupling agent [134-138], attributed to a reduction in PLA crystallinity [135], as a result of interaction of hydroxyl groups on highly branched polymer (see Figure 2.16) with C=O groups of PLA.

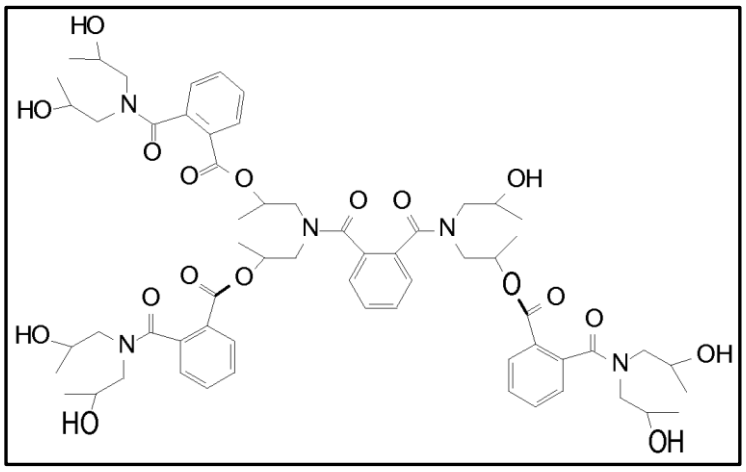

Figure 2.16: Chemical structure of HBP (Hybrane PS2550).

2.6 Thermoplastic Composites Processing

In general, processing methods used in natural fibre composites are similar to those used in synthetic fibre composite production. Composite quality, production cost and production speed are the main factors that determine the suitability of the processing method. In natural fibre thermoplastic matrix composite production, the most common methods used are extrusion, injection moulding and compression moulding.

2.6.1 Extrusion

Extrusion is the process where a solid matrix, usually in the form of pellets or powder is melted and mixed with the fibre and conveyed by means of a single or two rotating screws, compressed and forced out of the chamber at a steady rate through a die [139]. The speed and temperature are two critical factors for producing a good quality composite. High screw speed can result in air entrapment, excessive melt temperatures and fibre breakage. Low speeds, however, can lead to poor mixing and wetting between matrix and the fibres. If the temperatures are very high, it is possible to degrade the fibres, which limits the

thermoplastic matrices used to those with melting points lower than the temperature at which fibre degradation will occur. This method can be used alone for production or as a pre-cursor to injection moulding [140].

2.6.2 Injection Moulding

Injection moulding has been widely used in the automotive and construction industries. Short fibres and matrix materials in the form of pellets or powder are normally supplied via a hopper into a heated barrel with a plunger. The heated barrel transforms the polymer into a viscous liquid which can be injected by the plunger through a nozzle and forced into a tightly clamped mould cavity where the composite is cooled to solidify it [81]. During this process, the phenomenon called fountain flow occurs when the velocity of the melt flow varies between the centre of flow and flow closer to the wall [27, 41, 141-143]. Lower flow velocity along the wall due to friction produces more aligned fibre while higher flow velocity at the centre leads to more randomly and transversely aligned fibre. Injection moulding offers fast, economical processing with minimum warping and shrinkage. It also offers the ability to use a wide range of materials, low labour cost, minimal scrap losses, and little need to finish parts after moulding [144]. Due to the requirements of viscosity, injection moulding is generally limited to composites of less than 40 wt% fibre content.

2.6.3 Compression Moulding

Compression moulding is a method in which the moulding material is generally preheated and placed in an open, heated mould cavity. The mould is then closed under pressure to force the material to fill up the cavity; heat and pressure are

maintained until the moulding material has solidified. Composites can be made with continuous or chopped fibre either randomly oriented or aligned in mats, with a thermoplastic or thermoset matrix. The fibres are normally stacked alternatively with matrix before pressure and heat are applied. For thick composite samples, temperature gradients and holding times should be carefully optimised to ensure adequate heat is transferred from the surface of the composite to the core and the matrix is impregnated fully into the space between fibres. Good quality composites can be produced by controlling viscosity, pressure, holding time, temperature depending on the types of fibres and matrix [145]. Fibres with low heat resistance should be moulded with relatively low temperatures to avoid damage.

CHAPTER 3

The Effects of Alkali Treatment on Fibre Properties

3.1 Introduction

In this chapter, the effect of alkali treatment on the physical and mechanical properties of hemp and harakeke fibres is detailed. As previously mentioned, alkali treatment is among the most popular treatments used it removes components such as pectin, hemicellulose and waxes, enhance fibre properties and can provide good fibre dispersion within the composite [16, 38, 41, 146, 147]. Details of the materials used, the methods and the effects of treatments assessed using single fibre tensile testing, X-ray diffraction (XRD), scanning electron microscopy (SEM) and thermal analysis using thermogravimetric analysis (TGA) are included.

3.2 Experimental Methodology

3.2.1 Materials

Harakeke fibre was obtained from the Templeton Flax mill, Riverton. It was mechanically prepared and supplied in bundle form. Hemp fibre was locally grown from October 2012 and harvested in February 2013 after 120 days and donated by the Hemp Farm NZ Ltd. Green hemp stalks were dried exposed to air for two weeks and then the bast fibre was hand separated from the stalks.

3.2.2 Methods

3.2.2.1 Alkali Fibre Treatment

Alkali treatment was carried out using a laboratory scale pulp digester (normally used for paper making) at different temperatures and for different durations. Three alkali formulations were used in this investigation: 5 wt% sodium hydroxide (NaOH), 10 wt% NaOH and 5 wt% NaOH with 2 wt% sodium sulphite (Na_2SO_3). The chemicals used (purchased from Scharlau Chemie S.A.) were analytical grade Na_2SO_3 pellets and NaOH powder, both with 98% purity level. The abbreviations used for the fibres and treatments are shown in Table 3.1.

Table 3.1: Abbreviations used for fibre and treatment

Fibre and Treatments	Abbreviation
Harakeke – Untreated	**HR-U**
Harakeke – Treated with 5wt%NaOH	**HR-5**
Harakeke – Treated with 10wt%NaOH	**HR-10**
Harakeke – Treated with 5%wtNaOH/2wt%Na_2SO_3	**HR-5/2**
Hemp – Untreated	**HM-U**
Hemp – Treated with 5wt%NaOH	**HM-5**
Hemp – Treated with 10wt%NaOH	**HM-10**
Hemp – Treated with 5wt%NaOH/2wt%Na_2SO_3	**HM-5/2**

The three alkali solutions were used with a fibre (harakeke or hemp) to solution ratio of 1:8 by weight. Predetermined amounts of harakeke and hemp fibres were placed in stainless steel canisters with pre-mixed NaOH and Na_2SO_3 solutions. The canisters were then placed into a small lab-scale pulp digester with the treatment cycles, controlled by a 4-step controlled programme, chosen based on preliminary screening trials. Trials had previously been conducted raising the

temperature from ambient to a maximum temperature over 90 minutes. It had been demonstrated that treatment conducted for longer than 30 minutes at a temperature for more than 160 °C reduced the tensile strength of hemp fibre considerably. However, with treatment conducted at less than 160 °C the fibre tensile strength was maintained, but the separation of the fibre was very poor. Therefore, treatment at 160 °C for 30 minutes was chosen for hemp fibre. For harakeke, it was found that in order to get fibre separation, treatment was required to be conducted at 170 °C for at least 40 minutes, however, harakeke fibre treated at higher than 170 °C was slightly degraded even though the fibre separation was improved. This is supported by research conducted elsewhere, such that treatment at 170 °C was found to give the optimum fibre separation for harakeke [46]. Therefore, treatment at 170 °C for 40 minutes was chosen for harakeke fibre.

3.2.2.2 Scanning Electron Microscopy

SEM micrographs of untreated and treated fibres were taken using a Hitachi S-4100 field emission scanning electron microscope (SEM). Prior to SEM observation, the samples were mounted on aluminium stubs using carbon tape and then coated with plasma sputtering to avoid the sample becoming charged under the electron beam. SEM observation was carried out at 5 kV.

3.2.2.3 Single Fibre Tensile Testing

The tensile strength and Young's modulus of untreated, NaOH and NaOH/Na_2SO_3 treated harakeke and hemp fibres were tested according to the ASTM D3379-75: Standard Test Method for Tensile Strength and Young's Modulus for High-Modulus Single Filament Materials. Single fibres were

mounted on 2 mm thick cardboard mounting-cards with a 2 mm gauge length as schematically shown in Figure 3.1. PVA glue was applied to hold the fibres to the cardboard and define the gauge length.

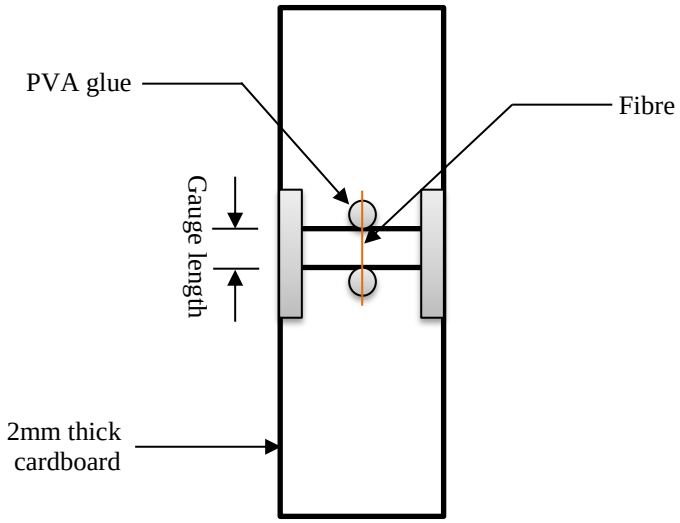

Figure 3.1: Schematic diagram of cardboard used in testing with mounted single fibre [148].

Harakeke and hemp fibres, similar to other cellulosic fibres generally have variable cross-sectional areas and diameters along their length. To account for this, the diameter of the fibres was measured at five different points along the fibres length by means of an Olympus BX60F5 optical microscope. Typical single harakeke and hemp fibres observed under optical microscope are shown in Figure 3.2 and 3.3 respectively. It can be seen that harakeke fibre is finer than hemp fibre, but otherwise looked similar.

Figure 3.2: Single harakeke fibre as observed under optical microscope.

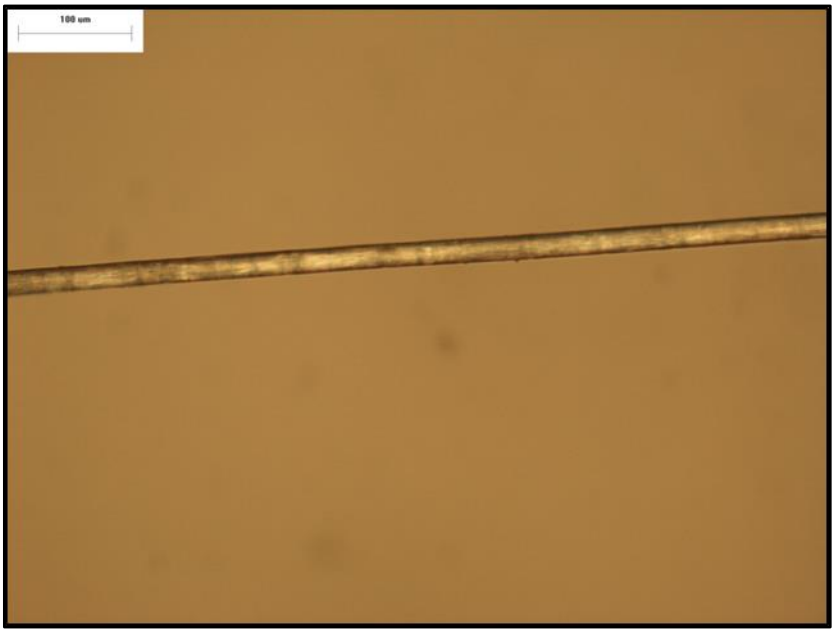

Figure 3.3: Single hemp fibre as observed under optical microscope.

The apparent cross-sectional area of each fibre was then calculated using the mean fibre diameter and assuming a circular cross-section. The measured and mounted fibres were then placed in the grips of an Instron-4204 universal testing machine and the supporting sides of the mounting cards were cut using a hot-wire cutter.

The fibres were then tensile tested to failure at a rate of 0.5 mm/min using a 10 N-load cell. 30 replicate samples were tested for each batch and average tensile strength (TS) and Young's moduli (YM) were obtained using the results from all specimens. One tailed student's t-test was used to check the significance of data population [149]. As an extensometer cannot be used on such thin specimens, elongation of single fibres was determined through the displacement of the testing machine cross head. The crosshead displacement, however, is actually a combination of the fibre elongation as well as the crosshead deformation, specimen grips, and the cardboard mounting card. For accurate measurement of fibre elongation and Young's modulus, system compliance is required and was determined experimentally using related procedures described in ASTM D3375-75 [150]. In this study, specimens of different gauge lengths of 5, 10 and 15 mm of hemp and harakeke were prepared using similar set up used in single fibre testing. From the corresponding load-displacement curves for each specimen, the inverse of the slope of the initial linear region of the force versus cross-head displacement curve representing indicated compliance was determined. By plotting the apparent compliance against gauge length and extrapolating this function to zero gauge length, leads to the testing device compliance which was then used to calculate Young's modulus.

The data obtained for the tensile properties were statistically analysed using the two-parameter Weibull equation, which expresses the cumulative density function of the strength of the fibres as [151]:

$$P_{f(L)} = 1 - \exp\left[-L\left(\frac{\sigma}{\sigma_0}\right)^w\right] \tag{3.1}$$

where $P_{f(L)}$ is the probability of failure of a fibre of length L at a stress less than or equal to σ, σ_0 is the Weibull scale parameter or characteristic stress, and w is the shape parameter or Weibull modulus which describes the variability of the failure strength. Weibull parameters were estimated through the linear regression method, using the following estimator [152]:

$$P = \frac{i}{n+1} \tag{3.2}$$

where n is the number of data points and i the rank of the i-th data point.

Rearrangement of the two-parameter Weibull cumulative distribution expression (Equation 3.1) gives the following [153]:

$$ln\, ln\left(\frac{1}{1-P_f}\right) = w \ln \sigma - w \ln \sigma_0 + lnL \tag{3.3}$$

The scale and shape parameters can be obtained from a plot of ln ln(1/1-P_f) versus ln σ (commonly referred to as a Weibull plot) which should produce a straight line, with gradient w and intercept σ_0 at ln ln(1/1-P_f) = 0.

3.2.2.4 Wide Angle X-ray Diffraction

A Philips X'Pert diffractometer fitted with a ceramic X-ray diffraction tube was used to assess the influence of alkali treatment on fibre crystallinity. Prior to the analysis, untreated and treated harakeke and hemp fibres were cut by hand into fine particles and compressed into disks using a cylindrical steel mould with appropriate amount of pressure. The diffracted intensity of CuKα radiation (λ = 1.54nm) was recorded between 12° and 30° (2θ-angle range) using a current and voltage of 40 mA and 40 mV with scanning speed of 0.02 degrees/second.

The percentage crystallinity index (I_c) was then determined using the Segal empirical method according to the following equation [117, 154]:

$$I_C = \frac{(I_{002} - I_{am})}{I_{002}} x\ 100 \tag{3.4}$$

where I_{002} is the maximum intensity of diffraction of the lattice peak at a 2θ-angle of between 22° and 23° and I_{am} is the intensity of diffraction of the amorphous material, which is taken at a 2θ-angle of between 18° and 19° where the intensity is at a minimum [64, 155].

3.2.2.5 Thermal Analysis

Untreated and treated fibre samples weighing between 8 and 12 mg were analysed using an SDT 2960 Simultaneous DTA-TGA analyser (shown in Figure 3.4). The analysis was operated in a dynamic mode, heating from ambient temperature to 500 °C at 10 °C/min in air purged at 150 ml/min with an empty pan used as a reference. Differential thermal analysis (DTA) and thermal gravimetric analysis (TGA) curves were obtained at the end of the operation.

Figure 3.4: SDT 2960 Simultaneous DTA-TGA analyser.

3.3 Results and Discussion

3.3.1 Fibre Morphology

SEM micrographs of harakeke fibres are shown in Figure 3.5 to Figure 3.7 and hemp in Figures 3.8 and 3.9. As can be seen in Figure 3.5a, untreated harakeke fibre bundles were composed of many single fibres attached to each other and coated with substances known to include hemicellulose, pectin, lignin, and other non-strengthening components [117].

In contrast, alkali treated harakeke fibres (shown in Figures 3.6 and 3.7) were separated from each other and appeared to have undergone removal of surface coating revealing less rounded sides and a rougher texture with a large numbers of grooves, believed to be cellulose rich as seen for treatment of other cellulosic fibres [34, 156, 157]. However, fibres treated with 5 wt% NaOH, 10 wt% NaOH and 5 wt% NaOH/2 wt% Na_2SO_3 are found to be physically similar with no obvious fibre degradation observed. The fibre separation resulting from the

removal of non-strengthening components along with the exposure of rougher texture would have increased contact area for bonding and could therefore be expected to improve fibre-matrix interfacial bonding. The improvement of fibre-matrix adhesion is also expected due to the exposure of more cellulose OH groups, which could bond with reactive sites on the matrix [156]. Likewise for hemp, all treated fibre was well separated and surfaces appeared to have increased overall rugosity compared to the untreated fibre as shown in Figure 3.8b and Figure 3.9.

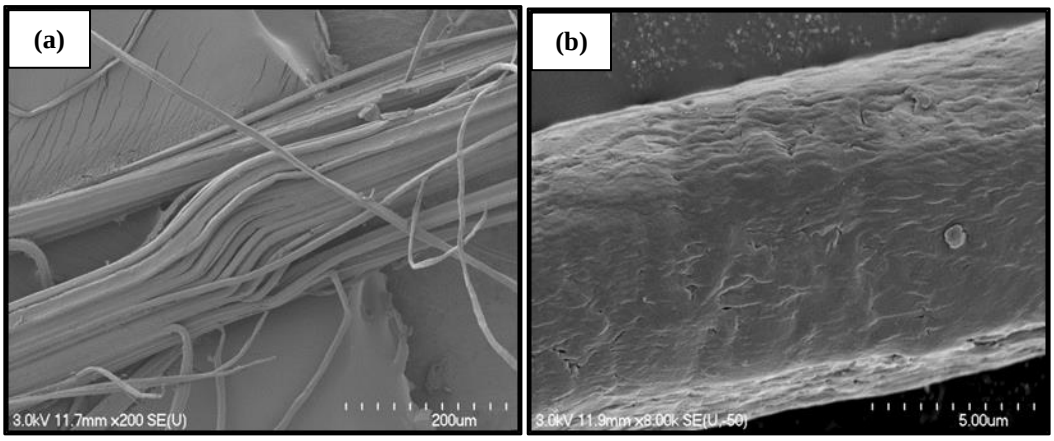

Figure 3.5: Scanning electron micrographs of untreated harakeke: (a) in bundle form, (b) a mechanically separated single fibre.

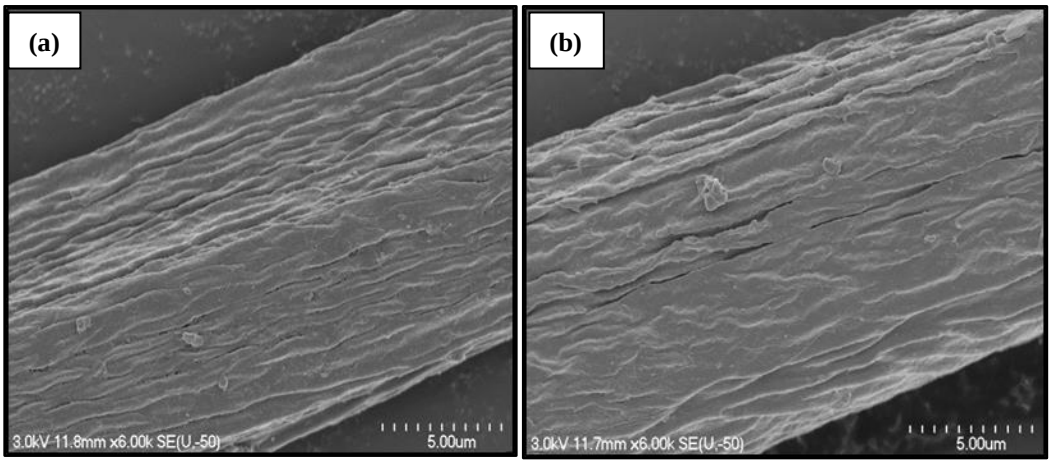

Figure 3.6: Scanning electron micrographs of treated harakeke fibre surface using: (a) 5 wt% NaOH and (b) 10 wt% NaOH.

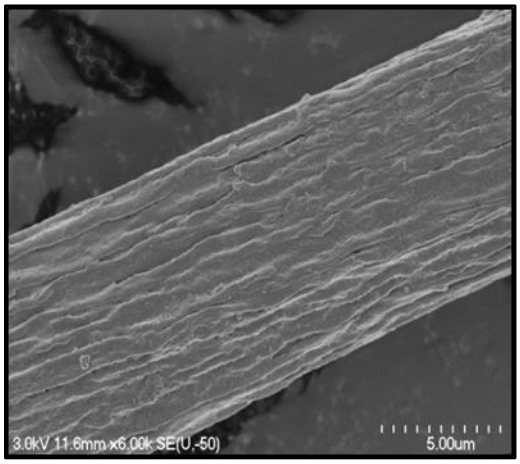

Figure 3.7: Scanning electron micrograph of treated harakeke fibre surface using 5 wt% NaOH/2 wt% Na_2SO_3.

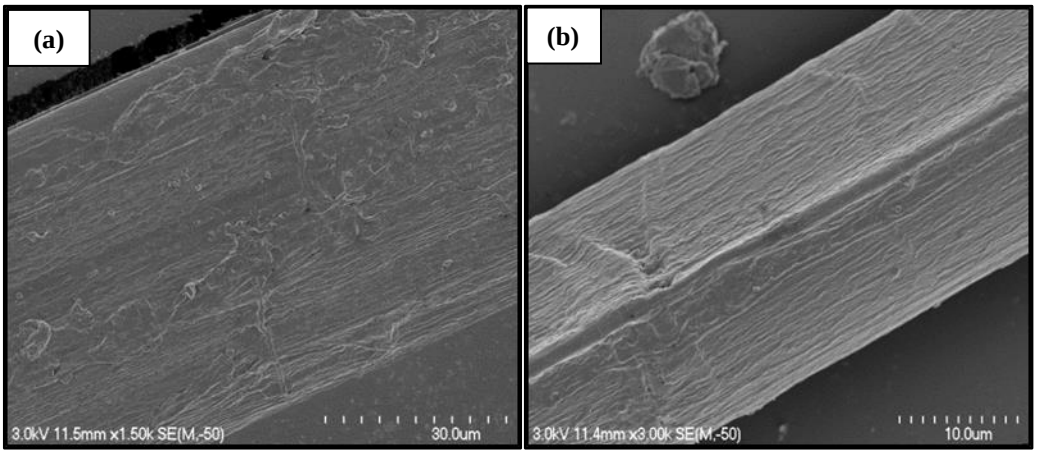

Figure 3.8: Scanning electron micrographs of (a) untreated hemp and (b) 5 wt% NaOH treated fibre surface.

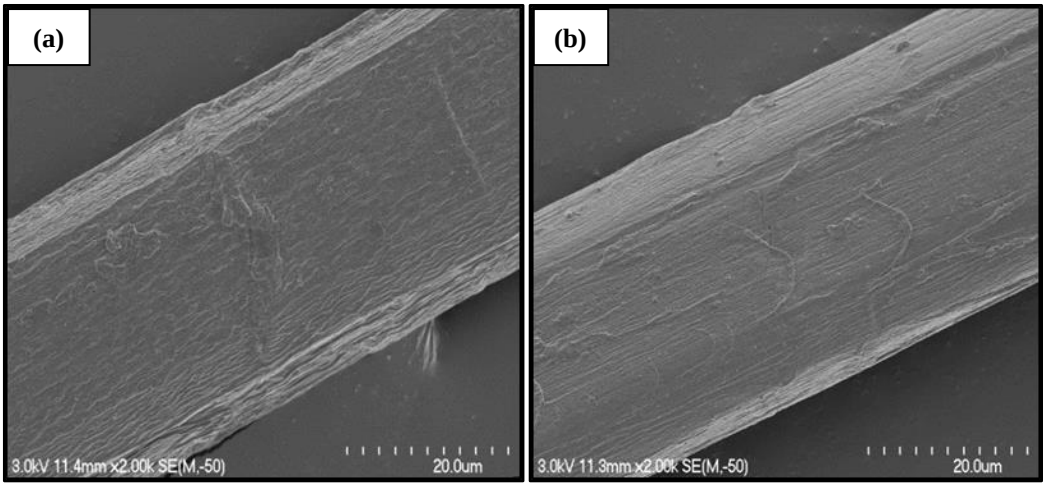

Figure 3.9: Scanning electron micrographs of treated hemp fibre surface using: (a) 10 wt% NaOH and (b) 5 wt% NaOH/2 wt% Na_2SO_3.

3.3.2 Single Fibre Tensile Properties

Alkali treatment of cellulosic fibres using NaOH and Na_2SO_3 is widely used in the pulp and paper industry to separate single fibres from their bundles and as mentioned previously has also been shown to remove non-reinforcing components and can improve the fibre properties, although overtreatment can decrease fibre properties significantly [38, 41, 158, 159]. Ideally alkali treatment should separate fibres, improve fibre dispersion within composites and offer an improvement to the fibre properties [63]. As can be seen in Table 3.2, the harakeke fibres were a lot finer than hemp fibres (as seen in optical micrographs). Alkali treatments resulted in a decrease of fibre diameter for both harakeke and hemp fibres, which can be attributed to the removal of alkali-soluble components from the fibre cell walls. For the treatments using NaOH only, the reduction in diameter for hemp and harakeke fibre was found to correspond to the severity of the treatment used, considered to be simply due to more alkali-soluble components removed from the fibre at higher alkali concentration. The diameter of harakeke reduced by 5.8% and 12.2% and that for hemp reduced by 16.3% and 16.8% when treated using 5 wt% NaOH and 10 wt% NaOH solutions respectively. Treatment using 5 wt% NaOH/2 wt% Na_2SO_3 was found to give maximum reduction in diameter for both fibres. The reductions in fibre diameter for harakeke and hemp treated with this solution were found to be 13.8 and 18.9% respectively. Addition of Na_2SO_3 has been shown elsewhere to assist NaOH in the removal of lignin and shorten treatment times required [36, 160, 161]. These effects are facilitated when sulphite groups (SO_2^{-3}) in the Na_2SO_3 are introduced into the lignin side chains by means of sulphonation, and enable the lignin to be quickly dissolved into the alkaline solution [43, 162]. Although no specific analysis was conducted to measure the

lignin content of treated fibres in this study, it is proven elsewhere that lignin was effectively removed by the application of Na_2SO_3 [158]. It was found that treatment with 10 wt% NaOH removed sufficient hemicellulose and pectin from hemp fibre to give good fibre separation, but similar separation was not obtained with 10 wt% NaOH for harakeke as harakeke contains greater amount of lignin compared to hemp [43]. However, good separation was achieved for harakeke using 2 wt% Na_2SO_3 with 5 wt% NaOH at the higher temperature and longer processing time required to remove a greater amount of lignin.

Table 3.2: Mechanical properties of untreated and alkali treated fibres. Standard deviations are included in parenthesis.

Fibre	Fibre Treatment	Fibre Diameter (μm)	Maximum Tensile Load (N)	Tensile Strength (MPa)	Young's Modulus (GPa)
Harakeke	HR-U	13.03 (1.74)	0.11 (0.05)	804.55 (305. 01)	20.76 (8.61)
	HR-5	12.26 (1.66)	0.08 (0.03)	641.34 (209.57)	20.44 (6.73)
	HR-10	11.44 (1.45)	0.06 (0.02)	540.28 (115.46)	18.68 (5.62)
	HR-5/2	11.23 (1.50)	0.08 (0.02)	782.401(277.18)	21.25 (7.32)
Hemp	HM-U	34.93 (12.90)	0.82 (0.30)	1077.55 (663.18)	20.93 (11.82)
	HM-5	29.22 (6.98)	0.58 (0.22)	911.33 (315.58)	26.44 (13.34)
	HM-10	29.04 (9.93)	0.50 (0.28)	790.16 (349.96)	26.72 (13.97)
	HM-5/2	28.33 (8.34)	0.46 (0.17)	866.06 (458.62)	28.86 (13.28)

From the tabulated results, it can be seen that the maximum tensile load carried by hemp and harakeke fibres decreased with treatment. Correlation of load reduction with diameter reduction was observed except for harakeke at higher treatment levels where the tensile load increased for HR – 5/2 compared to HR – 10. This suggests that the resulting structure, such as cellulose arrangement or non-cellulose distribution could depend on the composition of non-cellulosic

components of the fibres. The largest reductions in tensile load for harakeke and hemp fibres were 49.1% and 43.7% when treated with 10 wt% NaOH and 5 wt% NaOH/2% Na_2SO_3 solutions respectively. Given that only weak materials were meant to have been removed, this suggests that the structural components of the fibres were impaired by this treatment or that bonding between cellulose fibrils is adversely affected [163]. Similar to maximum tensile load, reduction in average tensile strength was observed for all treated harakeke and hemp fibres. Tensile strength of harakeke and hemp fibres reduced dramatically, up to nearly 30% relative to untreated fibres when treated with 10 wt% NaOH solution. The smallest reduction for treated harakeke and hemp fibres were 3 and 15.4% when treated using 5 wt% NaOH/2 wt% Na_2SO_3 and 5 wt% NaOH respectively. However, this reduction was found to be insignificant when the tensile strength data was analysed using a one-tailed Student's t-test and given that fibre separation had occurred, these were considered useful treatments. That different treatment should be required for hemp and harakeke is not surprising given the higher levels of non-cellulosic components removal in harakeke leading to the requirement of a higher concentration of alkali even when conducted at higher temperature and for a longer time.

Also from Table 3.2, Young's modulus can be seen to increase or decrease dependent on the treatment used. The average Young's modulus for treated harakeke fibres reduced by 1.54% and 10.0% when treated with 5 wt% NaOH and 10 wt% NaOH but increased by 2.36% when treated with 5 wt% NaOH/2 wt% Na_2SO_3. Statistical analysis did not support a significant reduction in Young's modulus of treated harakeke fibres when compared with those of the untreated

fibres, although high variability of data was observed considering experimental errors which at some level have influenced the variability in calculated values [159]. Surprisingly for hemp, the Young's modulus for all treated fibres was improved with treatment; treatment using 5 wt% NaOH/2 wt% Na_2SO_3 improved the most, (by 37.9%) and was found significant as suggested by the Student's t-test. The increase in Young's modulus could be due to improvement in cellulose rigidity resulting in removal of non-cellulosic components. Taking into consideration the desire for fibre separation as well as strength, harakeke fibre treated with 5 wt% NaOH/2 wt% Na_2SO_3 was selected along with hemp fibre treated with 5 wt% NaOH for further study.

The tensile strength of fibres was further statistically analysed using the Weibull cumulative distribution through linear regression and applying the estimator in equation 3.2. Weibull analysis is commonly used to describe the strength variation of fibers, which are believed to be caused by randomly distributed fiber flaws and defects. The strength of materials is normally found decreases with an increase in size due to a larger number of flaws in a larger material volume. Weibull characteristic strength and Weibull modulus are tabulated in Table 3.3. It is worthy of note that the two-parameter Weibull distribution approximated the experimental data relatively well, particularly for alkali treated fibres. As expected, Weibull characteristic strength has the same trend as the average tensile strength. Bearing in mind that natural fibres generally possess much larger property variability than commercially produced synthetic fibres in terms mechanical, physical, and chemical properties, low Weibull modulus representing a high variability of fibre strength was expected as is seen here. From Table 3.3, it

can be seen that, Weibull modulus for harakeke fibre varied from 2.43 to 4.88 and from 1.75 to 3.00 for hemp fibre with the lowest Weibull modulus observed in untreated harakeke and hemp fibres. These values follow the trend for fibre diameter and are comparable with those from other authors for cellulosic fibres [38, 152, 164-166]. The lower Weibull moduli values for untreated fibre may be explained by the fact that the untreated fibre is larger in diameter having a bigger volume and therefore is more likely to contain more defects.

Table 3.3: Experimental tensile strength and Weibull parameters of untreated and alkali treated fibres.

Sample	Tensile Strength (MPa)	Characteristic strength, σ_0 (MPa)	Weibull Modulus, w
HR-U	804.56	923.34	2.43
HR-5	641.34	713.37	3.40
HR-10	540.28	588.75	4.88
HR-5/2	782.41	882.71	2.92
HM-U	1077.55	1222.07	1.75
HM-5	911.33	1022.78	3.00
HM-10	790.16	895.32	2.48
HM-5/2	866.06	993.74	1.80

3.3.3 Wide Angle X-ray Diffraction

For most cellulosic fibres, peaks for crystalline phases are normally observed at around 2θ = 15, 17 and 20° (denoted as peaks 1, 2 and 3 respectively as shown in Figure 3.10) which represent the cellulose crystallographic planes (110), ($1\bar{1}0$) and (002). The amorphous phase peak (denoted as peak 4) was assigned according to the current literature [167] at the lowest point between peaks 2 and 3 (for ($1\bar{1}0$) and (002) planes). Generally, it is found in studies that cellulose crystallographic (002) planes are clearly represented, however, the cellulose crystallographic plane

peaks of (110) and (1$\bar{1}$0) are only clearly seen separately when the cellulose content is high [168], but when the fibre contains high amounts of amorphous material, these two peaks overlap and appear as one broad peak [111, 117].

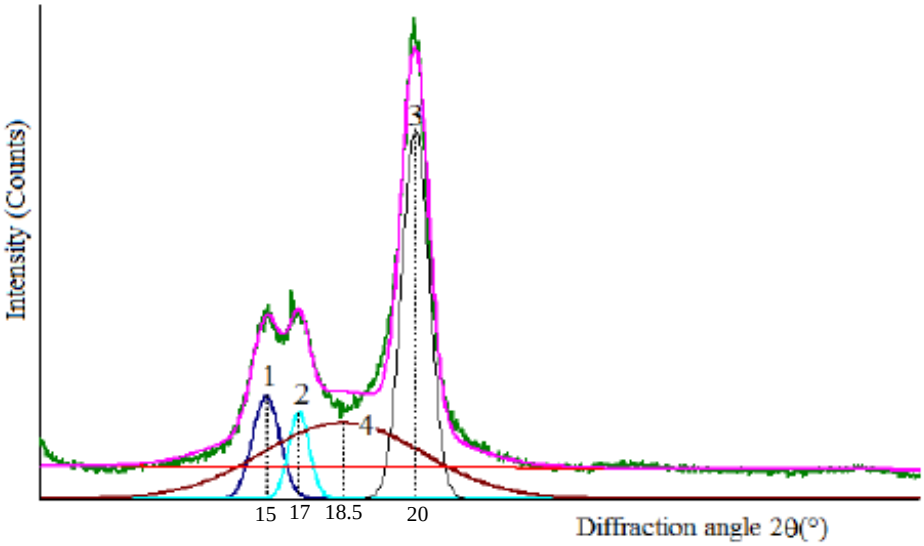

Figure 3.10: Typical diffraction curves of natural fibres used in calculating crystallinity index by the area method [167].

The X-ray diffractograms of untreated, NaOH treated and NaOH/Na_2SO_3 treated harakeke and hemp fibres are shown in Figure 3.11 and Figure 3.12. As expected, major crystalline peaks for harakeke and hemp fibres occurred at 2θ around 22°. It can be seen that intensity of the (002) crystallographic plane peak increased significantly as a result of alkali treatment suggesting removal of amorphous material.

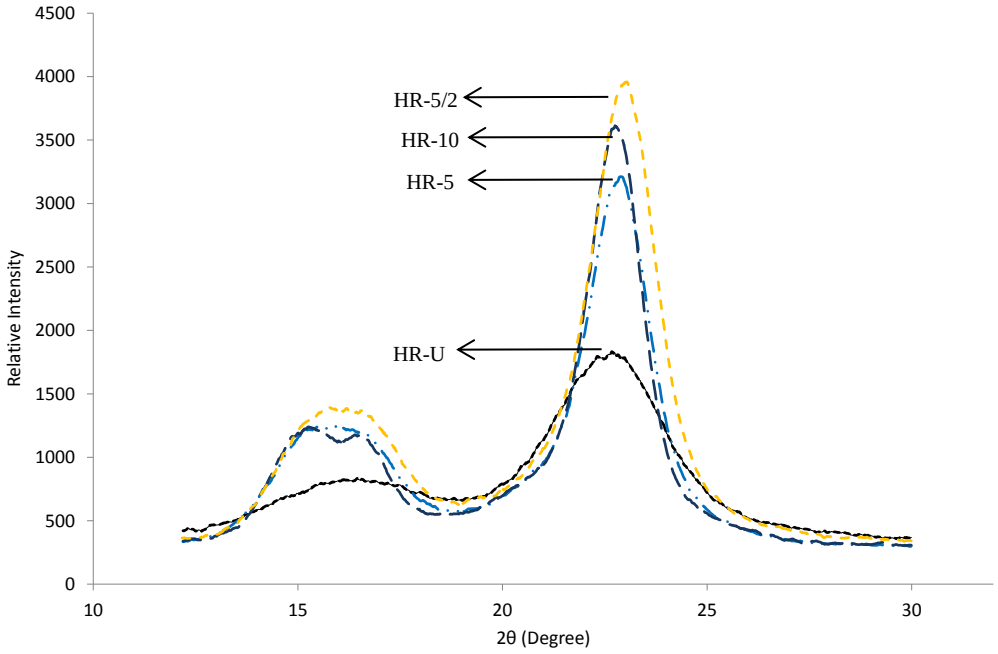

Figure 3.11: X-ray diffraction curves for untreated and treated harakeke fibres.

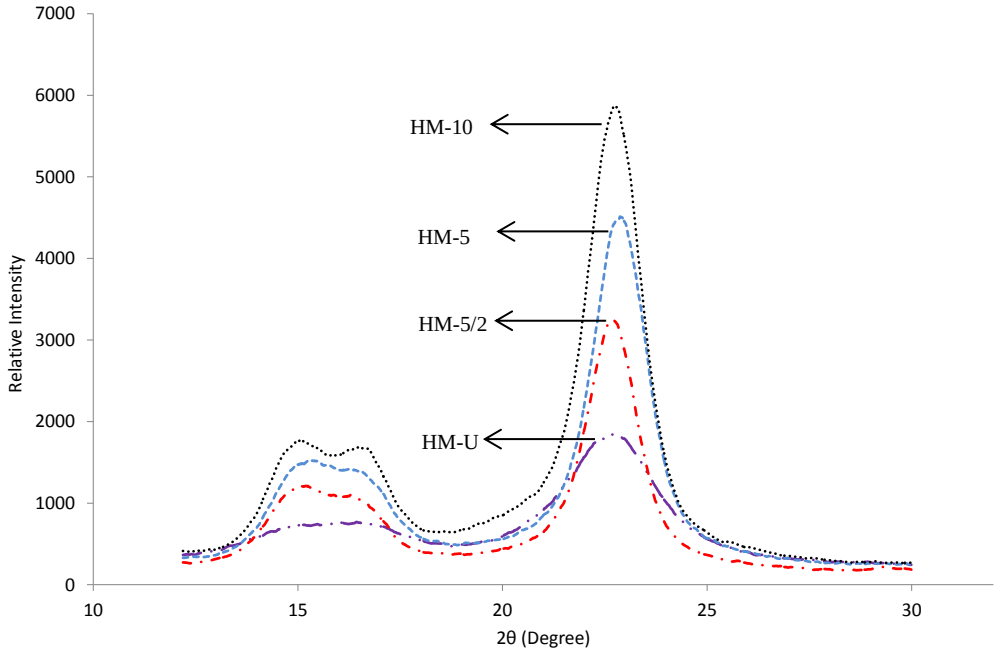

Figure 3.12: X-ray diffraction curves for untreated and treated hemp fibres.

Other peaks were present on the X-ray diffractograms for harakeke and hemp fibre at 2θ around 15 and 17°, which represent the cellulose crystallographic

planes of (110) and ($1\bar{1}0$) respectively. These peaks can be clearly observed individually for all treated hemp fibre but only with treatment using 10 wt% NaOH for harakeke, indicating high crystallinity due to greater removal of non-cellulosic materials. Although the (002) peak is not the highest for harakeke treated with 10 wt% NaOH, it is the peak areas that give most accurate information on crystallinity on which crystallinity index is established. The values of crystallinity index (I_c) for treated and untreated harakeke and hemp fibres are presented in Table 3.4. The values of crystallinity index (I_c) were calculated using Equation 3.4 considering the peaks for the crystalline (peak 3) and the amorphous (peak 4) phases as depicted in Figure 3.10 [167]. It should be noted that the crystallinity index is generally used for comparison rather than to define absolute crystallinity [158]. As can be seen in the presented results, the crystallinity index (I_c) of harakeke and hemp fibres was effectively increased by alkali treatment. The crystallinity index (I_c) of treated fibres was increased up to 20% (using 10 wt% NaOH solution) for harakeke and 15% (using 5 wt% NaOH solution) for hemp with low variation between treated fibres. Such behaviour is expected, as under the applied treatment, amorphous materials (e.g. lignin, hemicellulose and wax) would be removed from the fibres [38, 154]. Increase in fibre crystallinity with alkali treatment has also been suggested to occur due to better packing and stress relaxation of cellulose chains. However, the removal of excessive amounts of amorphous materials can possibly reduce the tensile strength by loss of adhesion between cellulose microfibrils [64].

Table 3.4: Crystallinity index (I_c) of untreated and alkali treated harakeke and hemp fibres

Fibre Treatments	I_{am} ($18° \leq 2\theta \leq 19°$)	I_{002} ($22° \leq 2\theta \leq 23°$)	Crystallinity Index (%)
HR-U	603.0	1912.0	68.5
HR-5	543.0	3285.0	83.5
HR-10	504.0	3691.0	86.3
HR-5/2	608.0	4061.0	85.0
HM-U	445.0	1913.0	76.7
HM-5	438.0	4586.0	90.4
HM-10	610.0	6076.0	90.0
HM-5/2	343.0	3331.0	89.7

3.3.4 Thermal Analysis

The TGA and DTA thermograms for harakeke and hemp fibres are shown in Figure 3.13 and 3.14 respectively.

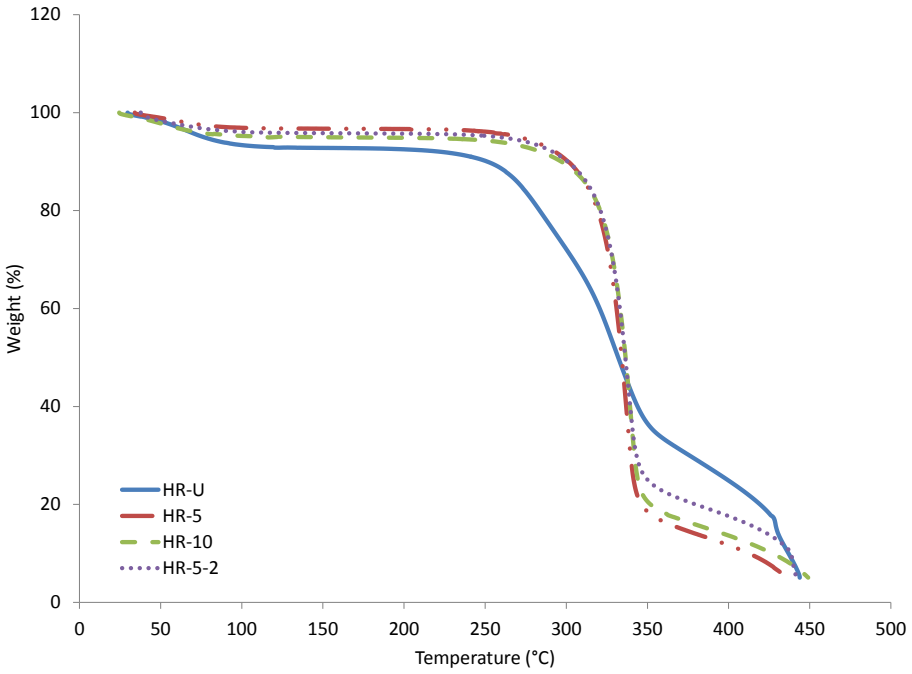

Figure 3.13: (a) TGA thermograms for untreated and treated harakeke fibres

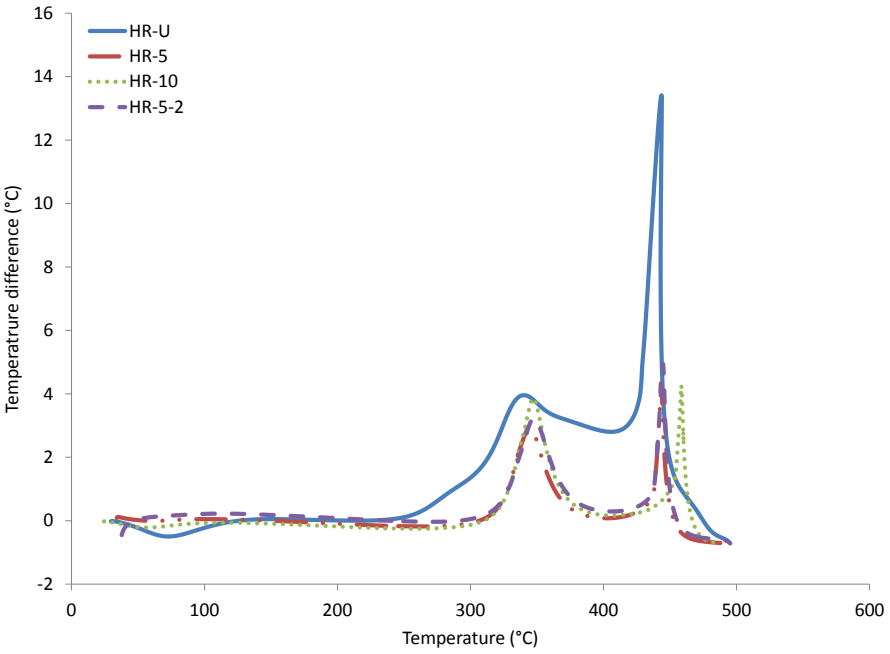

Figure 3.13: (b) DTA thermograms for untreated and treated harakeke fibres

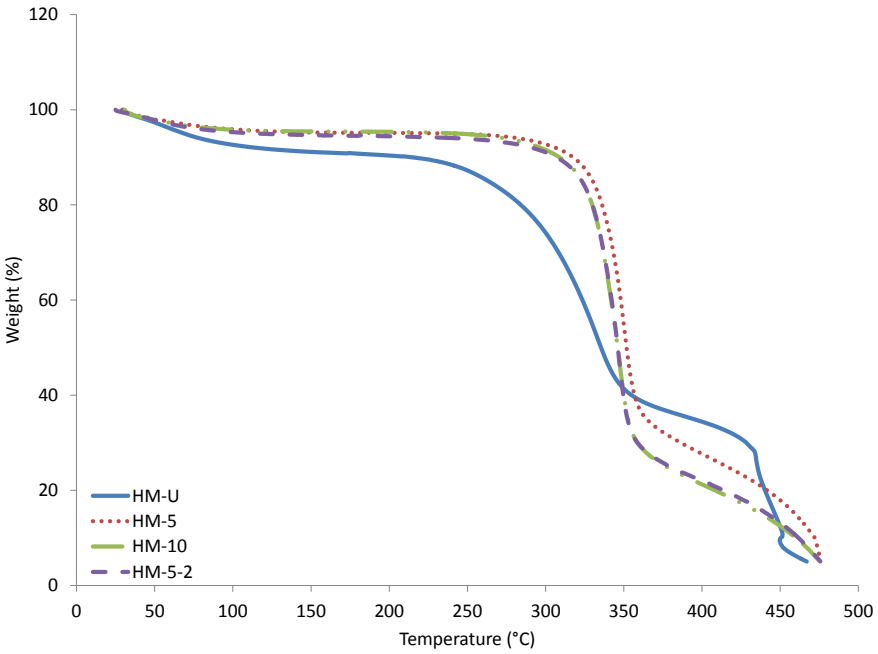

Figure 3.14: (a) TGA thermograms for untreated and treated hemp fibres

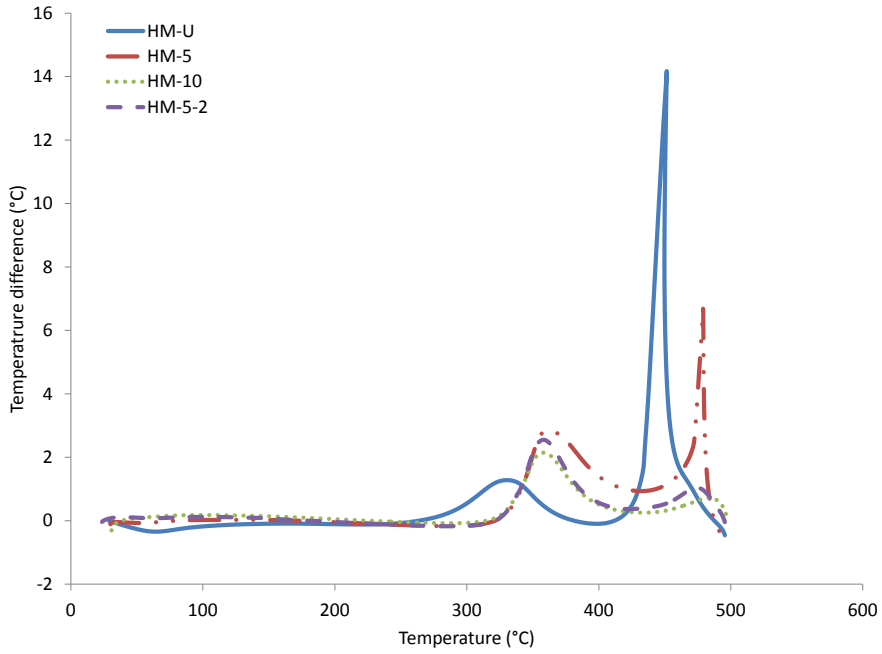

Figure 3.14: (b) DTA thermograms for untreated and treated hemp fibres

The thermal degradation of harakeke and hemp fibre can be identified by reduction in sample weight in TGA themograms and a temperature difference in DTA thermograms. This was evidenced as starting at around 70 °C for harakeke and hemp fibre when it is believed there is evolution of adsorbed moisture from the fibres. The fibre weight was then maintained until a reduction at around 250 °C for untreated fibre and around 300 °C for treated fibre, which has been associated with the initial thermal depolymerisation traces of hemicellulose and pectin followed by cellulose [109]. This stage was completed when the temperature reached around 345 °C for harakeke and 355 °C for hemp when the fibres had lost almost 60% for untreated and 80% for treated fibre of their initial weight. The final stage of thermal degradation occurred at temperatures between 400 to 450 °C when the fibres had lost almost 95% of their initial weight leaving behind ash and unburnt minerals [147, 158]. The weight loss of untreated and treated fibres at different stages of thermal degradation is presented in Table 3.5.

It can be seen that the degradation temperatures at different stages of thermal degradation for treated fibres were consistently higher than for untreated fibres indicating the heat resistance of fibre was effectively improved by alkali treatment [169]. DTA thermograms (Figure 3.13(b) and 3.14(b)) support the different stages of moisture loss and decomposition at the same temperatures as those evaluated by weight lost. Two main peaks were observed for all hemp and harakeke fibres. The first peak represents the multiple exothermic degradation reactions of cellulose, hemicellulose, lignin and other non-cellulosic materials and the second narrower peak represents the single exothermic degradation reaction of cellulose. Narrower peaks can clearly be observed for treated fibre, representing a more homogeneous cellulose content than for untreated fibre [170].

Table 3.5: Summary of TGA results for untreated and treated harakeke and hemp fibres.

Fibre Treatments	T_{10}/°C	T_{50}/°C	T_{90}/°C
HR-U	251	330	437
HR-5	301	334	412
HR-10	296	336	427
HR-5/2	300	336	438
HM-U	214	335	450
HM-5	317	351	472
HM-10	309	346	460
HM-5/2	321	347	478

T_{10}/°C, T_{50}/°C and T_{90}/°C means temperature at 10, 50 and 90% weight loss.

3.4 Chapter Conclusions

In this chapter, series of alkali treatments have been developed and conducted in order to improve the properties of harakeke and hemp fibres to further be used as

reinforcement in PLA composite. Experimentally, as compared to hemp fibre, harakeke fibre was found to be 25% weaker in its untreated state and required a harsher treatment to bring about fibre separation, which is believed to be due to the higher quantity of lignin in its composition. However, with a strength of 782 MPa it would generally be expected to provide significant reinforcement in most common polymer matrices. Treatment with NaOH and Na_2SO_3 was found to improve separation and remove surface constituents for harakeke as well as hemp fibre. As a consequence of constituent removal, fibre diameter, maximum tensile load and tensile strength were found to decrease in most cases. However, it was found that the tensile strength of hemp fibre treated with 5 wt%NaOH and harakeke fibre treated with 5 wt%NaOH/2 wt% Na_2SO_3 was not significantly affected as confirmed by a Student's t-test, although the average tensile strength suggests a slight reduction. It was also found that the crystallinity index (I_c) for all treated fibres increased significantly compared to untreated fibres. Furthermore, the application of alkali treatment was also found to lead to better thermal stability resulting in more homogeneous cellulose content as indicated with narrower peaks in DTA thermograms.

CHAPTER 4

Performance of Aligned Discontinuous Harakeke and Hemp Fibre Mat Reinforced PLA

4.1 Introduction

This chapter describes work carried out to fabricate and assess the structure and mechanical performance of PLA reinforced by aligned discontinuous natural fibre mats; harakeke and hemp fibres each treated with its optimum treatment developed in the previous chapter were used. The novel aspect of this work was in terms of composite processing, including the use of fibre mats produced using a dynamic sheet former (DSF) wherein discontinuous treated fibres were aligned. Details of materials used, the methods and the results of analysis are included in this chapter.

4.2 Experimental Methodology

4.2.1 Materials

Harakeke fibre treated with 5 wt% sodium hydroxide (NaOH) and 2 wt% sodium sulphite (Na_2SO_3) and hemp fibre treated with 5 wt% sodium hydroxide (NaOH) were used to produce fibre mats. The maximum length for both fibres was approximately 8 mm (cut using a granulator with 8 mm sieve size). NatureWorks® 3052D injection moulding grade PLA (polylactide) polymer with

a density of 1250 kg/m^{3}from Nature Works LLC, USA was used as a thermoplastic matrix.

4.2.2 Methods

4.2.2.1 PLA Sheet Production

The manufacture of PLA and composite samples in this work involved converting PLA granules into PLA sheets. PLA granules were used as purchased and extruded into sheets of about 0.5 to 0.6 mm thick using an extruder (Thermo-Prism TSE-16-TC) equipped with a coat hanger die. The extruder consists of 6 heating elements, for which the temperatures were set at 145 °C (barrel entrance), 165 °C, 180 °C, 180 °C, 170 °C (barrel exit) and 170 °C (die). The twin co-rotating screws were operated at 100 revolutions per minute (rpm). PLA sheets were cut to dimension of 150 mm x 90 mm to enable them to fit in a compression mould, with an approximate weight of 8 to 10 g each and kept in a sealed polyethylene bag.

4.2.2.2 Fibre Mat Production

Aligned fibre mats were produced using a Canpa automatic dynamic sheet former (DSF) as shown in Figure 4.1. In this study, fibre mats weighing 130 to 140 g/m^2 were produced using approximately 45 g alkali treated discontinuous harakeke or hemp fibre. Firstly, fibre was dispersed in water (approximately 10 litres of water was used to disperse 10 g of fibre) in a mixing drum fitted with a disintegrator. The disintegrator was set to rotate 90 degrees horizontally to ensure the fibres were fully suspended in water during fibre mats production. Mats were then produced by spraying a controlled quantity of this low concentration suspension

inside a spinning drum containing a porous medium to retain the fibre using a controlled pump and drum spinning speed.

Figure 4.1: Dynamic sheet former (DSF) used to produce aligned discontinuous fibre mats.

The fibre mats were finally rinsed and compacted by allowing the drum to spin for a further 2 to 3 minutes. They were then dried in an oven at 80 °C for 24 hours to ensure the moisture content less than 5% before being cut to size (150 mm x 90 mm) to enable them to fit in a compression mould. Samples of dried harakeke and hemp fibre mats are shown in Figure 4.2.

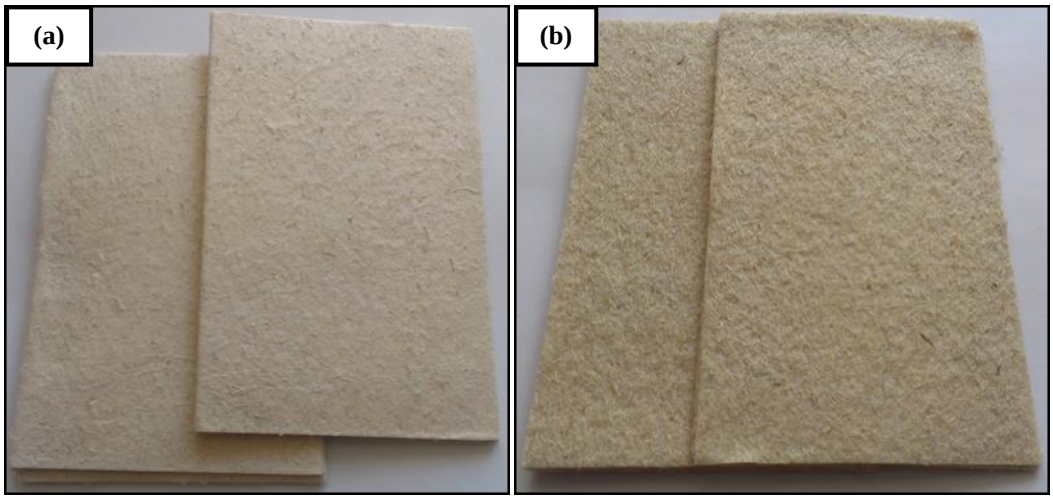

Figure 4.2: Fibre mats produced using DSF: (a) harakeke and (b) hemp.

Randomly oriented fibre mats were produced by mixing fibres in water in a large container. The water containing the suspended fibres was allowed to slowly drain out of the container and the fibres were deposited on a strainer at the bottom of the container. Randomly oriented fibre mats were finally left to dry in the oven at 80 °C for at least 12 hours before use.

4.2.2.3 PLA Sample Production

Figure 4.3 shows the aluminium mould used to mould PLA and composite samples. The mould consists of a base-plate onto which a central frame with internal dimensions of 150 mm x 90 mm was attached by screws to set the moulded plate width and length, as well as a T-shaped top section that could be inserted into the central frame, such that its flanges would rest on it to provide a gap of approximately 2.5 mm to determine the moulded material thickness. Small grooves were located at the bottom edges of the shorter sides of the central frame (as can be seen in Figure 4.3(c)) to allow trapped air within the melt and the excess PLA to be squeezed out from the mould. PLA sheets were inserted in the mould in between Teflon sheets (see Figure 4.3(d)) to give about 5-10% excess in

weight relative to the calculated final weight of the moulded material. This was to ensure that the polymer melt flowed under some pressure and took the shape of the mould with minimum air bubbles.

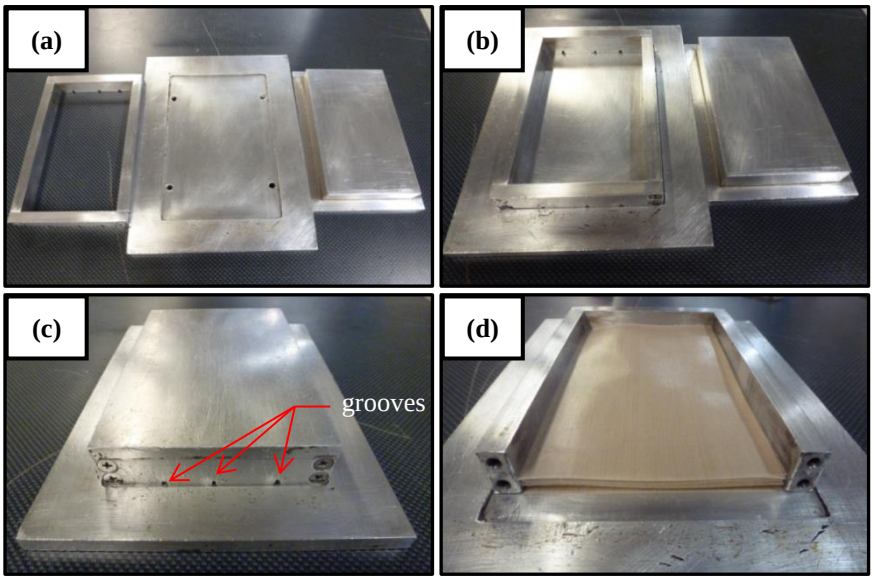

Figure 4.3: An aluminium mould showing: (a) separated mould parts; from left: middle, bottom and top sections, (b) middle section was screwed to bottom section, (c) aluminium mould in closed position showing grooves for venting and (d) aluminium mould filled with PLA sheets.

PLA sheets were first preheated in the mould with no pressure at a temperature of 170 °C for 10 minutes. They were then compressed at 170 °C and 3 MPa pressure for 3 minutes. The mould was finally removed from the hot press and allowed to cool down to room temperature, with a low pressure applied by placing a steel block (10 kg) on the top of the mould, before the moulded PLA was removed and stored in a sealed polyethylene bag.

4.2.2.4 Fabrication of Composite Material

Fibre mats and PLA sheets were dried overnight at 105 °C (to ensure the moisture for fibre mats less than 5%) and 60 °C respectively. They were weighed and

arranged in a stack (in between Teflon sheets to prevent sticking to mould) with relative numbers of each based on the required fibre weight percentage following the arrangement as tabulated in Table 4.1 before inserting into the mould.

Table 4.1: Arrangement of fibre mats and PLA sheets in mould

Approximate fibre wt%	Number of fibre mats	Number of PLA sheets	Fibre mat (s) and PLA sheets (s) arrangement *
0	-	4	4PLA
5	1	4	2PLA/1MAT/2PLA
10	2	4	1PLA/1MAT/2PLA/1MAT/1PLA
15	3	4	1PLA/1MAT/1PLA/1MAT/1PLA/1MAT/1PLA
20	4	3	1PLA/2MAT/1PLA/2MAT/1PLA
25	5	3	1PLA/3MAT/1PLA/2MAT/1PLA
30	6	3	1PLA/3MAT/1PLA/3MAT/1PLA
35	7	3	1PLA/4MAT/1PLA/3MAT/1PLA
40	8	3	1PLA/4MAT/1PLA/4MAT/1PLA

*arrangement of PLA sheet and fibre mat from bottom to top of the stack; number represents the number of layer(s) used, PLA = PLA sheet and MAT = Fibre mat

Stacks were heated and pressed in a hot press as for PLA samples (at 170°C and pressed for 3 minutes at 3 MPa). Since fibre mat was easily distorted, consolidating PLA with fibre mats needed to be carefully conducted. It was ensured that PLA sheets were fully melted before slowly applying pressure; applying pressure onto insufficiently melted PLA sheets with viscosity that was too high distorted the fibre mats, which was assumed would reduce composite strength. Air bubbles and excess PLA melt were squeezed out of the mould (through the grooves) as for PLA-only moulding. After hot pressing, the moulded composite materials were removed from the press and allowed to cool down (with a weight on top to apply pressure as for moulded PLA) to room temperature. Composite samples were then weighed to determine the final fibre weight

percentage (from knowing the weight of fibre placed in mould) and stored in a sealed polyethylene bag. Examples of moulded composites are shown in Figure 4.4. It should be noted that, it was difficult to make smooth, rectangular uniform shape composites when the fibre content was higher than 30 wt%.

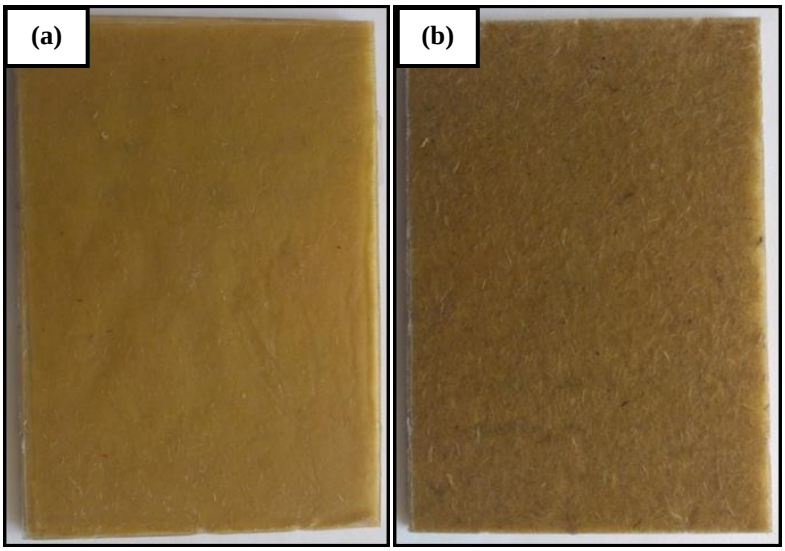

Figure 4.4: Fabricated composites produced by compression moulding: (a) harakeke and (b) hemp composites with 20%wt fibre.

4.2.2.5 Tensile Testing of PLA and Composites

In this work, all samples were cut into specimens of approximately 150 mm x 15 mm and their edges were ground to give a smooth and uniform section. Prior to tensile testing, all specimens were placed in a conditioning chamber at 23 °C ± 3 °C and 50% ± 5% relative humidity for at least 48 hours. Tensile testing followed the procedures detailed in ASTM D 638-03; Standard Test Method for Tensile Properties of Plastics. It consists of gripping a tensile test specimen in the jaws of an Instron-4204 tensile testing machine fitted with a 5 kN load cell; in order to prevent slippage and premature failure occurring near the grips, the specimen ends were cushioned with abrasive paper. The gauge length of the specimens was 90

mm. An Instron 2630-112 extensometer (50 mm) was attached to the central part of the test specimen to measure the specimen extension. The specimens were tested at a constant rate of 2 mm/min. Details and abbreviations of tensile tested specimens used are tabulated in Table 4.2. Stress versus strain graphs were obtained from which the ultimate tensile strength and Young's modulus could be determined; Young's modulus was obtained using the tangent to the initial linear portion of the stress–strain curve.

Table 4.2: Details and abbreviations of tensile tested composite samples

Sample		Layer (s) of fibre mat	Approximate Fibre wt%	PLA wt%	Load direction*
PLA		-	-	100	-
HARAKEKE	**HEMP**				
HR-5	**HM-5**	1	5	95	Parallel
HR-10	**HM-10**	2	10	90	Parallel
HR-15	**HM-15**	3	15	85	Parallel
P-HR-15	**P-HM-15**	3	15	85	Perpendicular
HR-20	**HM-20**	4	20	80	Parallel
HR-25	**HM-25**	5	25	75	Parallel
HR-30	**HM-30**	6	30	70	Parallel
HR-35	**HM-35**	7	35	65	Parallel
HR-40	**HM-40**	8	40	60	Parallel

Note:
* Parallel and perpendicular relative to DSF rotation direction, HR = Harakeke and HM = Hemp.

4.2.2.6 Preparation for Assesment of Fibre Mat and Composite Morphology

Light Microscopy

Transverse and longitudinal sections of composite samples were obtained for examination. Silicon moulds were initially wiped with a release agent to facilitate

specimen removal and epoxy resin was poured into the mould followed by placement of composite sections. Specimens were demoulded after 24 hours of curing at room temperature and ground and polished using a series of coarse and fine abrasive papers starting from 320 followed by 500, 1000, 2000 and 4000 grit for approximately three to five minutes for each step. Embedded composite specimens are shown in Figure 4.5. Optical images of fibre mats and composite sections were taken using an Olympus BX60F5 optical light microscope.

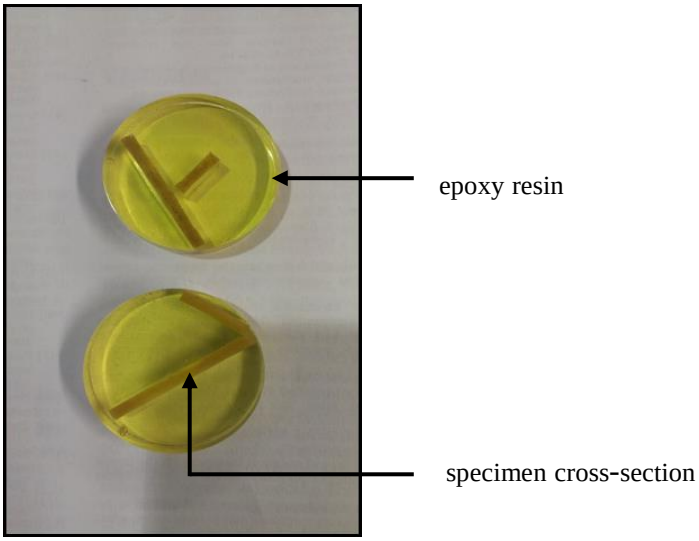

Figure 4.5: Composite cross-sections embedded in epoxy resin.

Scanning Electron Microscopy (SEM)

SEM was used to observe surface morphology and fracture surfaces of tested specimens. The observations were conducted using a Hitachi S-4100 field emission scanning electron microscope operated at 5 kV. Similar to the preparation for single fibres (section 3.2.2.2), samples were placed on aluminium stubs using double-sided adhesive tape and sputter coated with platinum and palladium to make them conductive.

4.2.2.7 Modelling of Composite Tensile Properties

Micromechanical models have been shown to be a useful method for predicting strength and Young's modulus of continuous and discontinuous fibre composites. Commonly, the basic Rule of Mixtures is used to predict strength and Young's modulus of composites reinforced with unidirectional continuous fibre in parallel and perpendicular to the loading direction. However, strength and Young's modulus prediction is more complex for discontinuous fibre composites that commonly have fibre with varying length and orientation. In this chapter, the main prediction models are presented, starting with the basic Rule of Mixtures followed by models developed to predict discontinuous fibre composites including, the Bowyer-Bader model which was used to determine fibre orientation factor (K_o) and interfacial shear strength (τ) by applying composite strength and fibre length distribution.

Rule of Mixtures Models (Parallel and Series)

The Parallel and Series Rule of Mixtures models are the most commonly applied models to represent the upper and lower bounds for strength and Young's modulus of unidirectional continuous fibre composites [171]. It is assumed that reinforcing fibres have perfect interfacial bonding with the matrix and iso-strain conditions exist for fibre and matrix. According to these models, strength and Young's modulus are calculated using the following equations:

Parallel model (parallel to fibre direction):

$$\sigma_c = \sigma_f V_f + \sigma_m V_m \tag{4.1}$$

$$E_c = E_f V_f + E_m V_m \tag{4.2}$$

Series model (90° to fibre direction):

$$\sigma_c = \frac{\sigma_m \sigma_f}{\sigma_m V_f + \sigma_f V_m} \tag{4.3}$$

$$E_c = \frac{E_m E_f}{E_m V_f + E_f V_m} \tag{4.4}$$

where σ, E and V are strength, Young's modulus and volume fraction respectively. The subscripts c, m and f represent composite, matrix and fibre, respectively. Since the composites in this work were designed according to weight fractions and the above equations rely on fibre volume fraction, in order to be able to use them, the fibre and matrix volume fractions (V_f and V_m) needed to be calculated from the fibre weight fraction (W_f) using the following equations:

$$V_f = \left(1 + \frac{\rho_f}{\rho_m}\frac{(1 - W_f)}{W_f}\right)^{-1} \tag{4.5a}$$

$$V_m = 1 - V_f \tag{4.5b}$$

such that ρ_f and ρ_m are density of fibre and matrix respectively [172]. It should be realised that there is the possibility that the actual matrix density may vary due to the presence of the fibres for a number of reasons (e.g. nucleation of matrix crystallinity at fibre surfaces or effects due to dissolution and reaction with sizing where this is present) which therefore results in a slight variation in calculated fibre volume fraction compared to the actual fibre volume fraction [173].

Hirsch's Model

Hirsch's model is based on a combination of the Parallel and Series models and can be applied to discontinuous and variably oriented fibre composites. It is fitted empirically to experimental data by means of a fitting parameter, x (between zero

to one) as seen in Equations 4.6 and 4.7, which can be considered to represent the stress transfer efficiency between fibre and matrix taking into account the fibre orientation, fibre length and stress amplification at fibre ends [174].

$$\sigma_c = x\left(\sigma_m V_m + \sigma_f V_f\right) + (1 - x)\frac{\sigma_f \sigma_m}{\sigma_m V_f + \sigma_f V_m} \tag{4.6}$$

$$E_c = x\left(E_m V_m + E_f V_f\right) + (1 - x)\frac{E_f E_m}{E_m V_f + E_f V_m} \tag{4.7}$$

This model has been found to give a good fit with actual composite strengths and Young's moduli [175].

Halpin-Tsai Model

The Halpin and Tsai model is a semi-empirical model that can be applied to tensile strength and Young's modulus of discontinuous fibre reinforced composites aligned in either the longitudinal or transverse direction as follows [176, 177]:

$$\sigma_c = \sigma_m\left(\frac{1 + \zeta\eta V_f}{1 - \eta V_f}\right) \tag{4.8}$$

$$E_c = E_m\left(\frac{1 + \zeta\eta^* V_f}{1 - \eta^* V_f}\right) \tag{4.9}$$

where η and η^* are given by:

$$\eta = \frac{\frac{\sigma_f}{\sigma_m} - 1}{\frac{\sigma_f}{\sigma_m} + \zeta} \tag{4.10a}$$

$$\eta^* = \frac{\frac{E_f}{E_m} - 1}{\frac{E_f}{E_m} + \zeta} \tag{4.10b}$$

and ζ is a shape fitting parameter to fit the Halpin–Tsai model to experimental data depending on fibre geometry and loading direction (longitudinal or transverse to fibre direction). ζ for circular-sectioned fibre is commonly given by:

$$\zeta = \frac{2l}{d} \tag{4.10c}$$

where l is the length of the fibre in the direction of the load, d is the diameter of the fibre (such that ζ can be taken as 2 for transverse tensile properties) [178-181].

The Halpin-Tsai model was further modified by Nielsen [182] taking into consideration a factor to account fibre arrangement as well as fibre content, ψ to enable a better prediction as given by the following equations:

$$\sigma_c = \sigma_m \left(\frac{1 + \zeta \eta V_f}{1 - \eta \psi V_f} \right) \tag{4.11}$$

$$E_c = E_m \left(\frac{1 + \zeta \eta^* V_f}{1 - \eta^* \psi V_f} \right) \tag{4.12}$$

and

$$\psi = 1 + \left(\frac{1 - \text{ø}_{max}}{\text{ø}_{max}^2} \right) V_f \tag{4.13}$$

where ø_{max} is the maximum fibre packing fraction for the relevant fibre arrangement and has a value 0.785 for a square arrangement of fibres, 0.907 for a hexagonal array of fibres and 0.82 for random packing of fibres [174].

Cox Model

Cox's model is amongst the earliest models used to predict the strength and Young's modulus of composites reinforced with aligned discontinuous fibres. It assumes that the interface between fibres and matrix is perfect, with both fibre and

matrix perfectly elastic and isotropic. This model is developed based on shear-lag theory which considers stress transfer into discontinuous fibre occurring by shear stress at the fibre/matrix interface when the fibre of length, *l* embedded in a matrix subjected to a strain in fibre direction [183]. The characteristic tensile and shear stress distributions along the fibre in the matrix derived from the Cox model are represented by Figure 4.6.

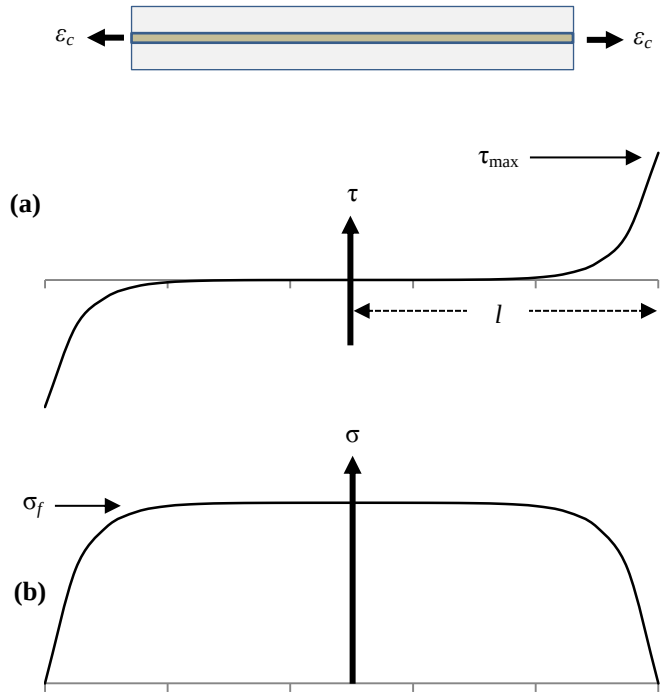

Figure 4.6: Fibre-matrix interfacial stress distribution along the fibre having different aspect ratio embedded in matrix for elastic stress transfer derived in Cox's model: (a) shear and (b) tensile.

As can be seen in the figure, shear stress is a maximum at the fibre ends and, decreases to zero at the centre which leads to a tensile stress profile within the fibre of zero at the fibre ends, increasing towards the middle of the fibre, limited by the breaking stress of the fibre [171, 178, 184, 185]. If the fibre is long enough, as the strain in the composite increases, eventually, the maximum stress at the centre of the fibre will reach the tensile strength of the fibre and fibre failure will

occur. However, for shorter fibre, fibre failure does not occur. In this instance, debonding would be expected, which will lead to pull-out during composite failure. According to this model, strength and Young's modulus of a composite can be predicted similarly to the Rule of mixtures by including a factor to account for the effectiveness of load transfer from matrix to fibre giving:

$$\sigma_c = \sigma_f V_f \left(1 - \frac{tanh\left(\frac{\beta l}{2}\right)}{\frac{\beta l}{2}} \right) + \sigma_m V_m \tag{4.14}$$

$$E_c = E_f V_f \left(1 - \frac{tanh\left(\frac{\beta l}{2}\right)}{\frac{\beta l}{2}} \right) + E_m V_m \tag{4.15}$$

where

$$\beta = \left(\frac{2\pi G_m}{E_f A_f ln\left(\frac{R}{r}\right)} \right)^{\frac{1}{2}} \tag{4.16a}$$

where r is radius of the fibre, G_m is the shear modulus of matrix, l is length of fibre and A_f is the area of the fibre and R is centre to centre distance of the fibres [186].

For hexagonally packed fibres,

$$R = \left(\frac{2\pi r^2}{\sqrt{3} V_f} \right)^{\frac{1}{2}} \tag{4.16b}$$

and for square packed fibres,

$$R = r \left(\frac{\pi}{4 V_f} \right)^{\frac{1}{2}} \tag{4.16c}$$

If ($\beta l/2$) is large, the value of reinforcement effectiveness reduction factor approaches unity, but if ($\beta l/2$) *is* small, it tends to zero [187].

Cox's model was further extended by Krenchel [188] to take into account fibre orientation by adding a fibre orientation factor, K_o into the basic Cox model giving:

$$\sigma_c = \sigma_f V_f K_{\emptyset} \left(1 - \frac{tanh\left(\frac{\beta l}{2}\right)}{\frac{\beta l}{2}} \right) + \sigma_m V_m \tag{4.17}$$

$$E_c = E_f V_f K_{\emptyset} \left(1 - \frac{tanh\left(\frac{\beta l}{2}\right)}{\frac{\beta l}{2}} \right) + E_m V_m \tag{4.18}$$

K_o has a value of unity for axially aligned fibre composites, 0.375 for planar random configuration and 0.2 for a three dimensional randomly oriented fibre composites [184, 189, 190].

Kelly - Tyson Model

The Rule of Mixtures model for fibres parallel to loading direction was modified using a different approach by Kelly and Tyson to predict the strength and Young's modulus of axially aligned discontinuous fibre composites [171]. It is derived based on stress distribution along the fibre embedded in an elastic-plastic matrix. The applied load is assumed to be transferred to the fibres by means of shear forces at the fibre-matrix interface as described for the Cox model, but the stress increases linearly with distance from the fibre ends up to yield stress, at which the shear stress at the interface is assumed to be constant until the strain in the fibre is equal to that in the matrix of which the fibre stress levels out and the shear stress

at the interface is zero (Figure 4.7) [183]. In this model, an average fibre length relative to a fibre length termed the critical fibre length is considered. The critical fibre length (L_c) is defined as the minimum length at which the stress in the fibre can reach the tensile strength (σ_f). It can be determined experimentally and/or using micromechanics such as through a model proposed by Bowyer-Bader (described in detail in next section) [191, 192]. The most common techniques used are the fibre fragmentation test [64] or a pull-out test [116] such that the critical fibre length can be determined using the following equation:

$$L_c = \frac{\sigma_f D}{2\tau} \tag{4.19}$$

where, D is the mean fibre diameter and τ is the interfacial shear strength. It is obvious that the improvement of interfacial shear strength results in lower critical fibre lengths. For a fibre having length equal to L_c, the ultimate fibre tensile stress is only achieved at the centre of the fibre (see Figure 4.7). As fibre length increases to $L > L_c$, the fibre reinforcement becomes more effective and the ultimate tensile stress could be achieved within the fibre over a greater length. Fibre lengths less than the critical fibre length L_c, cannot be broken and will eventually debond and be pulled out of the matrix. The average stress of supercritical length fibre ($L > L_c$) is given by the area under the curve in Figure 4.7(a) divided by the fibre length and the average stress of critical and subcritical length fibre ($L \leq L_c$) is given by the area under the curve in Figure 4.7(b and c) divided by the fibre length.

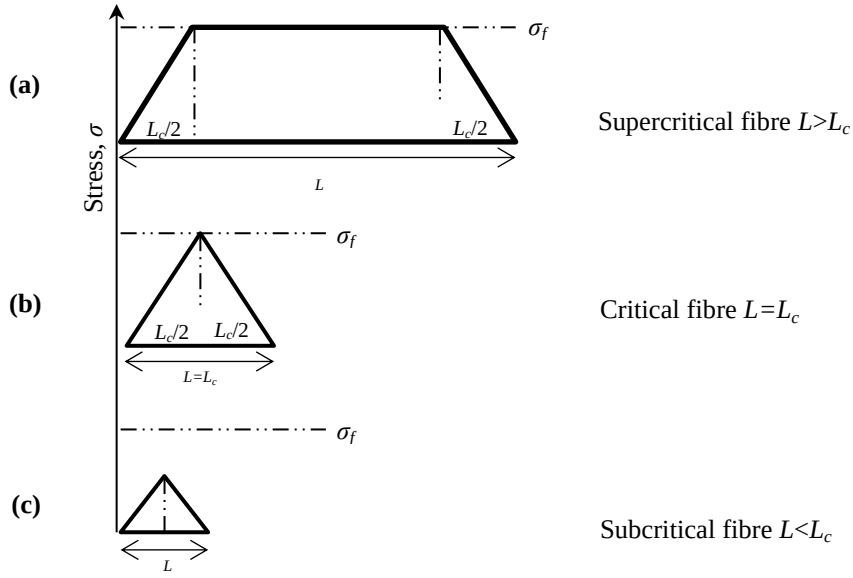

Figure 4.7: Schematic illustration indicating tensile stress distribution along the fibre having: (a) supercritical, (b) critical and (c) subcritical length embedded in elastic-perfectly plastic matrix.

According to this model, the strength and Young's modulus of a composite depends on a fibre stress transfer factor, denoted as K_{st} which determines the stress transfer efficiency from matrix to fibres; dependent on whether the average fibre length (L) is longer than L_c or shorter than L_c such that:

$$\sigma_c = \sigma_f V_f K_{st} + \sigma_m V_m \tag{4.20}$$

$$E_c = E_f V_f K_{st} + E_m V_m \tag{4.21}$$

with K_{st} determined using the following equations:

$$K_{st} = \frac{L}{2L_c} \qquad \text{for } L < L_c \tag{4.22a}$$

or

$$K_{st} = 1 - \frac{L_c}{2L} \qquad \text{for } L > L_c \tag{4.22b}$$

Therefore, the tensile strength and Young's modulus of composites containing fibre shorter than L_c is thus given by:

$$\sigma_c = \sigma_f V_f \left(\frac{L}{2L_c}\right) + \sigma_m V_m \tag{4.23}$$

$$E_c = \sigma_f V_f \left(\frac{L}{2L_c}\right) + E_m V_m \tag{4.24}$$

and the tensile strength and Young's modulus of composite containing fibre longer than L_c is given by:

$$\sigma_c = \sigma_f V_f \left(1 - \frac{L_c}{2L}\right) + \sigma_m V_m \tag{4.25}$$

$$E_c = \sigma_f V_f \left(1 - \frac{L_c}{2L}\right) + E_m V_m \tag{4.26}$$

The Kelly-Tyson model has been further modified to account a different the fibre orientation [173, 193, 194]. The fibre orientation factor (K_o) was fitted to the model giving the following which is commonly called the Modified Rule of Mixtures (MROM):

$$\sigma_c = \sigma_f V_f K_{st} K_\Theta + \sigma_m V_m \tag{4.27}$$

$$E_c = E_f V_f K_{st} K_\Theta + E_m V_m \tag{4.28}$$

The common values for K_o for respective fibre direction are as given in Cox model.

Bowyer - Bader Model

Bowyer and Bader model predicts the tensile strength of discontinuous fibre composites of varying fibre alignment by considering the sum of the contributions of different fibre lengths, as well as that of the matrix [191, 192]. It should be noted that, in the Bowyer-Bader, the following assumptions are used [172]:

- stress transfer across the interface increases linearly along the fibre from its ends to some maximum value
- a perfect interface exists between the fibre and the matrix
- an orientation correction factor K_o may be applied to account for fibres not oriented in the loading direction
- the composite matrix properties are the same as the resin properties
- K_o is independent of strain and is the same for all fibre lengths at least at small strains
- τ is independent of loading angle
- fibre diameter is monodispersed
- fibre and matrix stress-strain curves are linear

The Bowyer-Bader model can be expressed as follows:

$$\sigma_c = K_\Theta(X + Y) + Z \tag{4.29}$$

where σ_c is the composite strength, Z the is strength contribution of the matrix, X and Y are the strength contributions of fibres with subcritical and supercritical fibre lengths respectively, relative to a critical fibre length defined in Equation 4.19. As previously mentioned, this model can also be used to estimate fibre orientation factor (K_o) and interfacial shear strength (τ) if the composite strength and fibre length distribution are known. This model is found to give a good approximation relative to the values determined experimentally [172, 192, 195-198]. In this work, the Bowyer-Bader model was used to determine K_o and τ considering the difficulty to experimentally measure the actual fibre orientation with irregularly shaped fibre cross-sections particularly with fibre aggregation (found in most natural fibre composites) and also the challenge in measuring

interfacial shear strength between the treated fibres (particularly harakeke fibre) and the PLA matrix as treated fibres are too short with small fibre diameters for fibre pull out or fragmentation testing. For the calculation of K_o and τ, subcritical and supercritical fibre lengths are defined as the length of fibre shorter or longer relative to the critical fibre length at any particular strain (L_ε), given by [191]:

$$L_\varepsilon = \frac{E_f \varepsilon_c D}{2\tau} \tag{4.30}$$

such that, L_ε is the fibre length, where, at particular strain, the fibre stress reaches a maximum only at the centre of the fibre. The average stress in the fibres of length equal to or shorter than L_ε at a particular strain according to the Bowyer-Bader model is given by:

$$\sigma_{f\varepsilon} = \frac{L\tau}{D} \tag{4.31a}$$

and for the fibres longer than L_ε is given by:

$$\sigma_{f\varepsilon} = E_f \varepsilon_c \left(1 - \frac{E_f \varepsilon_c D}{4L\tau}\right) \tag{4.31b}$$

Considering fibres having different lengths with respect to L_ε, Equation 4.29 can thus be expanded using the following:

$$X = \sum_{i}^{L_i < L_\varepsilon} \frac{\tau L_i V_i}{D} \tag{4.32a}$$

$$Y = \sum_{j}^{L_j > L_\varepsilon} E_f \varepsilon_c V_j \left(1 - \frac{E_f \varepsilon_c D}{4\tau L_j}\right) \tag{4.32b}$$

and

$$Z = E_m \varepsilon_c \left(1 - V_f\right) \tag{4.32c}$$

giving the overall composite stress at any strain level as:

$$\sigma_\varepsilon = K_\Theta \left[\sum_i^{L_i<L_\varepsilon} \frac{\tau L_i V_i}{D} + \sum_j^{L_j>L_\varepsilon} E_f \varepsilon_c V_j \left(1 - \frac{E_f \varepsilon_c D}{4\tau L_j}\right) \right] + E_m \varepsilon_c (1 - V_f) \quad (4.33)$$

where σ_ε is composite stress at a particular strain, V_i and V_j are the volume fractions of the subcritical and supercritical fibre lengths, respectively, and L_i and L_j are the subcritical and supercritical fibre lengths, respectively, in reference to L_ε. In order to determine K_o and τ, the following steps are employed. Firstly, values of two strains, ε_{c1} and ε_{c2} are selected from tensile stress-strain curve and the corresponding composite stresses σ_{c1} and σ_{c2} are determined. Strength contributions of the matrix (Z) from a tensile test of neat PLA are also determined at the same strain levels. These parameters (σ_{c1}, σ_{c2} and Z) are then used to calculate R, the ratio of the fibre load bearing contribution using the following equation:

$$R = \frac{\sigma_{c1} - Z_1}{\sigma_{c2} - Z_2} \quad (4.34)$$

Then, an assumed value of τ is taken and the corresponding values of $L\varepsilon_1$ and $L\varepsilon_2$ calculated using Equation 4.30. Accordingly, the fibre contribution terms X_1, Y_1 and X_2, Y_2 were calculated using Equations 4.32(a) and 4.32(b) for the different strain levels respectively, and used to calculate R', the theoretical value of R using the following equation:

$$R' = \frac{X_1 + Y_1}{X_2 + Y_2} \quad (4.35)$$

The assumed value of τ is adjusted until $R'=R$ and finally used in Equation 4.33 to obtain a value of K_o using strength and failure strain of the composite [199].

4.3 Results and Discussion

4.3.1 Assessment of Fibre Mat and Composite Morphology

Figure 4.8 shows the optical images of randomly oriented fibre mats produced by allowing randomly dispersed fibre to settle from a suspension (a and b) and aligned fibre mats produced by the DSF (c and d). It can be observed that in contrast to randomly oriented fibre mats, fibre mats produced by the DSF had fibres that were aligned to a reasonable degree parallel to the DSF rotation direction. It can also be observed that fibre mats produced using the DSF had improved fibre dispersion relative to randomly oriented fibre mat indicated by lesser fibre agglomeration which could help to further improve the mechanical properties of composites. Figure 4.9 shows composite surfaces, displaying fibre orientation within composites.

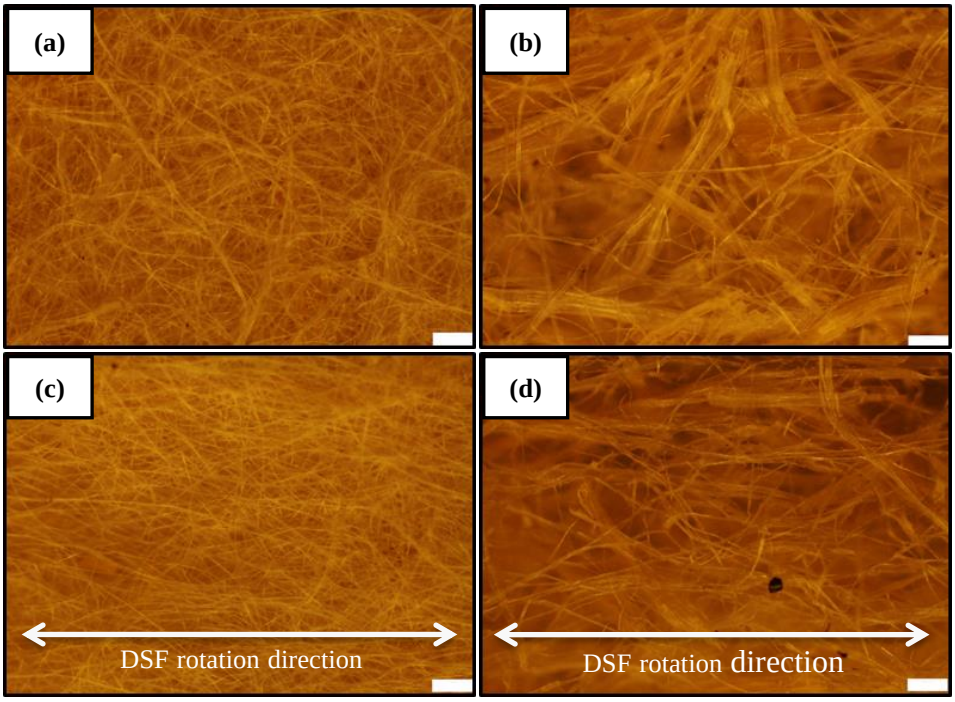

Figure 4.8: Optical images of fibre mats: randomly oriented (a) harakeke and (b) hemp; aligned (c) harakeke and (d) hemp.

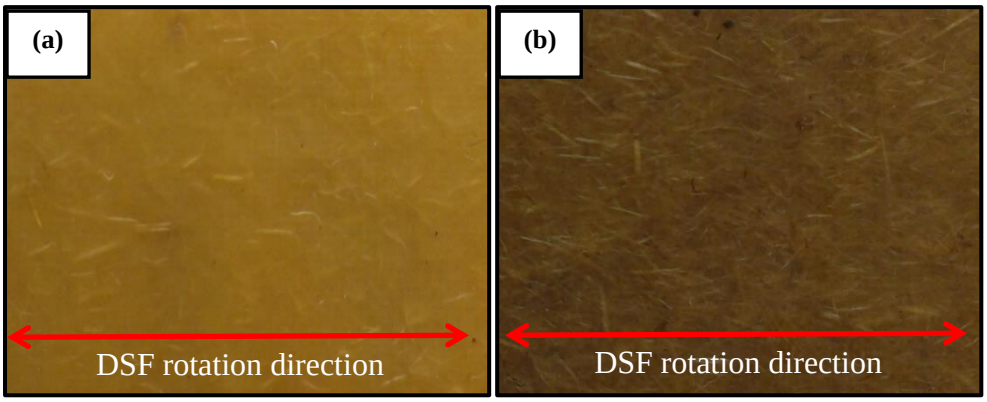

Figure 4.9: Photograph images of the surface of: (a) harakeke and (b) hemp composites.

Representative images of cross-sections of harakeke and hemp composites with 20 wt% fibre content sectioned parallel and perpendicular to the DSF rotation direction are shown respectively in Figures 4.10 and 4.11 (parallel (a), perpendicular (b)). Fibres sectioned longitudinally appear as dark lines whereas those sectioned transversely appear as light circles. It is clearly evident that the fibres have reasonable alignment in the DSF rotation direction as more transverse fibre cross-sections were observed within the sections cut perpendicular to DSF direction and more longitudinal fibre sections were observed within the sections cut parallel to the DSF rotation direction. It can also be observed that the fibres are well dispersed without obvious fibre agglomeration. Similar orientation was seen at 30 wt% content (Figures 4.12 and 4.13); however, at this fibre content, there are some voids and fibre agglomerates in the hemp composites. The formation of voids at high fibre content could be due to the evaporation of a greater amount of moisture from the fibre which would be expected to reduce the effect of reinforcement.

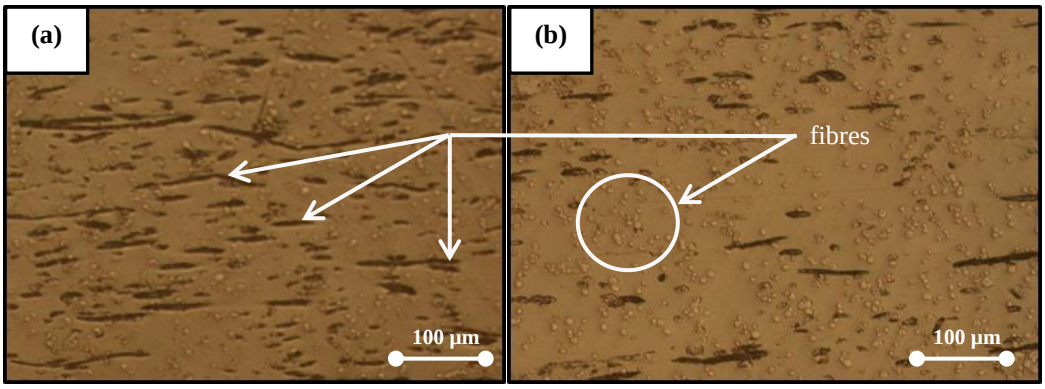

Figure 4.10: Optical microscopy images of cross-sections of harakeke composite with 20 wt% fibre content: (a) parallel and (b) perpendicular to DSF rotation direction.

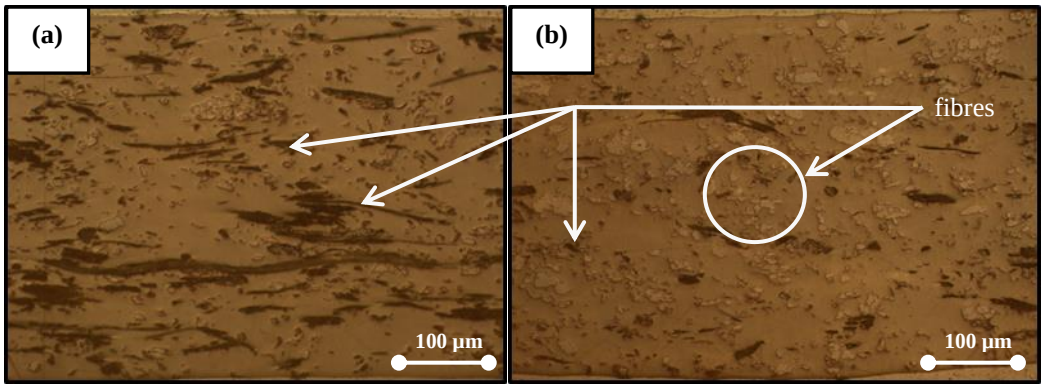

Figure 4.11: Optical microscopy images of cross-sections of hemp composite with 20 wt% fibre content: (a) parallel and (b) perpendicular to DSF rotation direction.

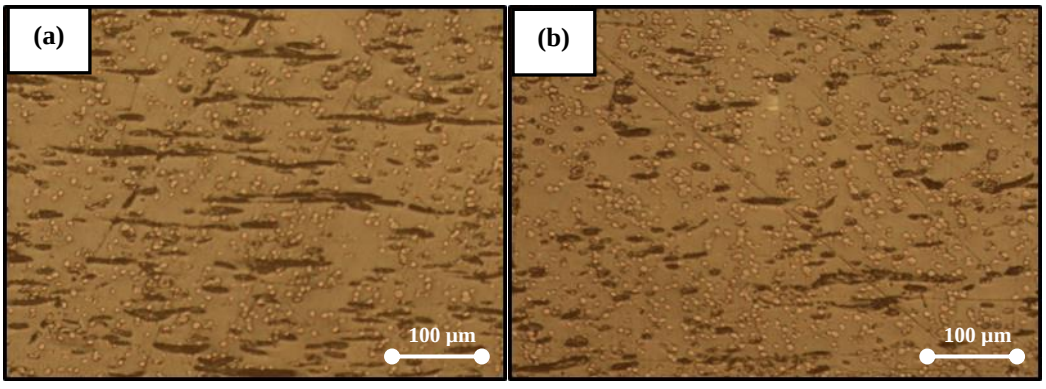

Figure 4.12: Optical microscopy images of cross-sections of harakeke composite with 30 wt% fibre content: (a) parallel and (b) perpendicular to DSF rotation direction.

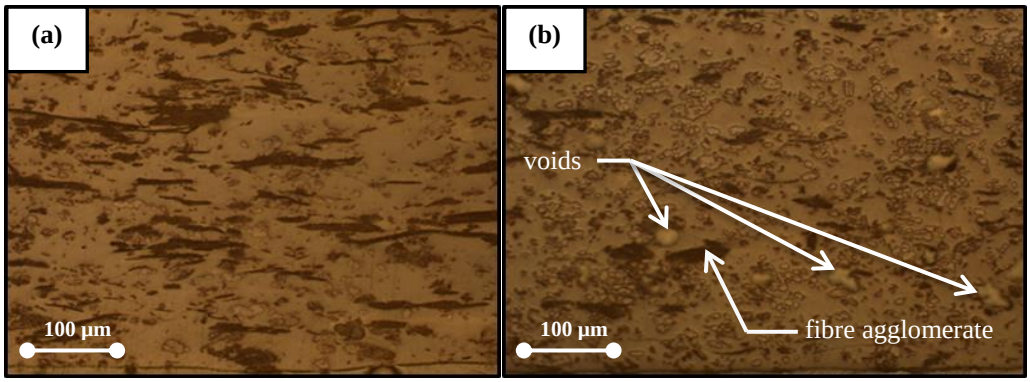

Figure 4.13: Optical microscopy images of cross-sections of hemp composite with 30 wt% fibre content: (a) parallel and (b) perpendicular to DSF rotation direction.

SEM micrographs of fracture surfaces of harakeke and hemp composites that were tested perpendicular (15 wt% fibre) and parallel (20 wt% fibre) to the DSF rotation direction are shown in Figures 4.14 and 4.15. Figure 4.14 further confirms that alignment of harakeke and hemp fibres has been obtained using DSF (as seen in the light microscope observations). Some holes in the matrix can be observed as well as protruding lengths of fibre (Figures 4.15a and b) suggesting fibre pull-out has occurred, which could be related to poor interfacial strength or fibres having lengths shorter than the critical fibre length, leading to fibre debonding rather than fibre failure [200]. The gaps between fibres and matrix (shown in Figures 4.15(c) and (d)) were smaller compared to untreated fibre composites observed elsewhere [201], suggesting a good degree of wetting known to be benefitted as a result of alkali treatment which would encourage good bonding. Furthermore, improved interfacial bonding is supported by longitudinal splitting of hemp fibres as seen in Figure 4.14(b), therefore suggesting the pull-out described above, being related to lengths of fibre shorter than the critical length rather than a weak interface, considering high variation in fibre lengths in composites.

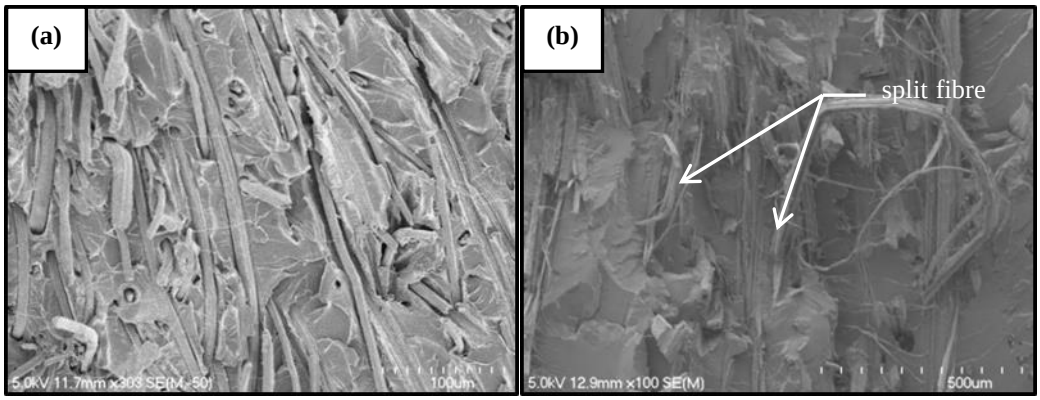

Figure 4.14: Scanning electron micrographs of fracture surfaces of: (a) harakeke and (b) hemp composites tensile tested perpendicular to DSF rotation direction (15 wt% fibres).

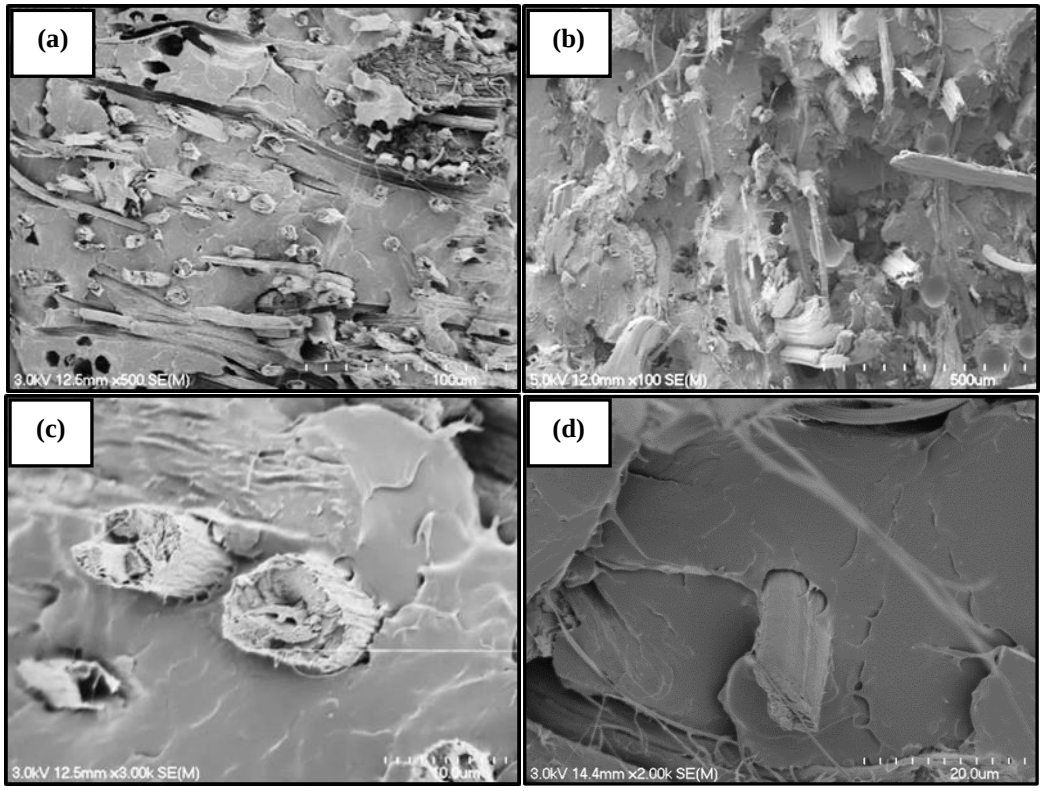

Figure 4.15: Scanning electron micrographs of fracture surfaces for composites reinforced tensile tested parallel to DSF rotation direction with 20 wt%: (a) and (c) harakeke, (b) and (d) hemp fibres.

4.3.2 Composite Tensile Properties – Effect of Fibre Content and Fibre Orientation

Figure 4.16 presents stress versus strain graphs for composites with 15 wt% fibre tested parallel and perpendicular to the main fibre alignment direction along with

that for neat PLA for comparison purposes. Both harakeke and hemp composites tested in both directions failed in a brittle manner at low strain without noticeable yielding. The stiffness for composites loaded parallel to the main fibre alignment direction (HR-15 and HM-15) was significantly increased as expected due to reinforcement and the failure strains remained comparable or increased attributed to effective stress transfer (HR-15) relative to neat PLA. Increases in stiffness can also be observed in composites tested perpendicular to the main fibre alignment direction particularly for harakeke composite (very small though for hemp), but the failure strains for the composites loaded perpendicular to the main fibre alignment direction were significantly lower, expected to be due to fibre debonding [202-206].

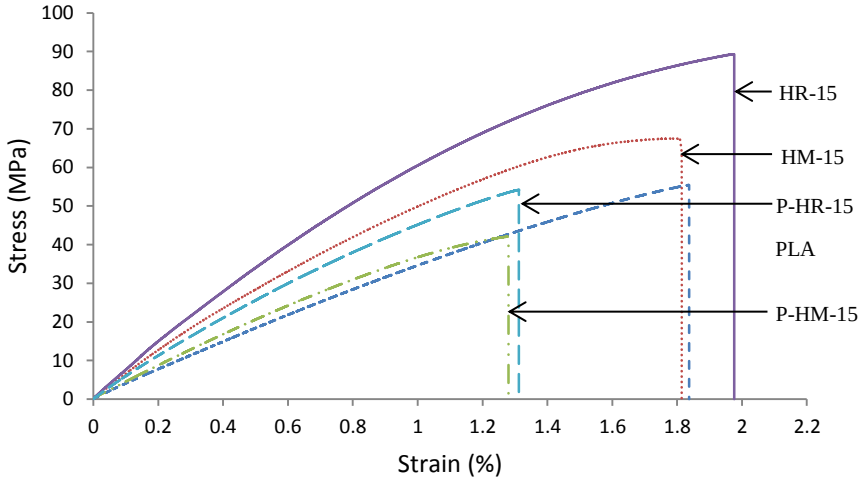

Figure 4.16: Typical stress versus strain curves for samples reinforced with 15wt% fibre loaded in parallel and perpendicular to main fibre alignment direction.

Tensile strengths for harakeke and hemp composites versus fibre content are presented in Figure 4.17. Clearly, for composites tested parallel to the main fibre

alignment direction, the inclusion of fibres up to 30 wt% for harakeke and 25 wt% for hemp increased the tensile strength of the composites.

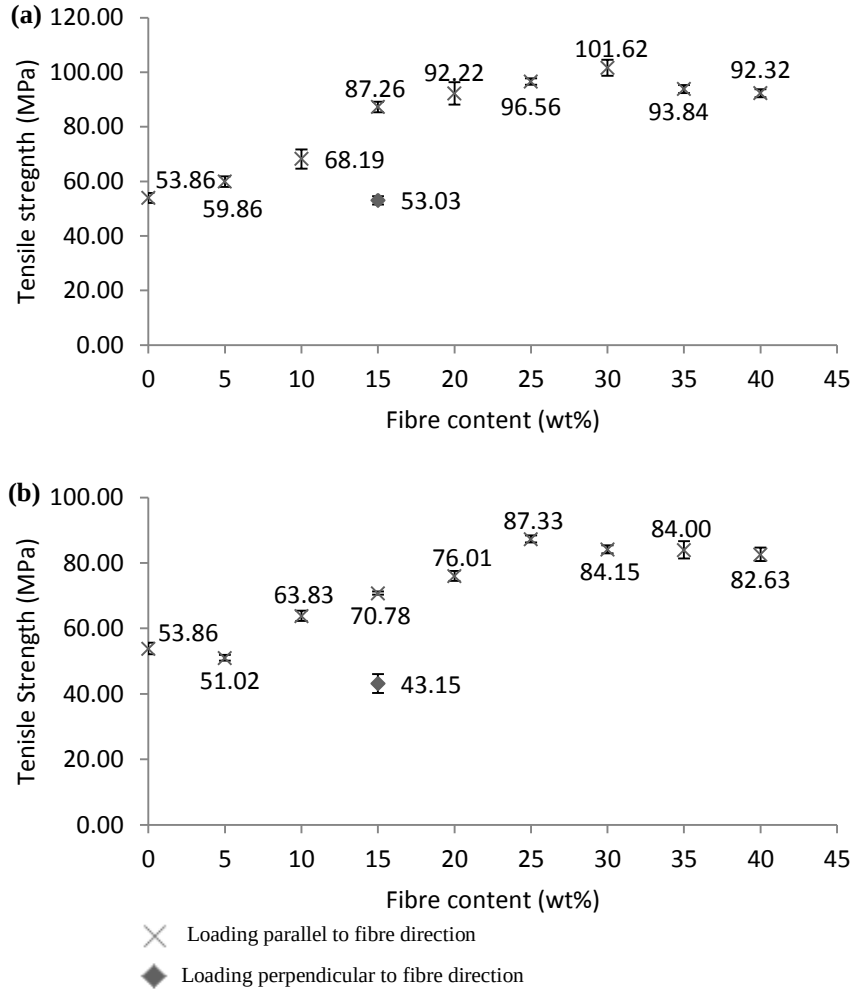

Figure 4.17: Tensile strength as a function of fibre content and loading direction for: (a) harakeke and (b) hemp reinforced PLA. Error bars each corresponds to one standard deviation.

Maximum tensile strengths of harakeke and hemp composites were 101.6 MPa and 87.3 MPa respectively, which were approximately 90 and 60% higher than for that PLA (53.9 MPa) with small standard deviations observed, as indicated by the error bars, suggesting good uniformity of fibre distribution throughout the composite. Higher improvement in tensile strength for harakeke composites could

be due to a larger interfacial area as a result of smaller diameter fibres. Tensile strengths attained in this work with discontinuous fibre in PLA are better than those in other reported works with PLA and discontinuous fibre at similar fibre contents [63, 91, 203, 207-214]; this is assumed to be due to improved fibre alignment and conserved fibre length relative to other composites produced where extrusion and injection moulding have been used resulting in more random orientation and where lengths of fibres are generally reduced due to processing. Reduction of strength above 30 wt% for harakeke and 25 wt% for hemp could be due to insufficient polymer for adequate wetting and increased possibility of fibre-fibre interaction resulting in fibre agglomeration [215], as well as an increase in the structural porosity component in the composite [216]. Furthermore, fibre was more easily displaced during processing at higher fibre contents due to the transverse pressure in polymer melt which could have contributed to a decrease in harakeke and hemp composite tensile strengths through reduced orientation and increased agglomeration (see Figures 4.10 to 4.13).

Unsurprisingly, lower strength was obtained for composites tested perpendicular to the main fibre alignment direction. Although in the main fibre alignment direction, composite properties are strongly dependent of fibre properties and the interface, in the perpendicular direction, properties are more dependent on fibre-matrix interfacial bonding and the matrix [91]. Also, in this direction, the dimension (diameter) of the fibre is very small relative to the critical fibre length for shear stress to bring about tensile load in the fibre. Furthermore, it is likely that the strength of the fibre is lower due to orientation of microfibrils which has shown to give different properties in different fibre direction [216].

Reduction in tensile strength for hemp composites with 5 wt% fibre tested parallel to the fibre direction relative to PLA could be due to the fibre content being lower than that referred to as the critical fibre volume fraction for reinforcement. The concept of minimum and critical fibre volume fractions for unidirectionally-aligned continuous fibre composites is illustrated schematically in Figures 4.18 ($V_{f,min}$) and 4.19 ($V_{f,min}$ and $V_{f,crit}$) for the two different possible cases such that the fibre has a higher or lower failure strain than the matrix [185].

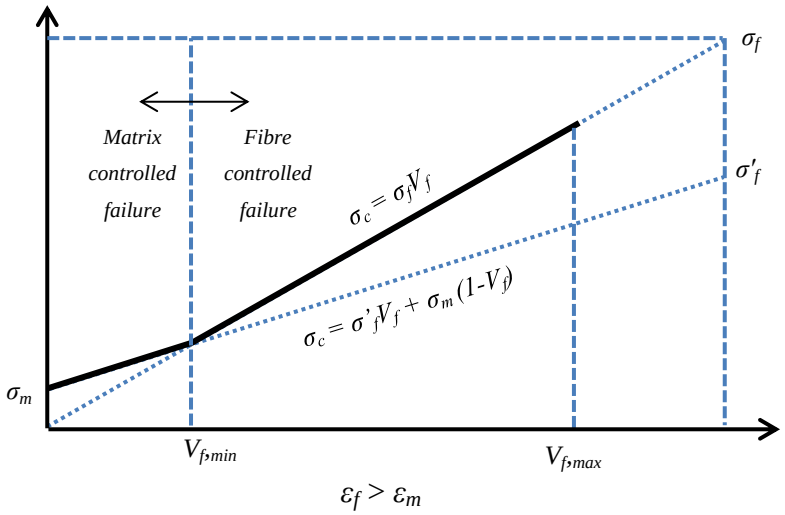

Figure 4.18: Schematic illustration of the variation of composite strength with fibre content showing minimum fibre volume content for composites with fibre failure strain higher than that of matrix.

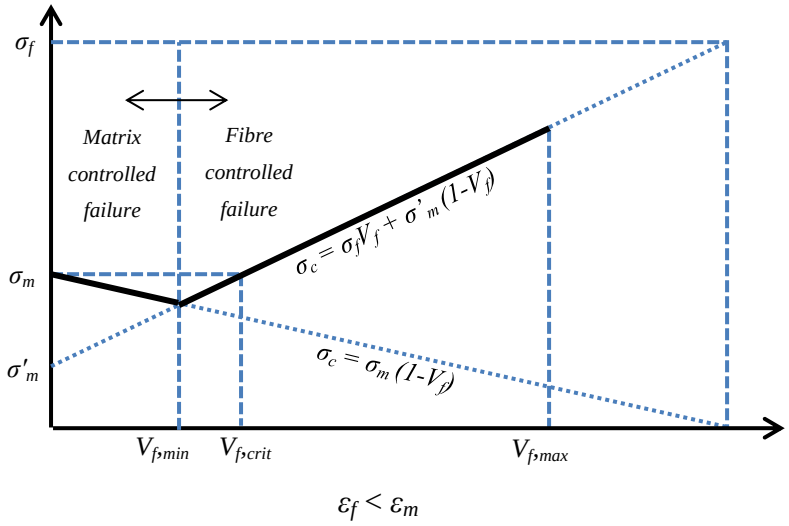

Figure 4.19: Schematic illustration of the variation of composite strength with fibre content showing minimum and critical fibre volume contents for composites with fibre failure strain lower than that of matrix.

Typical stress-strain curves for harakeke, hemp and PLA in this work are shown in Figure 4.20, showing that the material with the highest failure strain is harakeke followed by PLA followed by hemp with the lowest failure strain, so for harakeke composites the fibre failure strain is higher than the matrix and for hemp composites the fibre failure strain is lower.

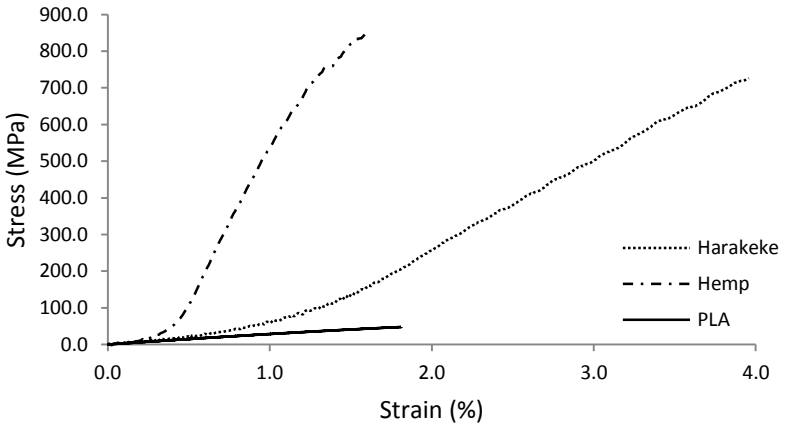

Figure 4.20: Typical stress-strain curves for harakeke, hemp and neat PLA.

In the case where failure strain of the fibre is higher than that for the matrix (Figure 4.18 ($\varepsilon_f > \varepsilon_m$)), as the strain is the same in the fibre and the matrix during testing, the matrix fails first. At low fibre volume fractions, load is largely supported by the matrix and the fibre will not be able to support the load transferred from the matrix, so composite failure will occur when the matrix fails (matrix controlled failure); at higher fibre volume fractions, the fibre will be able to support the transferred load until the strain of the composite reaches the failure strain of fibre (fibre controlled failure). Ideally, (see Figure 4.18) composite failure occurs when the fibre stress reaches σ_f, when the composite strength is given by $\sigma_f V_f$. The fibre volume fraction where the transition between matrix controlled failure and fibre controlled failure occurs is called the minimum fibre volume fraction ($V_{f,min}$). Above this point an increased gradient in composite strength versus fibre fraction occurs as the reinforcement becomes more efficient, until it reaches maximum fibre volume fraction ($V_{f,max}$). Beyond $V_{f,max}$ the composite strength deteriorates due to significant increase in porosity, poor wetting and inefficient stress transfer as a result of limited fibre-fibre spacing [217].

For the case where the fibre has a lower failure strain than the matrix (Figure 4.19 ($\varepsilon_f < \varepsilon_m$)), which is the situation for hemp fibre, at low fibre contents, as the strain on the composite surpasses the fibre failure strain, the fibre fails first leaving the matrix unreinforced with the fibres effectively acting as holes (matrix controlled failure). Consequently, tensile strength of a composite reduces with increased fibre content and is a minimum at $V_{f,min}$ [185, 217]. As the fibre content increases beyond $V_{f,min}$, when the fibres fail, the composite fails (fibre controlled failure),

however, with more fibre, more load is carried and so the strength increases and equal to that of the matrix can be seen to be obtained at a fibre volume fraction higher than that defined as the critical fibre volume fraction ($V_{f,crit}$). Beyond $V_{f,min}$, the maximum stress on the matrix (σ'_m) is dependent on the failure strain of the fibre.

Figure 4.21 shows the experimental data for tensile strength as a function of fibre content as previously presented in Figure 4.17, with lines fitted to enable minimum, critical and maximum fibre volume fractions to be obtained. From Figure 4.21(a), it can be seen that $V_{f,min}$ and $V_{f,max}$ for harakeke are about 10 and 32% respectively. The $V_{f,min}$, $V_{f,crit}$ and $V_{f,max}$ for hemp are about 4.5, 6 and 22% respectively (Figure 4.21(b)). Furthermore, σ'_f (defines the fibre stress at composite failure strain) for harakeke fibre is found to be approximately 358 MPa and σ'_m (defines the matrix stress at fibre failure strain) is found to be approximately 40 MPa. Clearly, for the case of hemp composites, strength greater than that of PLA can only be expected if the fibre volume fraction is higher than 6%. Notably, the $V_{f,min}$ and $V_{f,crit}$ in this work are lower compared to those reported for other short fibre composites. For instance, the $V_{f,min}$ and $V_{f,crit}$ for short banana fibre reinforced vinyl-ester were found to be around 15 and 25% respectively [218], while for hemp fibre reinforced unsaturated polyester composites were around 20 and 40% respectively [219]. This indicates that composites reinforced with these aligned natural fibre mats have better reinforcement efficiency as a result of better fibre alignment and interfacial properties. However, the values obtained from this work are still considerably

higher compared to those obtained for aligned carbon-polyester composites which were found to be around 2.3 and 2.4% [217].

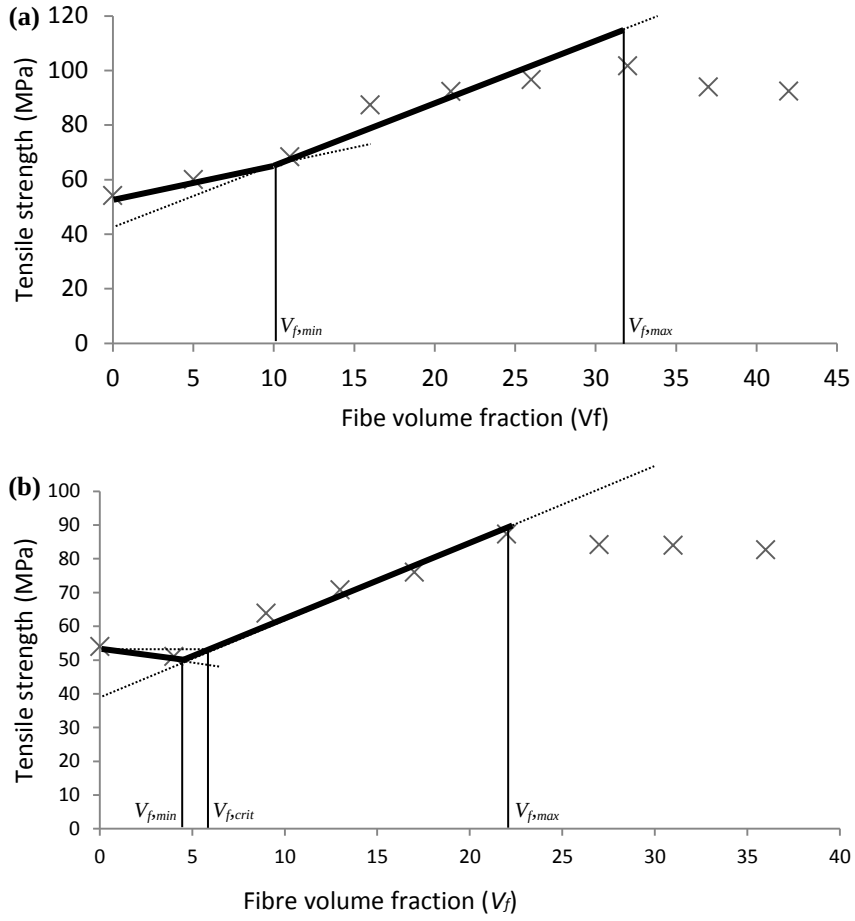

Figure 4.21: Variation of composite strength with fibre content showing minimum and critical fibre volume contents for: (a) harakeke and (b) hemp.

$V_{f,min}$ and $V_{f,crit}$ for harakeke and hemp fibre composites can be predicted by plotting strength versus fibre content according to the Rule of Mixtures model equations given in Figures 4.18 and 4.19 and plotted in Figure 4.22, along with the strength for harakeke and hemp fibre composites obtained experimentally. It should be kept in mind that this model assumes a perfect interface between fibre and matrix and that the fibres are continuous and perfectly aligned.

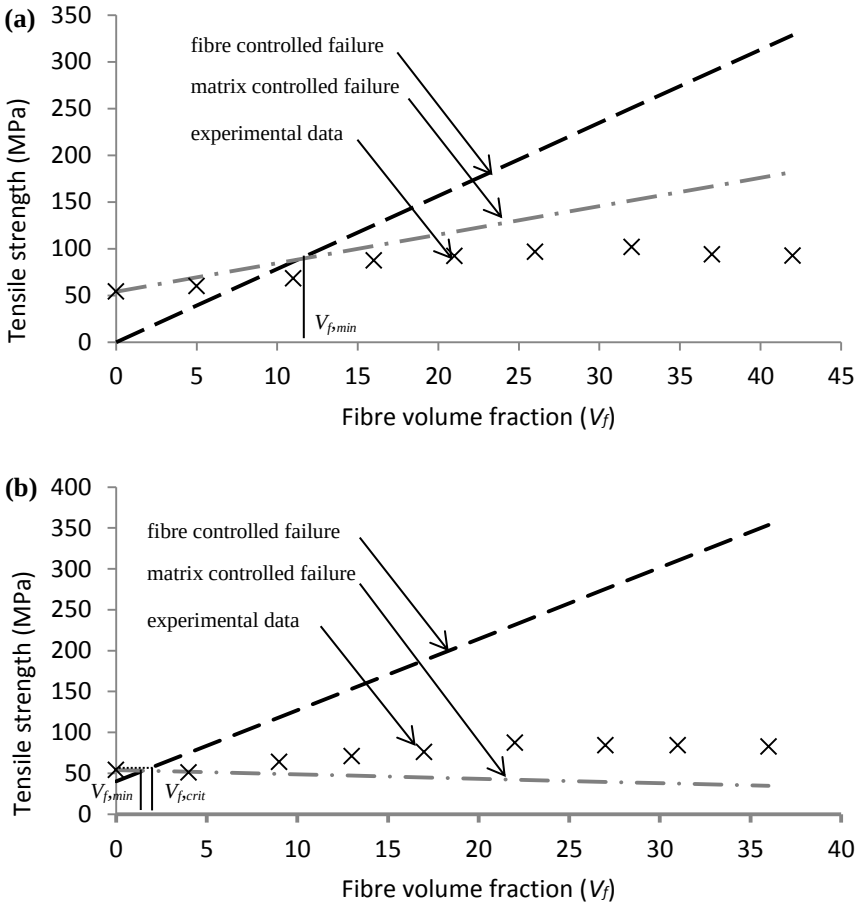

Figure 4.22: Variation of tensile strength with fibre volume fraction obtained using simple Rule of Mixtures with predicted $V_{f,min}$ and $V_{f,crit}$ for: (a) harakeke and (b) hemp. Experimental data represented by symbol x.

It can be seen from Figure 4.22, that the predicted $V_{f,min}$ for harakeke is about 12% and the predicted $V_{f,min}$ and $V_{f,crit}$ for hemp are about 2 and 2.5% respectively which differ from those determined from experimental data particularly for hemp fibre. Furthermore, a large discrepancy for composite strengths predicted by the Rule of Mixtures is also obtained, particularly in the region of fibre controlled failure which is not surprising given the assumptions used (fibres are continuous and perfectly aligned) in the model. Although good alignment was obtained when using DSF as supported by Figure 4.8, fibre with different directions and different lengths still need to be taken into consideration to improve the accuracy of the

model, hence modification factors were introduced to take account of alignment (see Figures 4.18 and 4.19) and the corrected Rule of Mixtures can then be expressed for the case $\varepsilon_f > \varepsilon_m$ as follows:

$$\sigma_c = K_{ø} K_{st} V_f \sigma_f \text{ for fibre controlled fracture} \quad (4.36)$$

$$\sigma_c = K_{ø} K_{st} V_f \sigma'_f + \sigma_m (1 - V_f) \text{ for matrix controlled fracture} \quad (4.37)$$

and for the case $\varepsilon_f < \varepsilon_m$

$$\sigma_c = K_{ø} K_{st} V_f \sigma_f + \sigma'_m (1 - V_f) \text{ for fibre controlled fracture} \quad (4.38)$$

where K_o is the fibre orientation efficiency factor and K_{st} is the stress transfer efficiency factor (defined previously in Section 4.2.2.7). By fitting K_o and K_{st} for harakeke and hemp obtained in Section 4.3.3 to the corrected Rules of Mixtures equations (Equations 4.36 to 4.38), the predicted strength for harakeke and hemp composites given by the corrected Rule of Mixtures is shown in Figure 4.23 along with the experimental strengths for comparison.

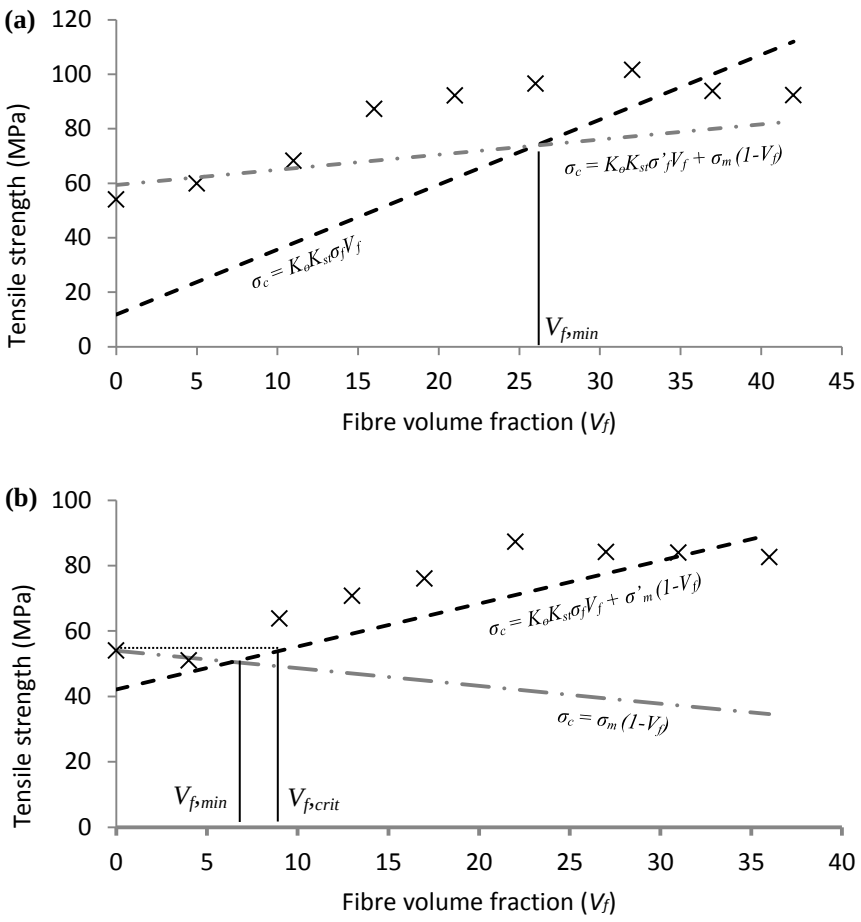

Figure 4.23: Variation of tensile strength with fibre volume fraction obtained from the corrected rule of mixture and experimental tensile strength (indicated with x) for: (a) harakeke and (b) hemp.

It is evident that the strengths given by the corrected Rule of Mixtures for harakeke and hemp composites have better agreement with experimental strength compared to that strength from uncorrected Rule of Mixtures. However, it can be seen that the corrected Rule of Mixtures fails to improve estimation for the $V_{f,min}$ for harakeke composite, which is found to be 26.5% (Figure 4.23(a)), considerably higher than that experimentally obtained. The predicted $V_{f,min}$ and $V_{f,crit}$ for hemp (Figure 4.23(b)) were found to be 7 and 9% respectively, relatively closer to the $V_{f,min}$ and $V_{f,crit}$ experimentally obtained.

Young's moduli of harakeke and hemp composites tested parallel to the fibre direction are shown in Figure 4.24. It can be seen that Young's modulus improved linearly with increasing fibre content up to 30 and 25 wt% for harakeke and hemp fibre composites respectively. This is expected due to the fact that fibre possesses higher Young's modulus than PLA [203].

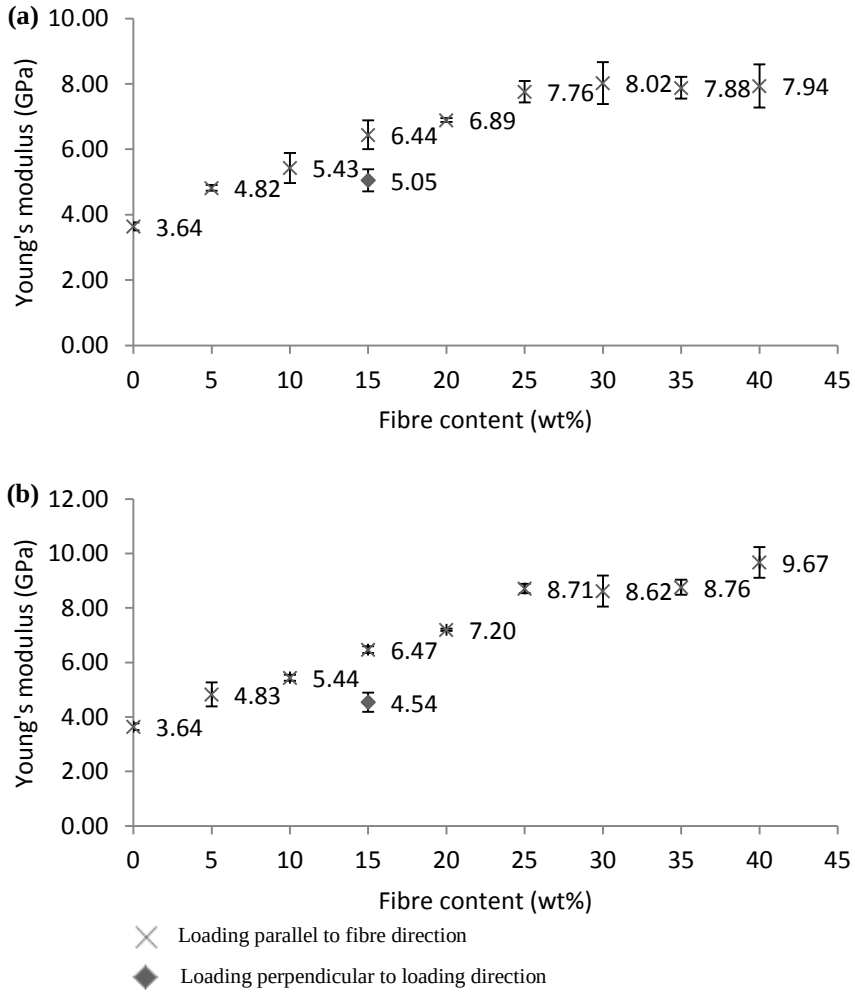

Figure 4.24: Young's moduli as a function of fibre content and loading direction for: (a) harakeke and (b) hemp reinforced PLA. Error bars each corresponds to one standard deviation.

Improvement in Young's moduli for harakeke and hemp were approximately 120% (8.02 GPa) and nearly 165% (9.67 GPa) at 30 and 40 wt% respectively,

compared to that for PLA (3.6 GPa). It may be seen that at the same fibre contents, Young's moduli for hemp composites are higher than that harakeke composites, reflecting the higher Young's modulus for hemp fibre (26.33 GPa) compared to harakeke (21.2 GPa). However, for composites tested perpendicular to the fibre direction (for 15 wt% fibre content), Young's modulus for harakeke composite is found higher compared to hemp composite; suggesting that Young's modulus for harakeke in this direction could be higher or possibly better interfacial bonding between the harakeke fibre and the matrix as a result of smaller fibre diameter and/or better fibre separation. In contrast to tensile strength, Young's moduli for composites tested perpendicular to fibre direction were found to have increased. This trend has been also found elsewhere [14, 91], which suggests that Young's modulus is less dependent on fibre orientation and fibre/matrix interface but more on fibre content, a higher fibre content providing increased constraint within the matrix.

Failure strains for harakeke and hemp composites are shown in Figure 4.25. As can be seen, failure strains for harakeke composites tested in the main fibre alignment direction were not greatly affected by the inclusion of fibres unlike for hemp composites for which failure strain reduced as fibre content increased. A greater reduction in failure strain for hemp fibre composites compared to harakeke fibre composites is not surprising given the lower failure strain of hemp fibre (1.58%) relative to that of harakeke fibre (3.95%). Lower failure strain for hemp composites could also be due to more fibre agglomerates and a higher void content particularly at higher fibre fractions resulting in increased stress concentration (refer to Figure 4.13) as reported elsewhere [139].

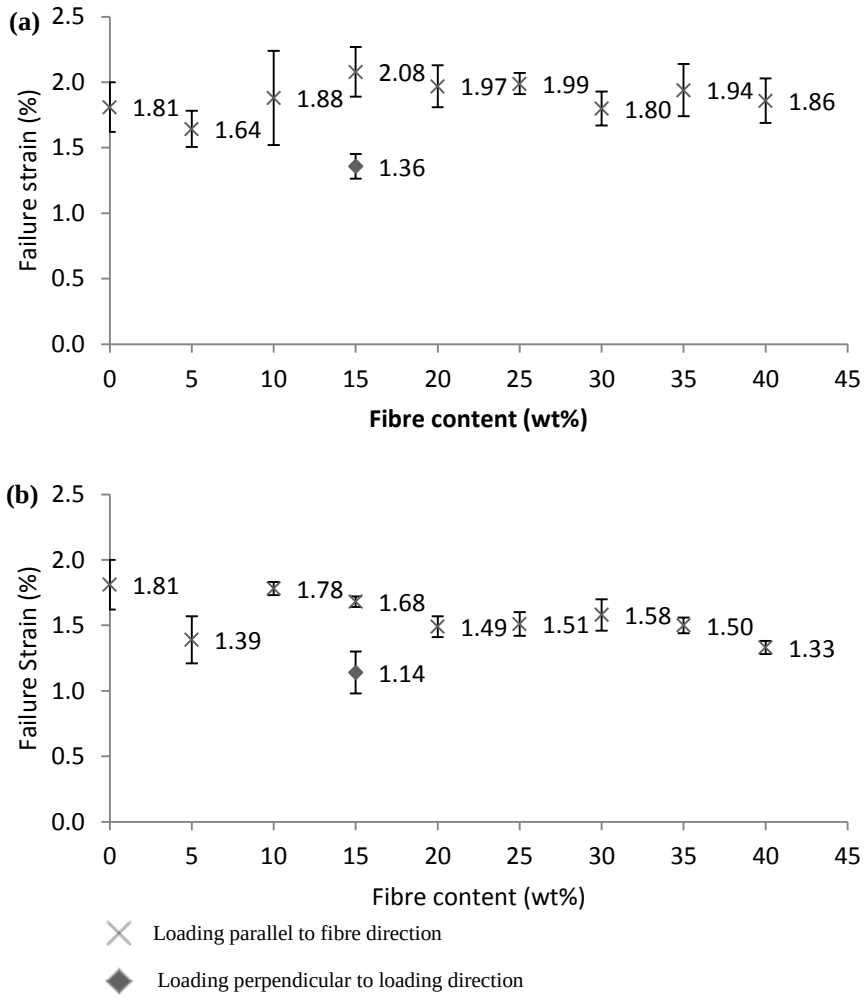

Figure 4.25: Failure strains as a function of fibre content and loading direction for: (a) harakeke and (b) hemp reinforced PLA. Error bars each corresponds to one standard deviation.

For composites tested perpendicular to the fibre direction (both harakeke and hemp), significant reduction in failure strains is noticed when compared to the failure strains of composites tested in the fibre direction, suggesting that the stress concentration as a result of fibre inclusion in this direction encourages matrix cracking to occur at strain level lower than the failure strain of PLA only [219].

4.3.3 Determination of Fibre Orientation Factor (K_o) and Interfacial Shear Strength (τ) According to the Bowyer - Bader Model

In this work, as previously mentioned, the Bowyer-Bader model has been employed to calculate fibre orientation factor (K_o) and interfacial shear strength (τ). K_o and τ were determined using the experimental tensile stress-strain curves and the fibre length distributions, following the procedure detailed previously. Most harakeke and hemp fibre composites failed with failure strains of less than 0.02 and so composite stresses (σ_1 and σ_2) corresponding to strain values well away from final fracture strain, $\varepsilon_1 = 0.005$ and $\varepsilon_2 = 0.01$, such that $\varepsilon_2 = 2\varepsilon_1$ were selected (as required by the model). Analysis was also conducted using strains of $\varepsilon_1 = 0.0075$ and $\varepsilon_2 = 0.015$ for comparison. Using higher strain levels has been shown to give lower values of K_o, as reinforcement efficiency decreased due to matrix cracking and fibre debonding occurring closer to the composite failure strain [192].

Typical composite stress-strain curves for harakeke and hemp fibre composites obtained from tensile testing are shown in Figure 4.26. The curves correspond to the experimental results that were close to the composites mean tensile strength values. It is well accepted that stress-strain curves of many thermoplastic composites are non-linear even at low strain levels. Due to this non-linearity, polynomial curve fitting parameters have been used to improve the accuracy of the analysis [172].

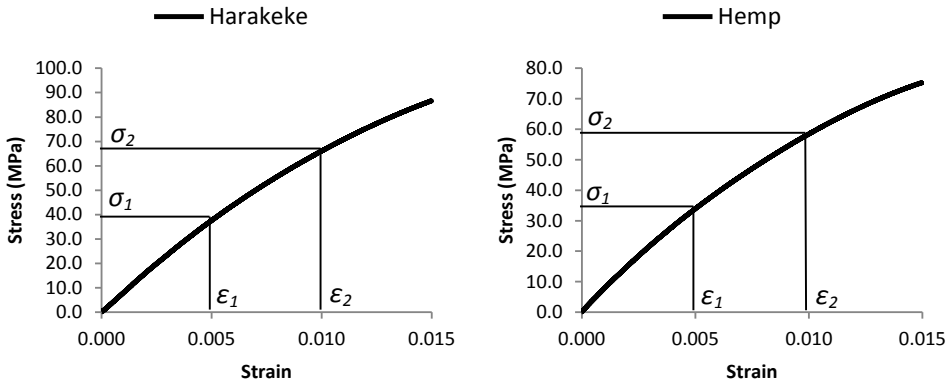

Figure 4.26: Typical tensile stress-strain curves of harakeke and hemp composites.

The relationship of composite stresses at strains of 0.005 and 0.01 versus fibre content is shown in Figure 4.27; stress can be seen to increase with increasing fibre content as expected from Equation 4.33. A linear regression line is used to fit the data and shows good agreement with the data. However, it may be observed that at 30wt% fibre content, the reinforcement efficiency is slightly decreased.

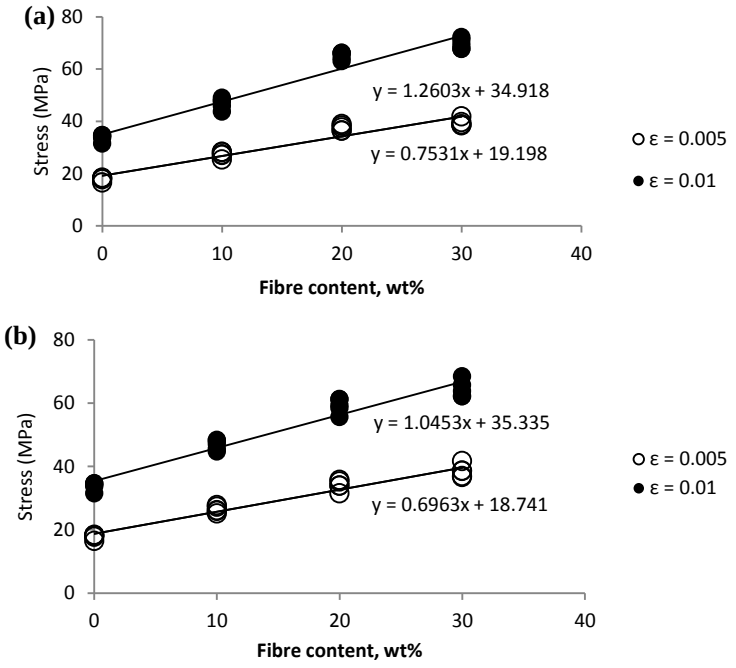

Figure 4.27: The composite stress data determined from the tensile stress-strain curves at strains of 0.005 and 0.01 (mm/mm) versus fibre volume fraction for: (a) harakeke and (b) hemp.

The analysis was conducted by substituting the following parameters into the model: E_f = 21.22 GPa for harakeke and 26.44 GPa for hemp, E_m = 3.64 GPa for PLA, σ_f = 782.4 MPa and 911.33 MPa for harakeke and hemp respectively, as reported in Chapter 3. It was found that at low strain levels, L_ε is small relative to the (measured) fibre lengths and so most of the length of fibres would be at the maximum stress. Therefore, the composite is tending towards behaving as a composite reinforced with continuous fibres [197]. K_o and τ and other related parameters obtained for composites at different fibre contents are tabulated in Table 4.3.

Table 4.3: Related parameters obtained according the Bowyer and Bader model and experiment for harakeke and hemp composites

Sample	Modelling				Experimental	
	Bowyer-Bader					
	Orientation factor, K_o *(ε_1 = 0.0075 and ε_2 = 0.015)*	Interfacial shear strength, τ (MPa) (ε_1 = 0.0075 and ε_2 = 0.015)	Orientation factor, K_o *(ε_1 = 0.005 and ε_2 = 0.01)*	Interfacial shear strength, τ (MPa) (ε_1 = 0.005 and ε_2 = 0.01)	Fibre aspect ratio (l/d)	Average fibre length (mm)
HR-5	0.542	9.0	0.545	8.7	55.8	0.625
HR-10	0.558	8.7	0.559	8.5		
HR-15	0.581	8.6	0.583	8.6		
HR-20	0.572	8.8	0.582	9.6		
HR-25	0.500	9.0	0.508	9.2		
HR-30	0.525	8.9	0.528	9.0		
HR-35	0.370	8.2	0.370	9.1		
HR-40	0.341	8.8	0.363	9.1		
HM-5	-	-	0.390	7.0	26.1	0.765
HM-10	0.421	8.1	0.430	8.6		
HM-15	0.365	8.5	0.371	8.2		
HM-20	-	-	0.438	10.5		
HM-25	0.362	9.0	0.390	8.6		
HM-30	0.263	9.1	0.363	8.8		
HM-35	0.245	8.9	0.317	8.6		
HM-40	-	-	0.310	8.6		

It can be seen from the table that K_o for harakeke fibres were higher than for hemp fibres at all fibre contents. K_o for both harakeke and hemp fibre composites were higher than values seen in the literature for that composites prepared using injection moulding and hot pressed using randomly oriented fibre mats (0.24 – 0.375) [64, 98, 195, 196, 198] and slightly lower compared to the highest values obtained with aligned flax/polypropylene nonwoven preforms (0.45 – 0.6) composites [93]. The highest K_o values for harakeke and hemp in this work were found to be 0.583 and 0.438 respectively at 20wt% fibre. Lower K_o values for hemp fibre composites compared to harakeke fibre composites could be related to lower aspect ratio and fibre agglomeration influencing orientation (refer to Figure 4.8). A similar trend has been observed in previous work, where decreased fibre length for composites at high fibre fractions can cause a decreased K_o in injection moulded samples [98, 195, 220]. Higher K_o values for injected moulded glass and carbon fibre composites than for injection moulded natural fibre composites have been obtained, which fits with the expectation that a higher degree of fibre straightness along with less possibility of fibre agglomeration can also contribute to an increase in K_o [172, 173, 191, 192, 197].

From our data, it was also found that the K_o obtained was not entirely independent of strain, in contrast with the assumption used in the model [191, 192]; K_o generally decreased at higher strain levels closer to composite failure, believed to be due to matrix cracking and fibre debonding as previously mentioned, particularly for hemp fibre composites for which the higher strain used was closer to the composite failure strain (indeed some had failed at strains lower than those used in analysis as reflected by a "–" in table) [196]. From Figure 4.28, it is also

evident that K_ϕ decreased as fibre content increased. A similar trend has also been observed in previous work [98, 195, 220]. Reduction in K_ϕ for harakeke and hemp composites with fibre contents of more than 30 wt% fibre is more evident, corresponding to a higher potential of fibre misalignment during processing due to fibre agglomeration as seen in Figures 4.12 and 4.13, which would be more likely at higher fibre contents due to fibre–fibre interaction from hydrogen bonding [221]. It should be noted that fibre alignment would also be expected to depend on matrix viscosity during processing, such that polymers with higher viscosity would cause a higher degree of fibre displacement as a result of higher pressure used during processing.

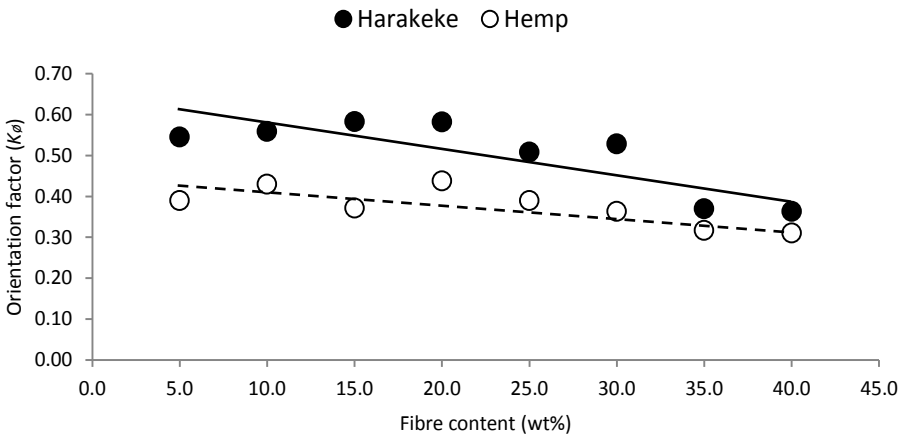

Figure 4.28: Fibre orientation factors for harakeke and hemp fibres at various fibre volume fractions.

General trends for τ versus fibre content for harakeke and hemp fibre composites are graphically presented in Figure 4.29. τ values obtained were found to be comparable to the values reported in previous studies [109, 165, 222-226]. Linear-trend lines fitted to the predicted τ values suggest a slight increase with increase

fibre content. This could be explained by the increased pressure used at higher fibre contents increasing interfacial bonding [98, 197].

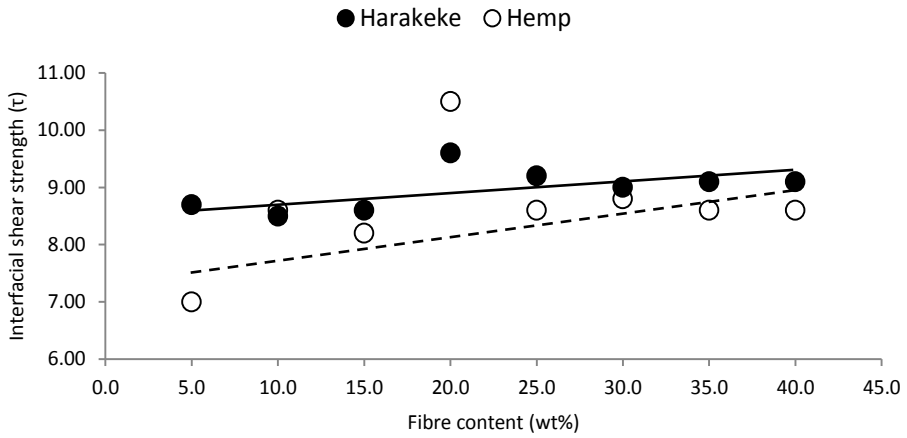

Figure 4.29: Interfacial shear strength (τ) for harakeke and hemp fibres at various fibre volume fractions.

It can be seen that τ for harakeke was slightly higher than for hemp fibre, except at 20 wt% fibre, which could be related to the greater surface area for harakeke fibre. Abnormality seen in τ for 20 wt% fibre content could be attributed to the most effective reinforcing effect as can be interpreted from Figure 4.27, supporting less fibre mat distortion and fibre agglomeration. A higher τ for harakeke fibre compared to hemp fibre could also be due to a higher degree of surface roughness for harakeke as supported by Figures 3.6 to 3.9.

4.3.4 Theoretical Modelling – Comparison between the Predicted and Actual Composites Tensile Properties

Figure 4.30 shows a comparison between the fitted (the Hirsch and Modified Halpin-Tsai ($\zeta = 2$)), predicted (the Cox, Modified Cox, Halpin-Tsai ($\zeta = 2(l/d)$) and MROM) and the experimental composite strengths for harakeke and hemp

composites at different fibre contents. Fitting parameters x = 0.13 for the Hirsch was found to give good correlation with the experimental strengths. This x value is relatively consistent with that found for aligned discontinuous sisal fibre LDPE composites (0.15) [175] and higher as would be expected due to better fibre orientation, than those reported for discontinuous fibre composites (0.09 – 0.1) produced by injection moulding [227] or hot pressed composites with randomly oriented fibre mats [175, 205, 228-230].

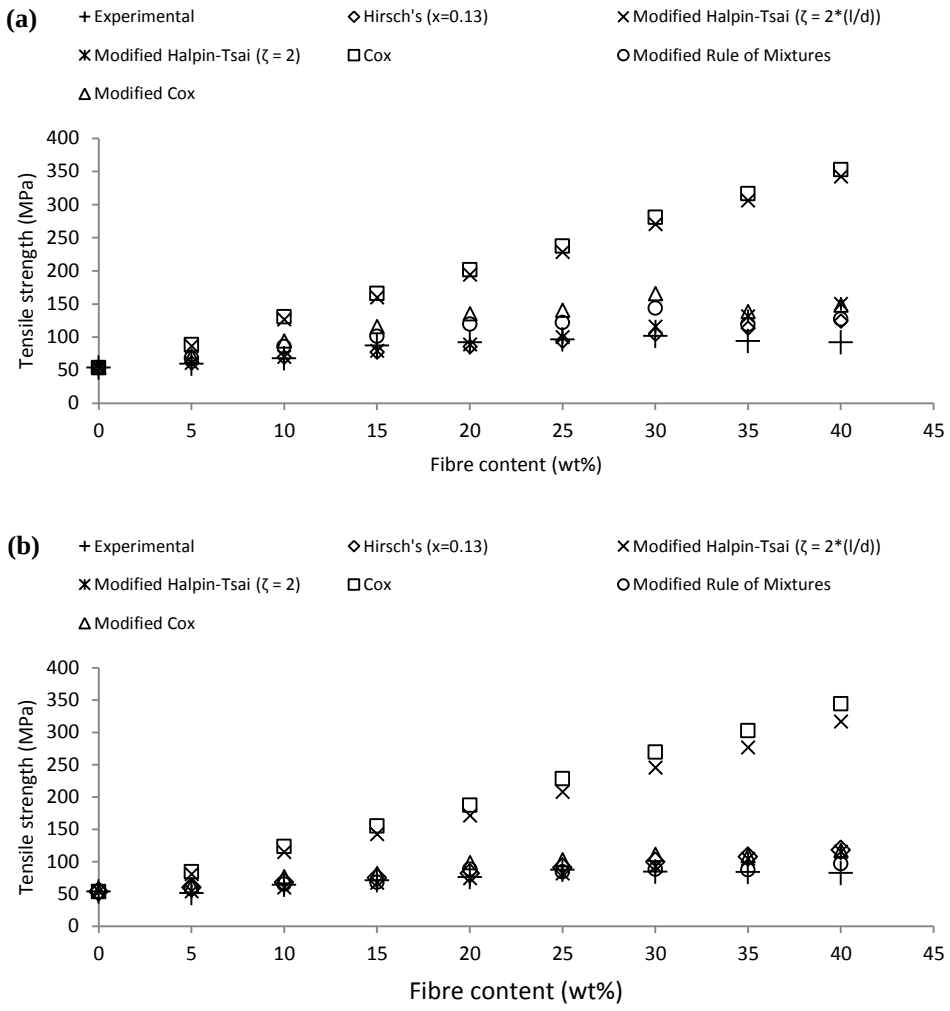

Figure 4.30: Variation of predicted and actual strengths composites taking into consideration fibre orientation factor for: (a) harakeke and (b) hemp fibre.

For the Modified Halpin-Tsai model, it can be seen that large disparity between the predicted and the experimental values is obtained when ζ according to Equation 4.10c is used (111 for harakeke and 52 for hemp). Discrepancy is not surprising given that this factor is used for composites with fibres that are perfectly aligned to the loading direction. Much better agreement to the experimental strengths is obtained using $\zeta = 2$, which matches with that generally found to fit experimental composite strengths for discontinuous random fibre composites [175, 180]. As can be seen in Figure 4.30, using ζ according to the Equation 4.10c would predict strengths up to about 2.2 times higher than that predicted using $\zeta = 2$, suggesting that if an orientation factor (K_o) of approximately 0.45 (1/2.2) were applied, good agreement would be obtained. However, this value varies by 12% and 19% respectively from those achieved for harakeke and hemp fibre using the Bowyer-Bader model. It should be kept in mind that the Modified Halpin-Tsai is a simple model and does not take into account failure mechanisms and in particular stress concentrations as a result of fibre orientation and fibre ends as well as fibre debonding which would be believed to influence the predicted strengths and the calculated K_o.

Large disparity (up to 280%) is also seen for the strength predicted using the Cox model, larger than that found for other short aligned natural fibre composites (35%) [175]. However, large disparity is again not surprising given that this model assumes that fibres are perfectly aligned and the interface between fibres and the matrix is perfect. However, harakeke and hemp fibres used in this work are not perfectly aligned, and at high stress where the strength is measured, fibre debonding is most likely to occur and stress transfer is expected to be much lower

even than for an imperfectly bonded interface. A weakness regarding the predictions of composite strength conducted in this work using the Modified Cox and MROM models is that K_o values as well as K_{st} are obtained from the Bowyer-Bader model using experimental values of composite strength. However, it is possible to avoid this; K_o can also be obtained without mechanically testing composites through imaging to find fibre angle using the following equation [98, 231, 232]:

$$K_{\emptyset} = \sum a_n \cos^4\theta_n \tag{4.36}$$

where a_n is the fraction of fibres with orientation angle, θ_n with respect to the loading direction [93]; K_{st} can be obtained from L_c from interfacial shear strength which can be obtained using a fibre fragmental and/or pull-out test as discussed previously (Section 4.2.2.7).

The Modified Cox and MROM show disparity with the experimental strengths obtained for harakeke up to about 62% and 41% respectively. The difference between the predicted and the actual strengths for harakeke fibre composites obtained using the Modified Cox and Modified Rule of Mixtures can be seen to become larger as the fibre content increases up to 30 wt% fibre, with better agreement at fibre content greater than 30 wt% than at 30 wt%. For hemp fibre composites, better agreement with experimental strengths compared to that of harakeke fibre composite is observed; the highest differences were about 41 and 17% for the Modified Cox and MROM models respectively. The differences obtained here are not surprising given that similar large disparity with these models has also been reported in previous work with other natural fibre composites [92, 233], where generally lower values of K_o have been used for less

aligned fibre composites (as previously discussed K_o is commonly taken as unity for axially aligned fibre composites, 0.375 for planar random configuration and 0.2 for a three dimensional randomly oriented fibre composites). Generally large disparity highlights potential fault with the assumptions for these models. Indeed, they are simplistic in nature and do not take account of failure mechanisms. A major oversight is the influence of stress concentrations on premature failure of composites as a result of different fibre orientations. It should be noted that the K_o values used for the Modified Cox and MROM models are based on average fibre orientation, whereas some are oriented at very large angles to the loading direction. The difference of stress concentration is supported experimentally by Figure 4.16, where the failure strains for composites tested perpendicular to the main fibre alignment direction are significantly lower compared to those tested parallel to the fibre alignment direction. Furthermore, fibre debonding is also not taken account of, which could be expected to have a significant influence on strength. For the Modified Cox model, it is assumed that the interface between the fibre and the matrix is perfect [234]. High interfacial shear strength is generally indicated by matrix tearing/fibre fracture depending on failure strain of the material. According to Von Mises yield criterion, the shear stress (τ_m) required to bring about matrix tearing can be estimated from the tensile strength of the matrix using the following equation [64]:

$$\tau_m = \frac{\sigma_m}{\sqrt{3}} \tag{4.37}$$

where σ_m is the matrix tensile strength. Taking the tensile strength of PLA as 53.86 MPa, the obtained τ_m based on the Equation 4.37 is 31.1 MPa; this is higher than the interfacial strength obtained here (calculated using the Bowyer-Bader model) for harakeke and hemp fibre composites, suggesting that fibre debonding

will occur during testing. The mechanism of pull-out is also neglected by these models. Furthermore, the fibre strength used in both models is the average fibre strength; in actual composites some fibres could fail at much lower stresses than the average fibre strength.

A comparison between the fitted, predicted and the experimental Young's moduli for harakeke and hemp fibre composites with different fibre contents are shown in Figure 4.31.

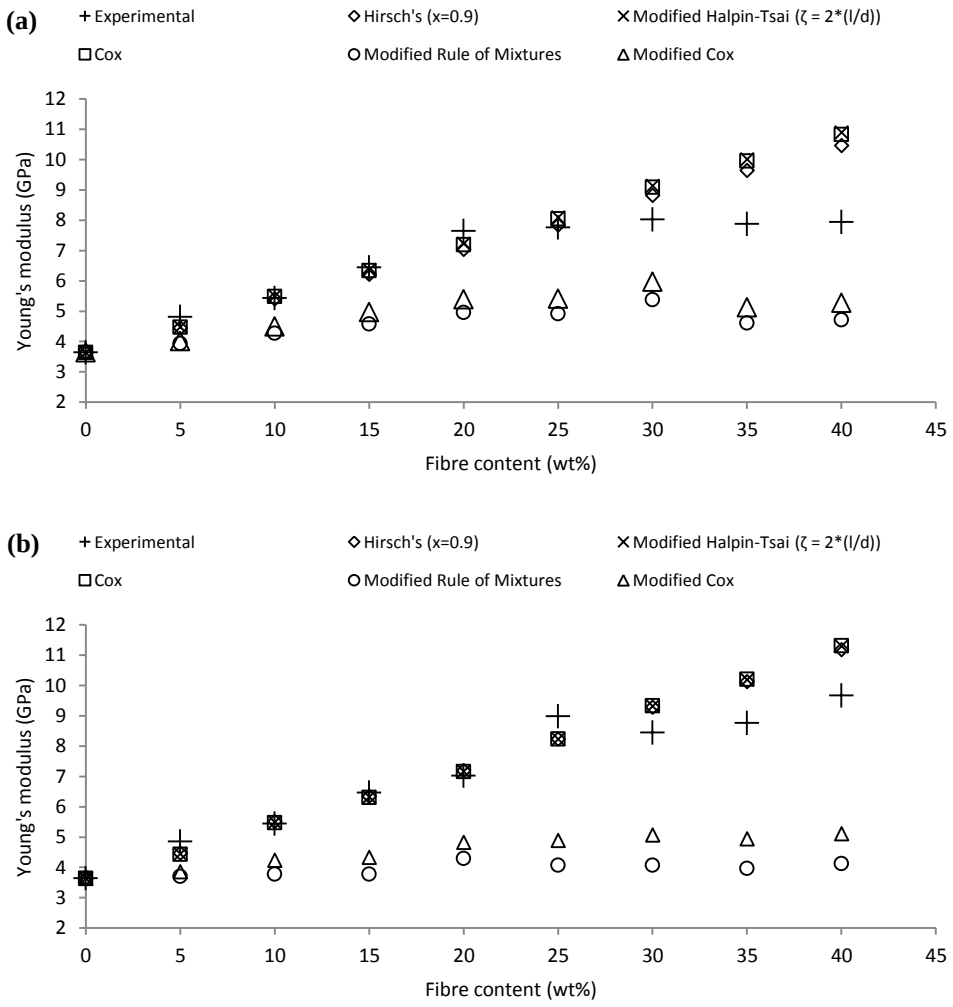

Figure 4.31: Variation of predicted and actual Young's moduli for: (a) harakeke and (b) hemp fibre.

It can be seen that good agreement (< 10% difference) between the theoretical and experimental values are obtained for the Hirsch, Modified Halpin-Tsai and Cox models up to 25 wt% fibre with a noticeable increase in disparity at fibre contents higher than 25 wt%, which is believed to be due to fibre agglomeration. At fibre contents lower than 25 wt%, the differences are found to be relatively lower than those found in the literature for other discontinuous fibre composites for which there was a less linear trend for experimental values which can be explained by less uniform fibre distribution [229, 235]. For the Hirsch model, the value of x (0.9) for harakeke and hemp fibre composites, however, is close to that expected for continuous fibre composites (x=1) and higher (0.2 – 0.8) than those for other discontinuous natural fibre composites made using injection moulding [17, 148, 198, 235, 236], suggesting better reinforcement efficiency from fibre mats can be obtained. It is much higher than that obtained when fitting for strength (0.13); given that x is meant to represent stress transfer, this suggests that less stress transfer may be occurring at the point where strength is measured which occurs at higher stress (at which point debonding can be reducing stress transfer) than where Young's modulus is measured, which could explain to an extent the difference seen. It is interesting to note that for the Modified Halpin-Tsai model, these predicted Young's moduli are obtained using the fitting parameter ζ according to the Equation 4.10c (111 for harakeke and 52 for hemp), which over-predicted strength (taken as 2 for strength), the higher value for ζ for Young's modulus compared to that for strength can again be attributed to the higher stress transfer at where Young's modulus is measured compared to where strength is measured, supporting a reasonable fibre alignment obtained using a DSF. Good agreement with the experimental data given by these models could also be

attributed that at low stress where Young's modulus is measured, much less or no fibre debonding occurs unlike at where the strength is measured, so more in agreement with the assumption used by the model that the interface between fibres and matrix is perfect.

The Modified Cox and the MROM models are found to largely underestimate Young's moduli (Figure 4.31). A similar discrepancy has also been observed in other work for discontinuous fibre composites for which discrepancies of up to 300% [237] and 60% [238] have been found for the Modified Cox and the MROM respectively. Differences predicted for Young's modulus using the Modified Cox (71 and 120% for harakeke and hemp respectively) and the MROM (54 and 84% for harakeke and hemp respectively) models in this work are much larger than those obtained for strength. Large disparity obtained from these models is believed to be due to smaller values for stress transfer reduction factors, K_o and K_{st}, determined from composite strength (using the Bowyer-Bader model); the actual values for these stress transfer factors at low stress level where Young's modulus is measured would be expected to be higher as discussed previously due to less (or no) debonding.

From the presented results for Young's modulus, it is clearly observed that except for the Modified Cox and MROM, the predicted Young's moduli obtained from the other models fit reasonably well with experimental data, particularly for fibre contents less than 25 wt%, which is interesting considering these are simple models. It should be kept in mind that the assumptions made for Young's modulus are much more accurate than for strength, and so simple prediction should be

expected to be more accurate. However, it is acknowledged that larger discrepancy (up to 140%) has been seen in the literature when these models used to predict Young's modulus for other natural fibre composites. The Cox model predicted Young's modulus for harakeke and hemp fibre composites the best, as found generally in the literature which could be due to the fact that it takes more account of fibre (fibre radius) and matrix (shear modulus) properties.

4.4 Chapter Conclusions

The alignment of fibres within composites reinforced using fibre mats produced using a DSF and the tensile strength of PLA composites reinforced using these fibre mats with different fibre contents tested parallel and perpendicular (for composites with 15wt% fibre) to the fibre direction were investigated. It was found that using a DSF to make fibre mats lead to better fibre alignment and dispersion compared to that for composites made using injection moulding and composites reinforced with randomly oriented fibre mats. Tensile strengths of composites tested parallel to fibre direction were higher than for composites tested perpendicular to the fibre direction. For composites tested parallel to fibre direction, tensile strengths were found increased by 90% for harakeke and 60% for hemp composites at fibre contents of 30 wt% and 25 wt% respectively, relative to PLA only. Young's moduli for harakeke and hemp fibre composites were also increased by 120% and 165% relative to neat PLA. Furthermore, it was found that the minimum and critical fibre volume fractions were lower compared to composites made using injection moulding, believed to be as a result of higher reinforcement efficiency through fibre alignment obtained using a DSF. Higher reinforcement efficiency obtained in this work is also indicated by a higher value

of x used for the Hirsch model for both strength and Young's modulus compared to that used for other discontinuous fibre composites made either using injection moulding or using randomly oriented fibre mat. The Modified Cox and MROM models were found to give accuracy within 45% for up to 25 wt% fibre contents for composite strengths, supporting their use as first order approximations, with the Modified Halpin-Tsai and Cox models showing better agreement (<10%) for Young's modulus for fibre contents up to 25 wt%, not surprisingly, given the simpler mechanism involved.

CHAPTER 5

The Effect of Fibre Surface Treatment, Coupling Agents and Plasticiser on the Performance of Aligned Discontinuous Harakeke and Hemp PLA Composites

5.1 Introduction

This chapter describes work carried out to assess the effect of fibre treatments, coupling agent and plasticiser on the mechanical performance of PLA composites reinforced with 20 wt% fibre. The harakeke and hemp fibres used to produce fibre mats were first treated with the optimum alkali treatment described in Chapter 3. Alkali treated harakeke and hemp fibres were further treated with silane and dicumil peroxide (DCP). Maleic anhydride (MA) grafted PLA (MA-g-PLA) was used as a coupling agent, while hyper-branched polymer (HBP) was used as a plasticiser. Composites with fibres treated with silane and DCP and composites using MA-g-PLA were characterised by swelling testing, scanning electron microscopy (SEM), tensile testing, dynamic mechanical analysis (DMA) and thermogravimetric analysis (TGA), while composites with HBP were tensile and impact tested. Details of the materials, the methods, the results of the testing and conclusions are presented in this chapter.

5.2 Experimental Methodology

5.2.1 Materials

Harakeke fibre treated with 5 wt% sodium hydroxide (NaOH) and 2 wt% sodium sulphite (Na_2SO_3) and hemp fibre treated with 5 wt% sodium hydroxide (NaOH) were used to produce fibre mats. PLA (polylactide) polymer from NatureWorks® 3052D injection moulding grade in pellet form was used as a matrix. Maleic anhydride (MA) with 99% purity, dicumyl peroxide (DCP) with 98% purity, both in powder form and 3-aminopropyl triethoxy silane (APS) with purity more than 97% were purchased from Sigma-Aldrich. Hyper-branched polymer (Hybrane PS 2550) with molecular weight of 2500 was purchased from Polymer Factory in Sweden.

5.2.2 Methods

5.2.2.1 Fibre Surface Treatment

Silane treatment

Prior to silane treatment, alkali treated harakeke and hemp fibres were left exposed to air for about one week until reaching equilibrium moisture content; it has been found that a stable moisture content of about 10 wt% of fibre weight is important for hydrolysis of silane [221]. The silane treatment for harakeke and hemp fibres was carried out using an aqueous solution. A predetermined 5 wt% of silane relative to the fibre weight was added to acetone and was continuously stirred for 15 minutes to assure complete hydrolisation then the pH of the solution was adjusted to 3.5 – 4.0 whilst stirring by introducing acetic acid. The fibres were left immersed in this solution for 30 minutes at room temperature. A minimum amount of solution was used, just enough to wet all the fibres and to

allow hydrolysis of silane to take place effectively with the moisture on the fibre surfaces. The fibres were manually extracted from the solution and left for four hours to dry in the air, then oven dried at 80 °C overnight before further use.

Peroxide treatment

A predetermined 5 wt% DCP relative to the weight of fibres was first dissolved in 0.5 L acetone for at least 10 minutes to get a stable mixture. The fibres were then immersed in this solution at a temperature of 70 °C for 30 minutes. High temperature used in this work was to promote the decomposition of peroxide onto the fibres [239]. The fibres were then removed and air dried for four hours before oven drying at 80 °C overnight.

5.2.2.2 Fibre Mat Production

Alkali treated fibres including those subjected to further treatments using silane and peroxide were used to produce fibre mats. The method used to produce fibre mats was similar to that described in Section 4.2.2.2.

5.2.2.3 Grafting MA onto PLA

MA was grafted onto PLA (MA-g-PLA) during extrusion in the presence of DCP as an initiator. A predetermined amount of 3 wt% MA and 0.5 wt% of DCP relative to PLA were dissolved in 50 mL of acetone. The solution was then stirred for about 15 minutes to get a stable mixture. 500 g of PLA pellets were then added to the solution. The solution containing PLA pellets was then slowly stirred until the acetone was fully evaporated leaving the PLA pellets uniformly coated with MA. The PLA pellets coated with MA were extruded into sheets of about 0.5

to 0.6 mm thick using twin-screw extruder (Thermo-Prism TSE-16-TC) equipped with a coat hanger die as used to extrude the PLA only. It was observed the viscosity of extruded MA grafted PLA was slightly lower than that the viscosity of the extruded PLA alone, indicated by a decrease in torque during extrusion. In order to maintain the desired viscosity and thickness of the extruded sheets, the temperatures were reduced from that used for PLA alone (see Section 4.2.2.1) to 145°C (barrel entrance), 155 °C, 170 °C, 170 °C, 165 °C (barrel exit) and 160 °C (die).

5.2.2.4 Plasticising PLA with HBP

Plasticising PLA using HBP was carried out using extrusion. A predetermined amount of 1 wt % HBP relative to PLA was dissolved in 50 mL of tetrahydrofuran (THF). 500 g of PLA pellets were then added to the solution and slowly stirred until the THF was fully evaporated leaving the PLA pellets uniformly coated with HBP. The same method was repeated for 2 and 3 wt% HBP. The PLA pellets coated with HBP were extruded into sheets using the same method and temperature profile used to graft MA onto PLA.

5.2.2.5 Fabrication of Composite Material

Prior to fabrication, fibre mats, PLA and PLA with coupling agent or plasticiser sheets were dried at 105 °C, 60 °C and 60 °C respectively for at least 4 hours. Only composites with 20 wt% fibre content were prepared for this work based on that gave the best combination of tensile strength and processing convenience as noted in Chapter 4. Composite processing was conducted according to the method described in Section 4.2.2.4.

5.2.2.6 Assessment of Composite Morphology

The microstructure of the fractured surfaces of the tensile tested samples was observed using a Hitachi S-4700 scanning electron microscope (SEM). The samples were coated with a thin layer of platinum prior to observation at an accelerating voltage of 20 kV similar to the method described in section 4.2.2.5.

5.2.2.7 Tensile Testing of Composites

Tensile testing for all composites was conducted following the method described in Section 4.2.2.6. Five samples from respective treatments were tested and the tensile strengths averaged. Details and abbreviations of the specimens used can be seen in Table 5.1. Harakeke and hemp fibre composites using HBP were denoted as HR/HM-HBP-XX, with XX represents the amount of HBP relative to the amount of PLA.

Table 5.1: Abbreviations used for PLA and composite samples

Sample	Abbreviation
Neat PLA	PLA
Alkali treated harakeke composite	HR - ALKALI
Alkali-silane treated harakeke PLA composite	HR - SILANE
Alkali-peroxide treated harakeke PLA composite	HR - PEROXIDE
MA grafted PLA harakeke composite	HR - MA-g-PLA
Alkali treated hemp composite	HM - ALKALI
Alkali-silane treated hemp PLA composite	HM - SILANE
Alkali-peroxide treated hemp PLA composite	HM - PEROXIDE
PLA grafted MA hemp composite	HM - MA-g-PLA

5.2.2.8 Impact Testing

Impact testing was carried out in accordance to the EN ISO 179 Plastics – Determination of Charpy impact strength. Dimensions of five replicate samples were 80 mm × 8 mm × 4 mm with a single notch of 0.25 mm (type A). An advanced universal pendulum impact tester POLYTEST with an impact velocity of 2.9 m/s and a hammer weight of 0.475 kg at 21°C was used.

5.2.2.9 Dynamic Mechanical Analysis (DMA)

Dynamic mechanical analysis (DMA) was carried out using a Perkin Elmer dynamic mechanical analyser (DMA 8000). Storage modulus (*E'*), loss modulus (*E''*) and tan δ were measured over a temperature range of 30 °C to 120 °C. The analysis was conducted using a single-cantilever configuration. Samples of 40 mm in length and 5 mm in width were heated at a constant rate of 2 ºC/min with an oscillating sinusoidal stress at a constant frequency of 1 Hz.

5.2.2.10 Thermogravimetric analysis (TGA)

A 15 mg sample was taken from each type of composite and analysed using an SDT 2960 Simultaneous DTA-TGA analyser as described in Section 3.2.2.5.

5.2.2.11 Swelling Studies

The interaction between fibre and matrix was assessed using swelling studies. In this work, toluene was used as a solvent because of its availability and to increase the swelling rate. Prior to sample immersion, the weights of three replicate air dried samples with dimensions of about 30 x 5 x 3 mm were determined. The samples were then immersed in toluene for 48 hours at room temperature. After immersion, the samples were wiped with a soft cloth and the weight of toluene

absorbed was recorded and averaged. The swelling index which is a measurement of the swelling resistance of the composite is calculated using the following equation [240]:

$$Swelling\ Index, \% = \frac{A_s}{W} \times 100 \quad (5.1)$$

where A_s is the amount of solvent absorbed by sample and W is the initial weight of sample before swelling.

5.3 Results and Discussion: Part I – Effect of Silane, Peroxide and MA-g-PLA on Composite Properties.

5.3.1 Composite Morphology

SEM micrographs of the fractured surfaces of tensile tested specimens for composites treated with alkali only and composites with further fibre treatments using silane and peroxide and MA grafted onto PLA (MA-g-PLA) are shown in Figures 5.1 to 5.3. As can be seen in Figures 5.1 (a) and (b) for composites with fibre treated with alkali only, reasonable wetting between fibre and PLA has been obtained as a result of alkali treatment as the observed gaps are small; smaller gaps were obtained here for harakeke and hemp fibre composites compared to that found in the literature for PLA reinforced with kenaf fibre treated with 4 wt% NaOH at room temperature suggesting better wetting [147]. It may also be seen from the figure that the gaps between harakeke fibres and PLA are smaller compared to the gaps between hemp fibres and PLA, suggesting wetting for harakeke fibre is better. Better wetting for harakeke fibre is believed to be attributed to a more uniform or rounded fibre cross-section which provides better access for the high viscosity PLA melt to impregnate around the fibre.

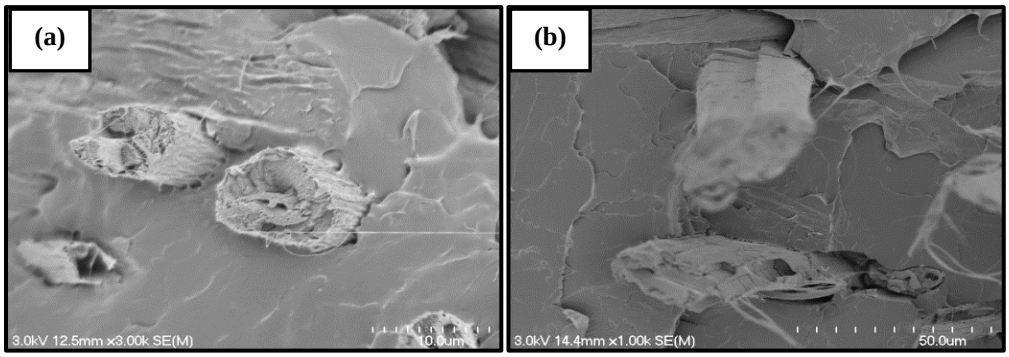

Figure 5.1: Scanning electron micrographs of fracture surfaces for composites reinforced with 20 wt% fibre treated with alkali only for: (a) Harakeke and (b) Hemp.

For composites with fibres treated using silane and peroxide shown in Figures 5.2 (a) to (d), long protruding fibres similar to composites with fibre treated with just alkali is observed, but the gaps between the fibres and matrix appeared to be slightly smaller. This suggests that the fibre wetting for fibres treated with silane and peroxide could be slightly improved from fibres treated with alkali only.

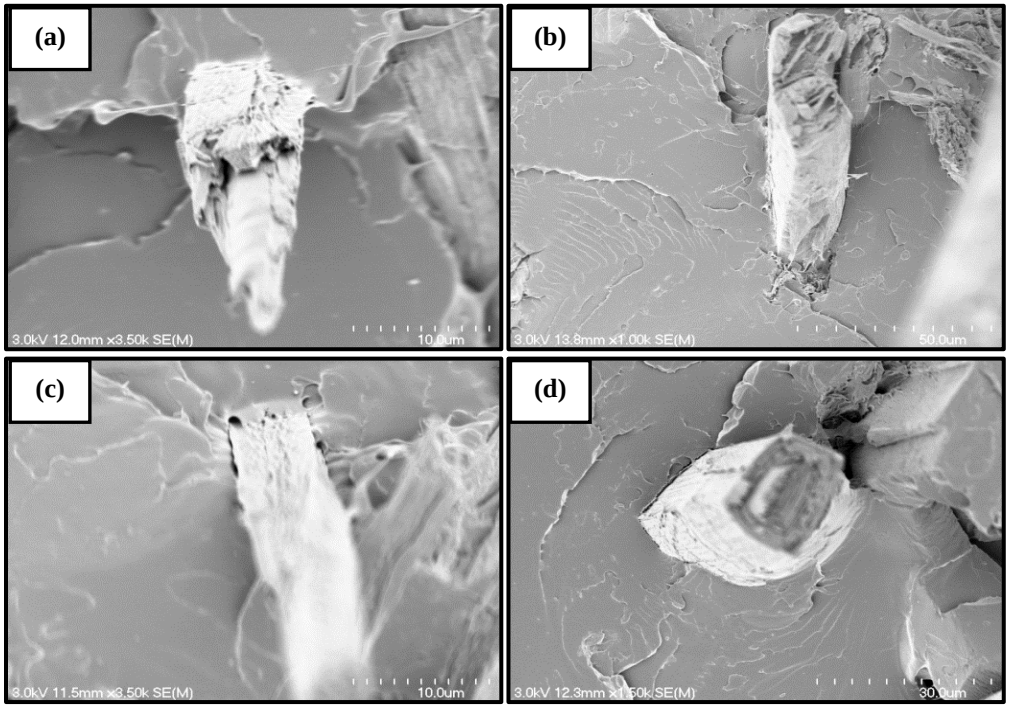

Figure 5.2: Scanning electron micrographs of fracture surfaces for composites reinforced with 20 wt% treated with: (a) and (b); silane, (c) and (d); peroxide. Figures on the left and the right represent harakeke and hemp composites respectively.

Comparing Figures 5.3 (a) and (b) for composites coupled with MA-g-PLA with composite surfaces shown in Figures 5.1 and 5.2, it is observed that composites with MA-g-PLA have shorter protruding fibres and even smaller gaps between fibres and matrix, indicating higher wetting than those composites with fibres treated with silane, peroxide and those treated with alkali only. For all composites, it may be seen that the pultruded fibres appeared to be clean, suggesting the interface is not too strong, or possibly brittle fracture of PLA has occurred close to the interface as seen elsewhere [147, 211, 241].

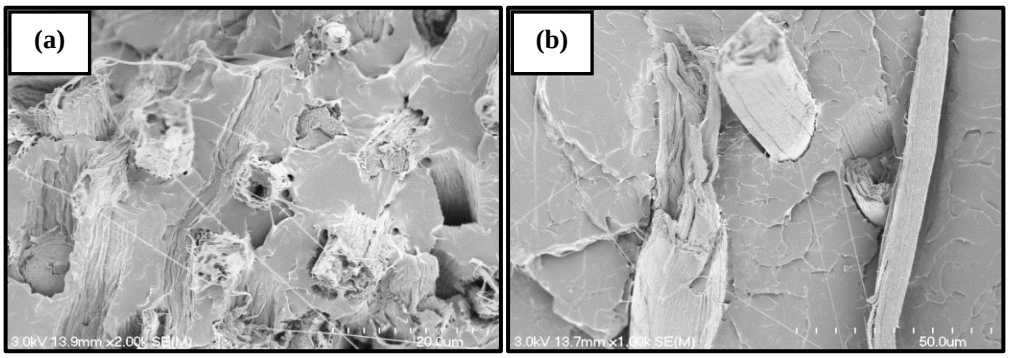

Figure 5.3: Scanning electron micrographs of fracture surfaces for composites reinforced with 20 wt% using MA-g-PLA as a coupling agent for: (a) Harakeke and (b) Hemp.

5.3.2 Swelling Studies

Swelling indices for PLA, harakeke and hemp fibre composites with and without further treatments and composites with MA grafted PLA are shown in Figure 5.4. The swelling index was highest for PLA on its own; for unreinforced polymers, the degree of swelling mainly depends on the bonding strength between their molecular chains which are weak in the case of PLA [242]. Inclusion of fibres has resulted in lower swelling index than that for neat PLA, as would be expected due to restriction from the fibres for solvent penetration [243]. Furthermore, swelling index for composites can be correlated with interfacial strength, as a weaker

interface is likely to have a higher solvent uptake due to the presence of voids between fibres and matrix.

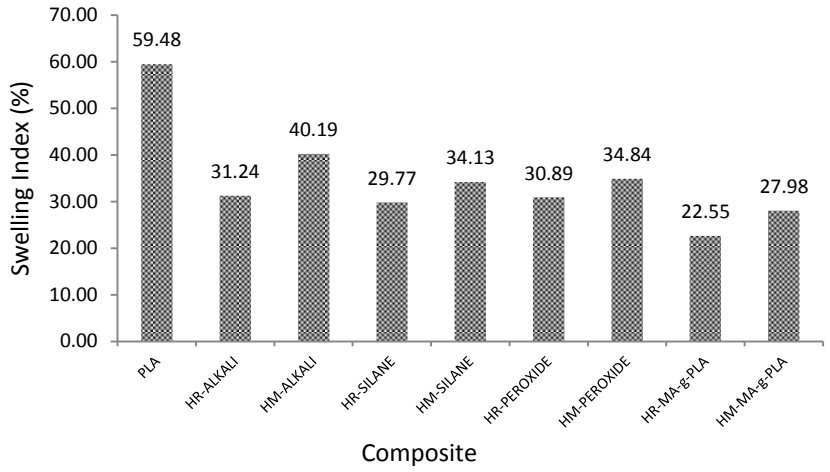

Figure 5.4: Swelling index for harakeke and hemp composites. Samples were subjected to immersion for 48 hour.

As can be seen in Figure 5.4, it is evident that the swelling indices for harakeke composites are lower compared to those of hemp composites, which can be explained by there being more fine fibres thus higher contact area between the fibres and the matrix in these composites (note that diameter of harakeke fibre is smaller compared to hemp fibre as found in Chapter 3) and were also believed due to a better fibre wetting as discussed previously. The swelling indices for composites with fibres treated using silane (HR and HM-SILANE) and peroxide (HR and HM-PEROXIDE) and composites coupled with MA-g-PLA (HR and HM-g-PLA) are lower compared to those composites treated with alkali only (HR and HM-ALKALI), supporting a further improvement for interfacial strength obtained. Excluding PLA and composites with fibres treated with alkali only, it can be seen that composites with fibres treated with peroxide has the highest swelling index followed by composites with silane treated fibres and composites

with MA-g-PLA for which swelling index is the lowest, suggesting the improvement in interfacial strength obtained for harakeke and hemp coupled with MA-g-PLA is the highest (see Figure 5.3).

5.3.3 Composite Tensile Properties

Tensile strengths for PLA, harakeke and hemp composites with fibre treated using silane and peroxide and composites coupled with MA-g-PLA are shown in Figure 5.5, with the percentage of improvement obtained from fibre inclusion, further fibre treatments and coupling agent being tabulated in Table 5.2, along with those values for composites treated with alkali only for comparison. It can be clearly observed that incorporation of the fibres into PLA increased tensile strengths of composites significantly as discussed previously in Chapter 4.

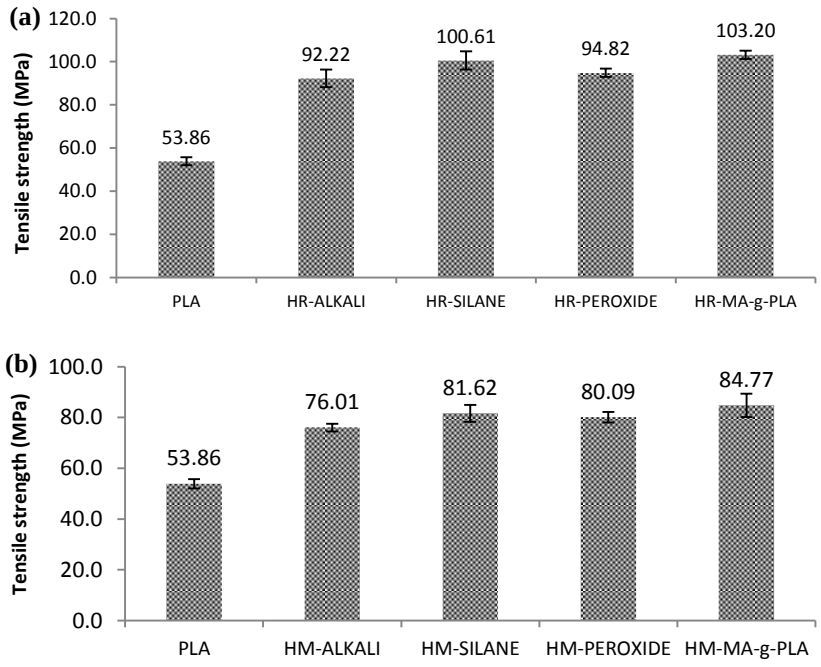

Figure 5.5: Tensile strength of harakeke (a) and hemp (b) composites as a function of various chemical treatments. Error bars each corresponds to a standard deviation.

Average tensile strengths for harakeke and hemp composites with fibre treated using silane, peroxide and composites coupled with MA-g-PLA were higher compared to those composites treated with alkali only. Harakeke and hemp composites treated with peroxide have the lowest tensile strengths, increased only by 2.8 and 5.4% respectively compared to those respective composites with fibres treated using alkali only.

Table 5.2: Improvements in tensile strengths of coupled composites over PLA and uncoupled composites

Sample	Tensile strength (MPa)	Improvement over PLA (%)	Improvement over composite treated with alkali only (%)
PLA	53.86	-	
HR - ALKALI	92.22	71.22	-
HR - SILANE	100.61	86.80	9.10
HR - PEROXIDE	94.82	76.05	2.82
HR – MA-g-PLA	103.20	91.61	11.91
HM - ALKALI	76.01	41.13	-
HM - SILANE	81.62	51.54	7.38
HM - PEROXIDE	80.09	48.70	5.37
HM - MA-g-PLA	84.77	57.39	11.52

Improvement of tensile strength for harakeke composites, however, was found to be statistically insignificant using the Student's *t*-test when compared with that of composites treated with alkali only, but comparable to those seen in the literature for sisal [244] and jute fibre [123] fibres and higher than that for ramie [245], flax [128] and kenaf [246] fibres reinforced PLA composites. Small differences in tensile strengths for composites treated with peroxide obtained from various

studies seen in the literature are believed to be due to different amount of hydroxyl groups available for bonding on fibre surfaces as well as different amount of peroxide used for treatment, in which could influence the decomposition of free radicals (RO) to react with fibre and matrix [244].

The second highest improvement was obtained for composites with fibres treated using silane; increased by 9.1 and 7.4% for harakeke and hemp composites respectively, relative to composites with fibres treated with alkali only. Improvement in tensile strength for composites with fibres treated using silane highlighting that, the amount of silane used in this work did not exceed the optimum silane content and believed only a single layer polysiloxane network on fibre surfaces was formed [247].

The highest improvement obtained here for tensile strength of composites coupled with MA-g-PLA supports the result obtained in SEM and swelling studies, believed to be attributed to the highest improvement for interfacial shear strength between fibre and the matrix that facilitates more stress transfer through bonding to the fibres, due to the presence of MA monomers which reacted with the hydroxyl group present in the fibre surfaces [248]. From the table, it can be seen that tensile strength for harakeke and hemp fibre composites coupled with MA-g-PLA increased to 103.2 and 84.77 MPa respectively; these were approximately 11.91% and 11.52% higher than the respective composites treated with alkali only and about 91.6% and 57.4% higher than PLA. However, it is acknowledged that reduction in tensile strength for other natural fibre PLA composites using MA-g-PLA has been reported elsewhere [249], believed to be due to non-homogeneous

mixture between the composite materials and coupling agent. Improvements obtained in this study for composites treated with MA-g-PLA were found higher than for ramie fibre PLA composites [250] and slightly lower than those obtained for bamboo fibres PLA composites [133] and sisal fibres PLA composites [251] reported elsewhere.

Figure 5.6 shows Young's moduli for PLA and all composites tested. It may be seen that, only slight improvement in Young's modulus for composites with fibres treated with silane and peroxide and composites coupled with MA-g-PLA is obtained; similar to those reported in previous work for other natural fibre composites [133, 250], suggesting that the improvement in interfacial strength did not greatly influence the Young's modulus for composites at the same fibre content.

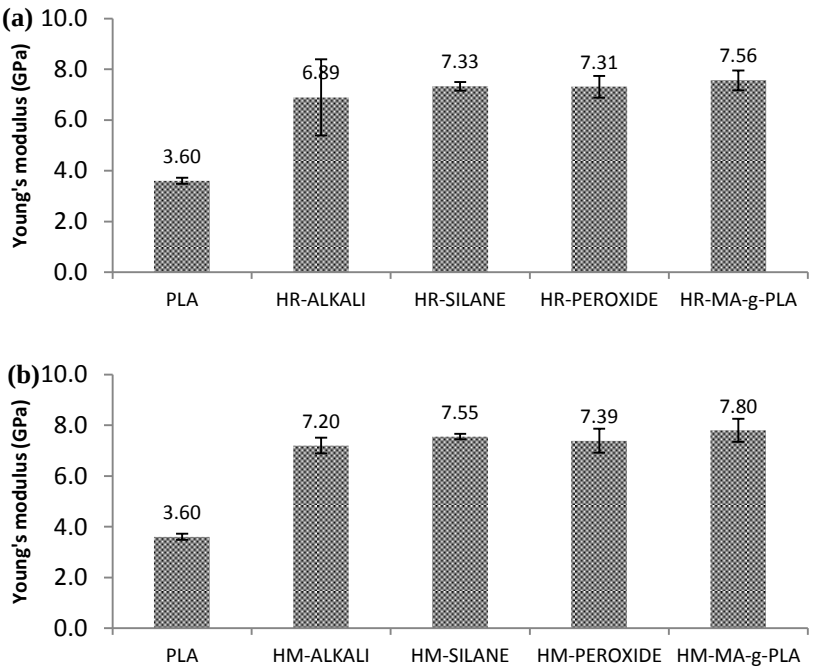

Figure 5.6: Young's modulus of harakeke (a) and hemp (b) composites as a function of various chemical treatments. Error bars each corresponds to one standard deviation.

Failure strains for all harakeke and hemp composites, along with PLA are shown in Figure 5.7. It can be seen that inclusion of harakeke and hemp fibres treated using just alkali increased failure strain for harakeke composites but decreased it for hemp composites. This is not surprising given the higher (3.95%) and lower (1.58%) average failure strains of harakeke and hemp fibres relative to the failure strain of PLA, respectively. Indeed, failure strain for hemp composites with fibres treated with just alkali can be seen to be even lower compared to the average failure strain of hemp fibres. Failure at low strain for hemp composites could possibly be attributed to the facture of fibres at failure strains lower than the average failure strain (it is known that there is a distribution of failure strains). However, it could also be related to lower interfacial strength between fibres and matrix, at which fibre debonding occurred at failure strain levels lower than the average failure strain for hemp fibres, causing matrix cracking and composite failure, which is supported by pull-out of fibres. Increased interfacial strength reduces the potential of fibre debonding and would allow fibres having failure strain higher than the average fibre failure strain to be loaded to the higher strain level prior to matrix cracking, leading to a higher composites failure strain.

Furthermore, additional fibre treatments using silane and peroxide and using MA-g-PLA as coupling agent increased the failure strain of composites considerably (similar to the improvement seen previously for tensile strength) and following the order of presumed interfacial strength discussed from swelling experimentation, with only composites containing hemp fibres treated using peroxide (that suspected to have the second lowest interfacial strength after just alkali treatment) retaining a failure strain less than that for PLA. Using silane,

peroxide and MA-g-PLA as additional fibre treatments, composite failure strain increased by 11, 19 and 30%, respectively for harakeke composites and by 13, 24 and 30% respectively for hemp composites compared to those composites with fibres treated by alkali only.

A further contribution to increased failure strain seen for both harakeke and hemp composites coupled with MA-g-PLA is believed to be the plasticisation effect of PLA [250], which may be associated with unreacted MA monomer playing a role as plasticiser and increasing the mobility of the PLA chain [250], as seen for other natural fibre PLA composites coupled with MA-g-PLA reported elsewhere [133, 250, 252], along with the improved interfacial strength.

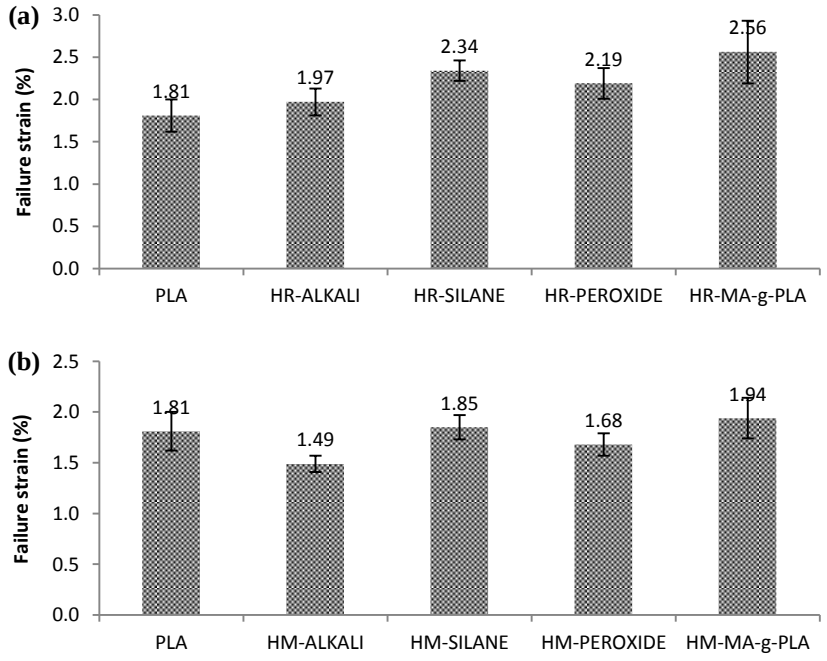

Figure 5.7: Failure strain harakeke (a) and hemp (b) composites as a function of various chemical treatments. Error bars each corresponds to one standard deviation.

5.3.4 Dynamic Mechanical Analysis (DMA)

Storage modulus and tan δ for harakeke and hemp fibre composites using different chemical treatments are shown in Figures 5.8 and 5.9 along with PLA only for comparison. It is obvious in Figure 5.8 that storage moduli for harakeke and hemp composites are higher than that of PLA only. Inclusion of fibres increases the storage modulus of composites due to increased composite stiffness as a result of decreased polymer chain mobility [86, 253]. Here, improved composite stiffness as a result of composite treatments can be seen even more clearly compared to those seen for composite Young's modulus. Storage modulus for composites with additional chemical treatments are higher than that for composites using only alkali treatment, supporting the higher stress transfer from the matrix to the fibre as a result of improved interfacial strength [91]. This is in agreement with swelling index and tensile properties discussed previously.

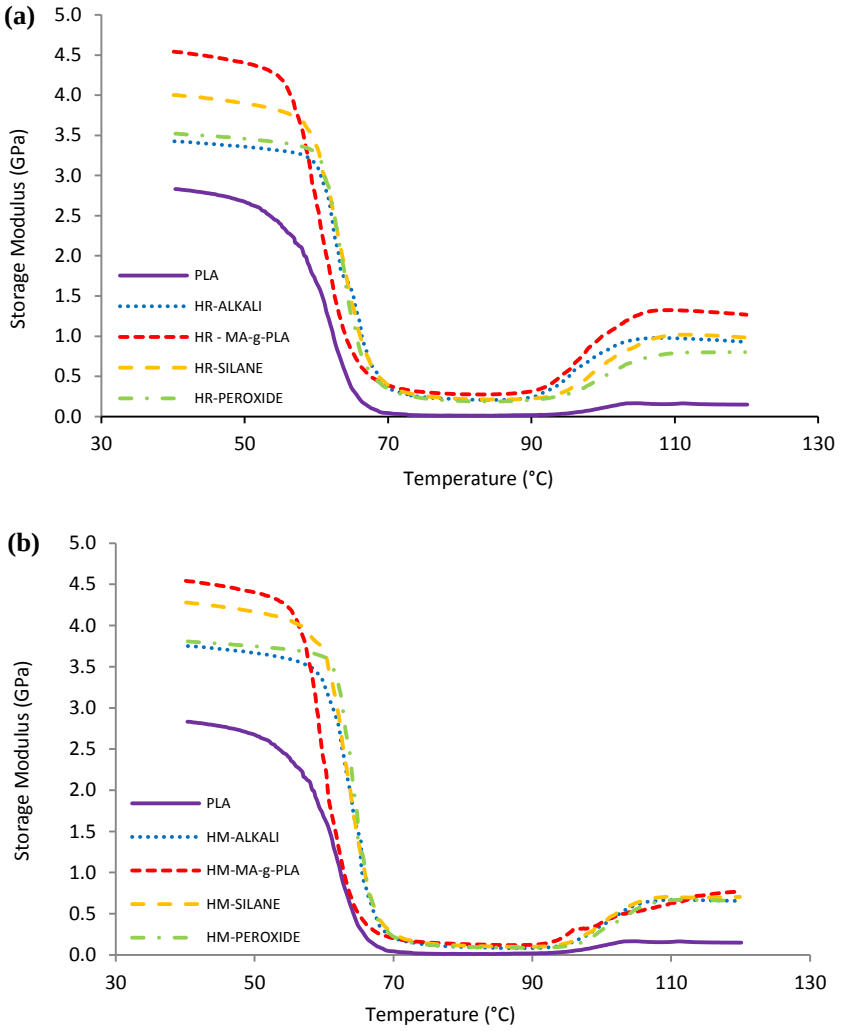

Figure 5.8: Influence of fibre inclusion and coupling agents on the storage modulus for harakeke and hemp fibre composites.

It can be seen from Figure 5.8, the storage modulus at 40 °C increased from 2.85 GPa for neat PLA to 3.5, 3.6, 4.0 and 4.6 GPa for composites with fibres treated using alkali only, composites with fibres treated using peroxide, composites with fibres treated using silane and composites coupled with MA-g-PLA respectively. For hemp fibre composites, storage modulus increase from 2.85 GPa for PLA to 3.7, 3.8, 4.4 and 4.6 GPa for composites with fibres treated using alkali only, composites with fibres treated using peroxide, composites with fibres treated using silane and composites coupled with MA-g-PLA respectively.

Decreasing storage modulus with increasing temperature was observed in the region between 50 °C and 70 °C, which is attributed to the softening effect of PLA due to polymer chain relaxation at the glass transition temperature (T_g) [91]. It can be seen that harakeke and hemp composites coupled with MA-g-PLA have the lowest softening temperatures, which is again attributed to plasticisation effect of PLA discussed previously, consistent to that trend reported in the literature for PLA composites coupled with MA-g-PLA [250, 253, 254]. Increase in storage modulus was observed after 90 °C due to the effect of cold crystallisation which is typically observed for PLA [246, 255].

The variations for tan δ at difference temperatures for PLA and all composites studied are shown in Figure 5.9. As expected, tan δ for PLA was found to be the highest indicating the highest degree of molecular chain mobility. Inclusion of fibres greatly decreases the values of peak tan δ due to the restriction to molecular chains mobility. For both harakeke and hemp composites, it may be seen that, the values of peak tan δ in descending order from the highest is composites with fibres treated using alkali, followed by composites with fibres treated using peroxide, followed by composites with fibres treated using silane and composites coupled with MA-g-PLA is the lowest, apparently relating to improved interfacial strength.

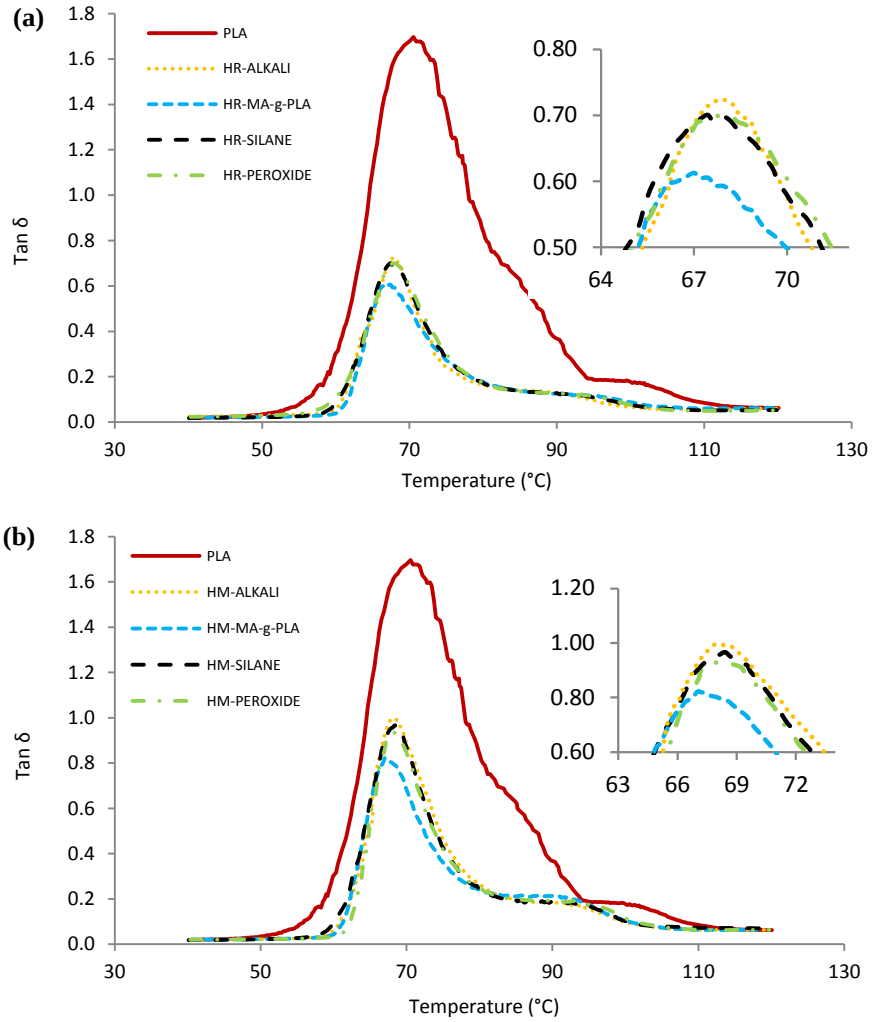

Figure 5.9: Influence of fibre inclusion and coupling agents on tan δ for harakeke and hemp fibre composites.

The lowest value of peak tan δ for composites treated with MA-g-PLA, seen for both harakeke and hemp composites, supports the highest improvement in composite stiffness as a result of higher interfacial strength between the fibres and matrix [256], highlighting that the improvement in interfacial bonding outweighed the effect of plasticisation. Indeed, it is also noticeable that the peak temperatures of tan δ for both harakeke and hemp fibre composites treated with MA-g-PLA are lower compared to other composites, revealing the effect of plasticisation could also reduce the T_g, of the matrix, as seen elsewhere [257].

5.3.5 Thermogravimetric analysis (TGA)

Thermogravimetric (TGA) curves for fibre, PLA and PLA composites are shown in Figure 5.10. Clearly, it is observed that harakeke and hemp fibres degraded at the lowest temperatures, particularly harakeke fibre. It may also be seen that PLA has only a single major decomposition step, displaying an onset temperature of 330 °C and final decomposition at 380 °C. For all harakeke and hemp fibre composites, there is a minor second decomposition step, which is attributed to the inclusion of fibres (and seen for the fibres on their own). It has been shown that, inclusion of fibre would generally decrease thermal stability of composites [125, 169, 258]. However here, inclusion of harakeke and hemp fibres has only a minor influence on the overall thermal stability of composites, supporting good compatibility between the fibre and the matrix [250].

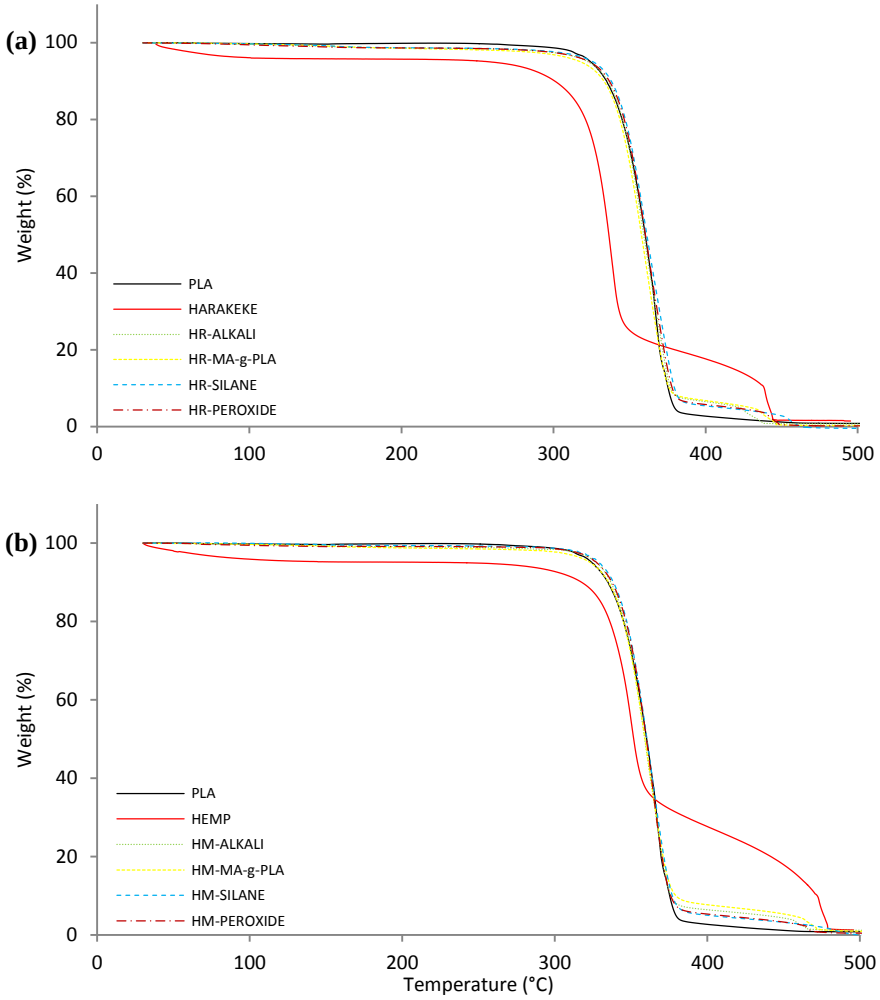

Figure 5.10: Thermogravimetric (TGA) curves fibres, PLA and PLA composites: (a) harakeke and (b) hemp composites.

The temperatures and residual weight of PLA and composites at different stages of thermal degradation are tabulated in Table 5.3. It is observed that at three different weight losses studied (10, 50 and 90%), the respective degradation temperatures for harakeke and hemp fibre composites in descending order is for composites with fibres treated using silane, followed by composites with fibres treated using peroxide, followed by composites with fibres treated using alkali only and followed by composites coupled with MA-g-PLA, whose degradation temperatures is the lowest. The order of reduction in thermal stability is consistent with the improvement obtained for interfacial strengths, except for composites

coupled with MA-g-PLA, which could be associated to a decreased molecular weight of the matrix as a result of unreacted MA monomer and possible molecular chain scission of PLA influencing thermal stability of the composites [259, 260]. However, the residue weights for composites with MA-g-PLA at 400 °C were seen to be higher compared to other composites, supporting a higher interfacial strength between fibres and matrix [246].

Table 5.3: Summary of TGA results for PLA and harakeke and hemp composites.

PLA and Composite sample	T_{10}/°C	T_{50}/°C	T_{90}/°C	Residue weight (%) at 400°C
PLA	334.68	360.29	375.12	2.70
HR-ALKALI	335.36	359.27	377.02	5.38
HR-SILANE	337.83	361.13	379.33	5.82
HM-PEROXIDE	336.37	360.15	377.98	5.72
HR-MA-g-PLA	333.05	357.50	376.87	6.75
HM-ALKALI	336.62	358.82	375.92	5.01
HM-SILANE	338.18	360.40	379.93	6.43
HM-PEROXIDE	337.50	359.95	375.79	5.32
HM-MA-g-PLA	333.75	358.00	373.33	7.70

T_{10}/°C, T_{50}/°C and T_{90}/°C means temperature at 10, 50 and 90% weight loss.

5.4 Results and Discussion: Part II – Effect of Plasticiser.

5.4.1 Composite Morphology

Figure 5.11 shows SEM micrographs of the tensile fracture surfaces of harakeke and hemp composites plasticised using HBP. It is observed that generally, all plasticised composites exhibited longer protruding fibres compared to those without plasticiser (see Figure 5.1). Visible gaps between the fibre and matrix as

well as voids from where fibres had pulled out are also observed, indicating a weak interface between fibres and matrix. However, the gaps here are smaller compared to those observed for other natural fibre plasticised PLA composites [212, 261, 262], suggesting increased wetting of harakeke and hemp fibres obtained in this work, benefitted from the alkali treatment.

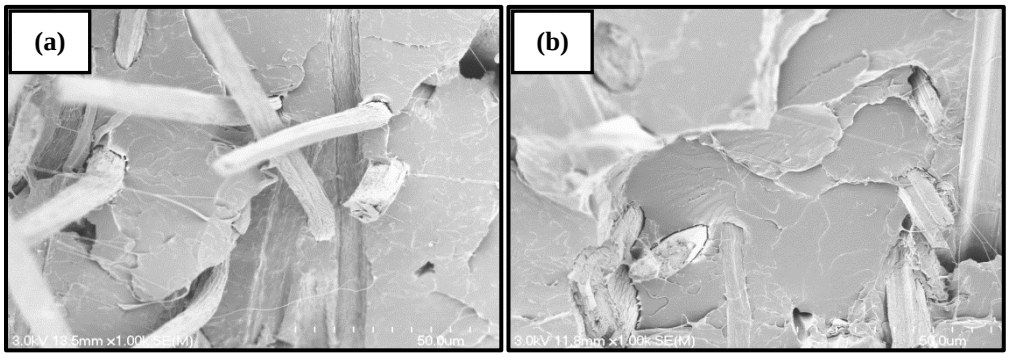

Figure 5.11: Scanning electron micrographs of fracture surfaces for composites reinforced with 20 wt% plasticised using HBP: (a) harakeke and (b) hemp.

Figure 5.12 represents higher magnification SEM micrographs of the tensile fracture surfaces of plasticised harakeke and hemp composites. As shown in Figure 5.12 (a), most of the PLA sample surfaces were relatively flat and smooth, which is an indication of brittle failure [135]. Figure 5.12 (b) shows the surface of composites with 3 wt% HBP, showing many circular features, believed to be precipitates of immiscible of HBP (some indicated by arrows), which is more likely to occur at higher HBP contents as seen elsewhere [263]. The plasticised composite surfaces appeared to be slightly rougher compared to neat PLA, which is suggestive of ductile behaviour [137], consistent with composites surfaces observed elsewhere [135, 137, 263, 264]. It may also be seen from the figure that, these HBP precipitates are uniformly dispersed, suggesting uniform distribution of HBP occurred during extrusion.

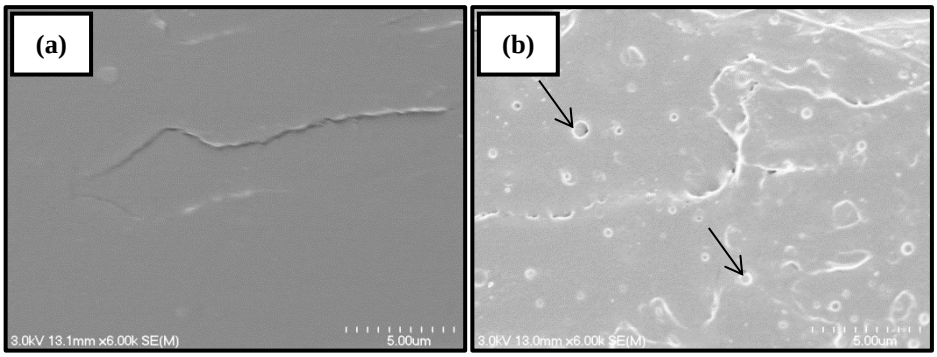

Figure 5.12: High-magnification scanning electron micrographs of fracture surfaces for composites reinforced with 20 wt% fibre looking between fibres showing: (a) surface of composite without HBP and (b) surface of composite with 3% HBP.

5.4.2 Composite Tensile Properties

Stress versus strain curves for the composites with various HBP contents is shown in Figure 5.13 and details of tensile properties are tabulated in Table 5.4. Harakeke and hemp fibre composites without plasticiser can be seen to fail without noticeable yielding with low failure strain (Figure 5.13) indicating typical brittle failure, as discussed in Chapter 4. It is observed that addition of HBP decreased the gradient of the stress-strain curves and composite tensile strengths, but increased failure strain of both harakeke and hemp composites.

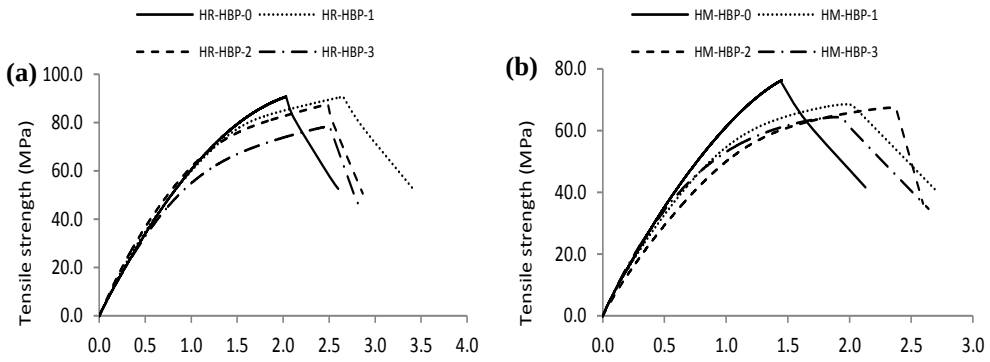

Figure 5.13: Typical stress versus strain curves for samples reinforced with 20 wt% fibre plasticised using various HBP contents: (a) harakeke and (b) hemp composites.

Decreased gradient of the stress-strain curves observed for all plasticised composites, particularly at higher strain level may be attributed to possible onset of fibre debonding and/or matrix cracking.

It can be seen from Table 5.4, addition of 1 wt% HBP to harakeke and hemp fibre composites reduced tensile strengths by approximately 3.5 and 11% respectively, while addition of 2 wt% HBP reduced the tensile strength of harakeke and hemp composites by 7 and 15% respectively, compared to those composites without plasticiser. A higher reduction of tensile strength was obtained for composites plasticised using 3% HBP, at which the tensile strength decreased by almost 15 and 18% for harakeke and hemp composites respectively, relative to those composites without plasticiser. Reduction in composite tensile strengths seen for both harakeke and hemp plasticised composites is attributed to a weaker interface between fibres and matrix indicated by big gaps (see Figure 5.14). However, it has been found elsewhere that using other plasticisers decreased composite tensile strengths even more significantly (up to more than 100%) [206, 212, 262], attributed to even weaker interface.

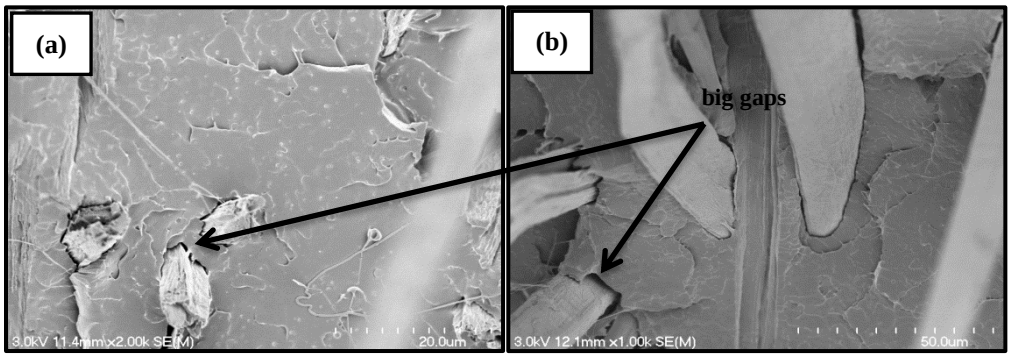

Figure 5.14: Scanning electron micrographs of fracture surfaces for composites reinforced with 20 wt% plasticised using 3 wt%HBP: (a) harakeke and (b) hemp.

Addition of 1 wt% HBP increased the failure strain of harakeke and hemp composites by nearly 25 and 35% compared to composites without HBP, while with 2 wt% of HBP, failure strains of harakeke and hemp composites increased by 35 and 52% respectively. However, a smaller increase of failure strain was obtained for composites with 3 wt% HBP than composites plasticised with 1 and 2wt% HBP, which is attributed to matrix weakening due to weaker intermolecular bonding of PLA. From the presented result, it can be acknowledged that 2 wt% of HBP can be used to effectively increase failure strains of harakeke and hemp fibre composites without greatly reduce composite tensile strength.

Table 5.4: Tensile properties of harakeke and hemp fibre composites with various plasticiser. Standard deviations are included in parenthesis.

Composite Sample	Tensile Strength (MPa)	Young's Modulus (GPa)	Failure Strain (%)
HR-HBP-0	92.22 (4.07)	7.64 (1.50)	1.97 (0.16)
HR-HBP-1	88.93 (1.25)	7.13 (0.21)	2.49 (0.17)
HR-HBP-2	85.56 (4.18)	6.81 (0.08)	2.65 (0.18)
HR-HBP-3	79.92 (1.91)	6.65 (0.04)	2.59 (0.09)
HM-HBP-0	76.01 (1.50)	7.02 (0.31)	1.49 (0.08)
HM-HBP-1	68.26 (2.97)	6.60 (0.39)	2.02 (0.32)
HM-HBP-2	66.92 (2.41)	6.27 (0.33)	2.27 (0.07)
HM-HBP-3	64.35 (1.89)	5.87 (0.24)	1.93 (0.16)

5.4.3 Composite impact strength

Figure 5.14 shows the effect of HBP on the notched impact strength of harakeke and hemp fibre composites. It can be seen that using HBP as a plasticiser increases impact strength of composites significantly, which can be attributed to interfacial weakening, as highlighted by SEM micrographs (Figure 5.14) and better fibre alignment for harakeke and hemp composites obtained here compared

to that obtained for composites produced using injection moulding, composites making crack propagation more difficult. Increased impact strength with the addition of HBP could also be attributed to a reduction in crystallinity of PLA [135]. From Figure 5.14, it may be seen that, with addition of 3 wt% HBP, impact strength for harakeke and hemp composites improved by 49 and 63% respectively. Substantial improvements obtained in this work are higher than those found in the literature for other natural fibre PLA composites with HBP produced using injecting moulding, supporting the influence of fibre alignment [265].

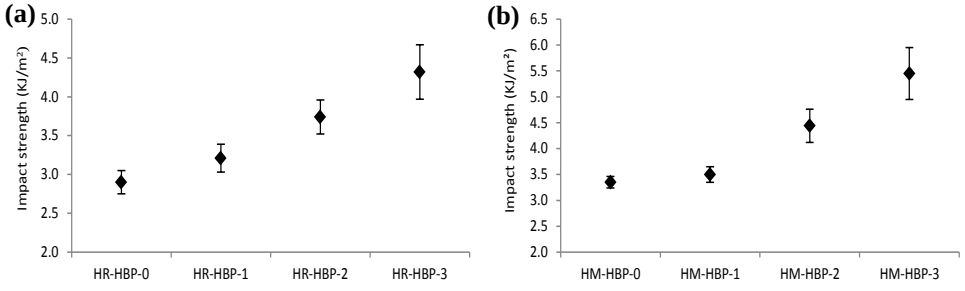

Figure 5.14: Notched impact strength for samples reinforced with 20wt% fibre plasticised using HBP with: (a) harakeke (b) hemp.

5.5 Chapter Conclusions

Silane, peroxide and MA-g-PLA have been employed to improve the tensile properties, while HBP was used to reduce the brittleness of harakeke and hemp fibre composites. Improved interfacial bonding for composites with fibres treated using silane and peroxide and composites coupled with MA-g-PLA is supported by lower swelling indices, higher tensile strengths and lower tan δ compared to those composites with fibres treated using alkali only. Harakeke and hemp fibre composites with MA-g-PLA exhibit the highest tensile strength followed by silane

and then peroxide. Addition of a HBP as plasticiser reduced the brittleness of harakeke and hemp fibre composites considerably. Addition of 2% HBP to composites increased failure strain by 35 and 52% respectively for harakeke and hemp composites. Furthermore, impact strengths of harakeke and hemp composites were also improved by up to 49 and 63% respectively, without greatly influencing composite tensile strength, suggesting that HBP can be effectively used to reduce the brittleness of PLA composites.

CHAPTER 6

Conclusions

6.1 Effects of Alkali Treatment

A series of alkali treatments were employed in order to improve fibre separation and interfacial bonding between fibres and the matrix. It was found that 5 wt% NaOH/2 wt% Na_2SO_3 and 5 wt% NaOH fibre treatments could be used to effectively remove non-cellulosic materials and separate harakeke and hemp fibres, respectively, from their bundles without greatly reducing the fibre tensile strength. Decreases of tensile strength by 3 and 15% compared to untreated fibres occurred for harakeke and hemp fibres respectively. Alkali treatments exposed a rougher texture with a large numbers of grooves. The crystallinity index (I_c) for harakeke fibres increased from 69% (untreated) to 86% (treated with 10 wt% NaOH). The crystallinity index (I_c) for hemp fibres increased from 77% (untreated) to 90% (treated with 5 wt% NaOH). Increased crystallinity index (I_c) is attributed to the removal of amorphous materials such as lignin, hemicellulose and wax allowing improved packing and alignment of micro fibrils. Insignificant change was found for Young's modulus of harakeke fibres but large increases in Young's modulus for all treated hemp fibres were obtained; at optimum alkali treatment, Young's modulus was found increased from 20.9 GPa for untreated fibre to 28.9 GPa. Higher increase in Young's modulus for hemp fibres is believed to be due the removal of greater amounts of non-cellulosic materials from hemp fibres compared to harakeke fibres, supported by greater reduction in fibre diameters.

Thermal stability of treated fibres was found improved with alkali treatment. The degradation temperatures at all stages of thermal degradation for treated fibres were consistently higher than those for untreated fibres. Onset fibre degradation for alkali treated harakeke and hemp fibres were seen increase from 250 °C for untreated fibres to about 300 °C for treated fibres. Increased onset temperature again supports the removal of non-cellulosic materials which have lower thermal stability.

6.2 Effects of Fibre Orientation and Fibre Content

The alignment of fibres in mats produced using a DSF and the tensile strength of PLA matrix composites reinforced using these fibre mats with different fibre contents were investigated. Visual inspection supported that alignment of harakeke and hemp fibre produced using a DSF had occurred. This led to lower minimum and critical fibre volume fractions for reinforcement. Using a DSF also led to better fibre dispersion compared to that for fibre mats produced by straining suspended fibre.

High fibre orientation factor (K_o) determined using the Bowyer-Bader confirmed the improvement of fibre alignment obtained using a DSF. The highest K_o values for harakeke and hemp were found to be 0.583 and 0.438 respectively, higher than those values for composites prepared using injection moulding and hot pressed using randomly oriented fibre mats (0.24 – 0.375), but slightly lower compared to the values obtained with aligned flax/polypropylene nonwoven preforms (0.45 – 0.6). K_o values were found to decrease as the fibre content increased, believed to be due to the higher pressure required with higher fibre content during processing

resulting in fibre misalignment. However, higher pressure for higher fibre contents resulted in increased interfacial shear strength.

Tensile strength of composites tested parallel to the main fibre alignment direction were higher than for composites tested perpendicular to the fibre direction supporting the influence of improved fibre alignment. At 30 wt% and 25 wt% fibre content, tensile strengths for harakeke and hemp composites tested parallel to the main fibre alignment direction were found increased up to 101 and 87 MPa respectively, from 53.8 MPa for PLA only; indeed, tensile strengths for harakeke and hemp fibre composites obtained in this work are higher than tensile strengths of any other PLA reinforced discontinuous natural fibre composites at the same fibre content. Young's moduli for harakeke and hemp fibre composites were found increased up to 8 GPa (30wt% fibre) and 9.7 GPa (40wt% fibre) respectively, from 3.6 GPa for neat PLA.

6.3 Effect of Fibre Surface Treatment, Coupling Agents and Plasticiser

The effect of fibre treatments, coupling agent and plasticiser on the mechanical performance of PLA composites reinforced with 20 wt% fibre were evaluated. Improvement in interfacial bonding using silane and peroxide treatments and coupling with MA-g-PLA was supported by lower swelling indices, higher tensile strength, storage modulus and lower tan δ compared to those composites with fibres treated using just alkali. The highest reduction in swelling index, increase in tensile strength and lowest tan δ was obtained for composites coupled with MA-g-PLA suggesting this gave the highest interfacial strength. The highest composites

strength was obtained for composites coupled with MA-g-PLA, followed by composites with fibres treated with silane and then composites with fibres treated with peroxide for both harakeke and hemp fibre composites. Tensile strength for harakeke and hemp fibre composites coupled with MA-g-PLA increased from 92 to 103 MPa and from 76 to 85 MPa respectively. Fibre treatments using silane and peroxide and using MA-g-PLA as a coupling agent also increased the failure strain of composites by 11, 19 and 30% for harakeke composites and by 13, 24 and 30% for hemp. Increased failure strains obtained here were believed to be attributed to the improved interfacial strength and plasticisation of PLA in the case of MA-g-PLA.

The storage modulus for harakeke and hemp composites with fibres treated using peroxide and silane and composites coupled with MA-g-PLA increased from 3.5 GPa for composites with fibres treated using just alkali to 3.6, 4.0 and 4.6 GPa and from 3.7 GPa (composites with fibres treated using just alkali) to 3.8, 4.4 and 4.6 GPa, respectively; the trend being the same as that for Young's modulus. The values of peak tan δ were decreased from 0.72 (alkali only) and 0.6 (MA-g-PLA) for harakeke and from 1 (alkali only) and 0.81 (MA-g-PLA) for hemp respectively.

TGA analysis showed that composites coupled with MA-g-PLA had lower thermal stability than composites with fibres treated using silane peroxide and alkali only. This was thought to be related to decreased molecular weight of the matrix attributed to unreacted MA monomer as well as molecular chain scission occurring during composite processing, but the residual weights for composites

with MA-g-PLA at 400 °C were found higher compared to other composites, believed to be due to a higher interfacial strength between fibres and matrix.

The failure strain of plasticised composites was found increased greatly without a great decrease of composite tensile strength; addition of 2% HBP increased failure strain of harakeke and hemp composites by 35 and 52% respectively. At the same HBP content, tensile strength for harakeke and hemp composites was found decreased from 92 and 86 MPa to 76 and 67 MPa respectively. Reduction in composite tensile strengths seen in this work, however, are less than those seen for PLA composites plasticised using other plasticisers. It was also found that impact strength for plasticised harakeke and hemp composites greatly increased with addition of HBP. The highest improvement in impact strength for plasticised harakeke and hemp composites was found to be 49 and 63% respectively, relative to composites without plasticiser. This large improvement in impact strength together with lower reduction in composite tensile strength suggests that HBP could be used to effectively reduce the brittleness of PLA.

Based on the presented results, it is believed that the research objectives set at the beginning of this study have been met upon the completion of this study. It can be conclusively said that fibre mats produced using a DSF can effectively increase the potential of harakeke and hemp to be used in broader applications as a result of improved composite mechanical properties due to improved fibre alignment. Depending on the application, where higher composite stiffness and tensile and impact strengths are required, the additional treatment using MA-g-PLA and HBP can be used.

CHAPTER 7

Recommendations and Future Works

The results obtained during the course of this research have laid an important platform to further improve the properties of discontinuous harakeke and hemp fibres reinforced PLA composites. Some recommendations for future work have been proposed:

- In this work, harakeke and hemp fibres were only cut into a maximum length of 8 mm prior to alkali treatment. Effect of different fibre lengths on fibre orientation and composite mechanical properties could be further investigated.
- Harakeke and hemp fibre mats in this work were produced using a dynamic sheet former (DSF) using constant parameters. The influence of different parameters such as drum rotation speed, pump speed and thickness of fibre mats on fibre alignment and composite mechanical properties could be investigated.
- Peroxide, silane and MA-g-PLA were found to be successfully improving mechanical properties of harakeke and hemp PLA composites as a result of improved interfacial strength. The use of combination of these treatments could be investigated.

References

1. Burgueno, R., et al., *Sustainable cellular biocomposites from natural fibers and unsaturated polyester resin for housing panel applications.* Journal of Polymers and the Environment, 2005. **13**(2): p. 139-149.
2. Dittenber, D.B. and H.V.S. GangaRao, *Critical Review of Recent Publications on Use of Natural Composites in Infrastructure.* Composites Part A: Applied Science and Manufacturing, 2011.
3. Stamboulis, A., et al., *Environmental durability of flax fibres and their composites based on polypropylene matrix.* Applied Composite Materials, 2000. **7**(5): p. 273-294.
4. Bodros, E., et al., *Could biopolymers reinforced by randomly scattered flax fibre be used in structural applications?* Composites Science and Technology, 2007. **67**(3): p. 462-470.
5. Brouwer, W., *Natural fibre composites: where can flax compete with glass?* Sampe Journal, 2000. **36**(6): p. 18-23.
6. Dweib, M., et al., *All natural composite sandwich beams for structural applications.* Composite structures, 2004. **63**(2): p. 147-157.
7. Satyanarayana, K., et al., *Fabrication and properties of natural fibre-reinforced polyester composites.* Composites, 1986. **17**(4): p. 329-333.
8. Wambua, P., J. Ivens, and I. Verpoest, *Natural fibres: can they replace glass in fibre reinforced plastics?* Composites Science and Technology, 2003. **63**(9): p. 1259-1264.
9. Zini, E. and M. Scandola, *Green composites: An overview.* Polymer Composites, 2011.
10. Drzal, L., et al. *Biobased structural composite materials for housing and infrastructure applications: opportunities and challenges*. in *Proceedings of the NSF Housing Research Agenda Workshop*. 2004.
11. Ibrahim, N.A., et al., *Poly (lactic acid)(PLA)-reinforced kenaf bast fiber composites: the effect of triacetin.* Journal of Reinforced Plastics and Composites, 2010. **29**(7): p. 1099-1111.
12. Yu, H., K. Potter, and M. Wisnom, *A novel manufacturing method for aligned discontinuous fibre composites (High Performance-Discontinuous Fibre method).* Composites Part A: Applied Science and Manufacturing, 2014. **65**: p. 175-185.
13. Zhang, L. and M. Miao, *Commingled natural fibre/polypropylene wrap spun yarns for structured thermoplastic composites.* Composites Science and Technology, 2010. **70**(1): p. 130-135.

14. Joseph, P., K. Joseph, and S. Thomas, *Effect of processing variables on the mechanical properties of sisal-fiber-reinforced polypropylene composites.* Composites Science and Technology, 1999. **59**(11): p. 1625-1640.

15. Chen, C.-S., et al., *Optimization of the injection molding process for short-fiber-reinforced composites.* Mechanics of Composite Materials, 2011. **47**(3): p. 359-368.

16. Beckermann, G., *The Processing, Production and Improvement of Hemp-Fibre Reinforced Polypropylene Composite Materials*. 2004, University of Waikato.

17. Sawpan, M.A., *Mechanical Performance of Industrial Hemp Fibre Reinforced Polylactide and Unsaturated Polyester Composites*. 2010, The University of Waikato.

18. Zhang, Q., et al., *Study on poly (lactic acid)/natural fibers composites.* Journal of applied polymer science, 2012.

19. Nyström, B., *Natural fiber composites: optimization of microstructure and processing parameters.* 2007.

20. Baillie, C., *Green composites: polymer composites and the environment*. 2005: CRC Press.

21. Mohanty, A., M. Misra, and G. Hinrichsen, *Biofibres, biodegradable polymers and biocomposites: An overview.* Macromolecular Materials and Engineering, 2000. **276**(1): p. 1-24.

22. Azeredo, H., *Nanocomposites for food packaging applications.* Food Research International, 2009. **42**(9): p. 1240-1253.

23. Corradi, S., et al., *Composite boat hulls with bamboo natural fibres.* International Journal of Materials and Product Technology, 2009. **36**(1): p. 73-89.

24. Kymäläinen, H.R. and A.M. Sjöberg, *Flax and hemp fibres as raw materials for thermal insulations.* Building and environment, 2008. **43**(7): p. 1261-1269.

25. Youssef, A.M., M.A.E. Samahy, and M.H.A. Rehim, *Preparation of conductive paper composites based on natural cellulosic fibers for packaging applications.* Carbohydrate Polymers, 2012.

26. Phillips, S. and L. Lessard, *Application of natural fiber composites to musical instrument top plates.* Journal of Composite Materials, 2012. **46**(2): p. 145-154.

27. Alvarez-Valencia, D., et al., *Behavior of natural-fiber/thermoplastic sheet piling.* Proceedings of the Composites & Polycon, 2009: p. 1-16.

28. Burgueño, R., et al., *Load-bearing natural fiber composite cellular beams and panels.* Composites Part A: Applied Science and Manufacturing, 2004. **35**(6): p. 645-656.

29. Lee, S.M., et al., *Novel silk/poly (butylene succinate) biocomposites: the effect of short fibre content on their mechanical and thermal properties.* Composites Science and Technology, 2005. **65**(3): p. 647-657.

30. Cheung, H.-y., et al., *Natural fibre-reinforced composites for bioengineering and environmental engineering applications.* Composites Part B: Engineering, 2009. **40**(7): p. 655-663.

31. Cao, Y. and Y. Wu, *Evaluation of statistical strength of bamboo fiber and mechanical properties of fiber reinforced green composites.* Journal of Central South University of Technology, 2008. **15**: p. 564-567.

32. Lee, B.H., H.J. Kim, and W.R. Yu, *Fabrication of long and discontinuous natural fiber reinforced polypropylene biocomposites and their mechanical properties.* Fibers and Polymers, 2009. **10**(1): p. 83-90.

33. Li, X., L.G. Tabil, and S. Panigrahi, *Chemical treatments of natural fiber for use in natural fiber-reinforced composites: A review.* Journal of Polymers and the Environment, 2007. **15**(1): p. 25-33.

34. Mehta, G., et al., *Novel biocomposites sheet molding compounds for low cost housing panel applications.* Journal of Polymers and the Environment, 2005. **13**(2): p. 169-175.

35. De Rosa, I.M., et al., *Tensile behavior of New Zealand flax (Phormium tenax) fibers.* Journal of Reinforced Plastics and Composites, 2010. **29**(23): p. 3450-3454.

36. Shahzad, A., *Hemp fiber and its composites–a review.* Journal of Composite Materials, 2012. **46**(8): p. 973-986.

37. Merfield, C.N., *Industrial Hemp and its Potential for New Zealand*, in *Report for the Kellogg Rural*. 1999.

38. Pickering, K., et al., *Optimising industrial hemp fibre for composites.* Composites Part A: Applied Science and Manufacturing, 2007. **38**(2): p. 461-468.

39. Barron, A., et al., *Integrating Hemp In Organic Farming Systems: A Focus on the United Kingdom, France.* 2003.

40. Franck, R.R., *Bast and other plant fibres*. 2005: CRC.

41. Beckermann, G., *Performance of hemp-fibre reinforced polypropylene composite materials*. 2007, The University of Waikato.

42. Keller, A., et al., *Influence of the growth stage of industrial hemp on chemical and physical properties of the fibres.* Industrial Crops and Products, 2001. **13**(1): p. 35-48.

43. Fortunati, E., et al., *Extraction of cellulose nanocrystals from Phormium tenax fibres.* Journal of Polymers and the Environment, 2013. **21**(2): p. 319-328.

44. Jayaraman, K. and R. Halliwell, *Harakeke (phormium tenax) fibre–waste plastics blend composites processed*

by screwless extrusion. Composites Part B: Engineering, 2009. **40**(7): p. 645-649.

45. Lowe, B.J., et al., *Understanding the variability of vegetable fibres: a case study of harakeke (Phormium tenax).* Textile Research Journal, 2010. **80**(20): p. 2158-2166.

46. Newman, R.H., et al., *Epoxy composites reinforced with deacetylated Phormium tenax leaf fibres.* Composites Part A: Applied Science and Manufacturing, 2007. **38**(10): p. 2164-2170.

47. Le Guen, M.J. and R.H. Newman, *Pulped Phormium tenax leaf fibres as reinforcement for epoxy composites.* Composites Part A: Applied Science and Manufacturing, 2007. **38**(10): p. 2109-2115.

48. Duchemin, B. and M.P. Staiger, *Treatment of Harakeke fiber for biocomposites.* Journal of applied polymer science, 2009. **112**(5): p. 2710-2715.

49. Duchemin, B., K. Van Luijk, and M. Staiger, *New Zealand flax (Phormium tenax) reinforced eco-composites.* Proc of EcoComp, 2003: p. 1-2.

50. Pérez, J., et al., *Biodegradation and biological treatments of cellulose, hemicellulose and lignin: an overview.* International Microbiology, 2002. **5**(2): p. 53-63.

51. Ramarad, S., *Preparation and properties of kenaf bast fiber filled (plasticized) poly (lactic acid) composites*. 2008, MSc. Thesis, Penang: Universiti Sains Malaysia.

52. Arial, E.S., E.S.T. NR, and E.S. Century, *Mechanical properties of flax fibers and their composites*, in *Division of Polymer Engineering*. 2006, Luleå University of Technology: Luleå University of Technology.

53. Evert, R.F. and S.E. Eichhorn, *Biology of plants*. 2004: WH Freeman.

54. Lilholt, H. and J. Lawther, *Natural organic fibers.* Comprehensive composite materials, 2000. **1**: p. 303-325.

55. Stamboulis, A., C. Baillie, and T. Peijs, *Effects of environmental conditions on mechanical and physical properties of flax fibers.*

Composites Part A: Applied Science and Manufacturing, 2001. **32**(8): p. 1105-1115.

56. Thomsen, A.B., et al., *Hemp raw materials: The effect of cultivar, growth conditions and pretreatment on the chemical composition of the fibres.* Risø National Laboratory. Report No.: R, 2005. **1507**.

57. Li, Y., *Processing of Hemp Fibre Using Enzyme/Fungal Treatment for Composites*. 2009, The University of Waikato.

58. Biswal, M., S. Mohanty, and S.K. Nayak, *Thermal stability and flammability of banana-fiber-reinforced polypropylene nanocomposites.* Journal of applied polymer science, 2012.

59. Summerscales, J., et al., *A review of bast fibres and their composites. Part 1–Fibres as reinforcements.* Composites Part A: Applied Science and Manufacturing, 2010. **41**(10): p. 1329-1335.

60. Dos Santos, P.A., et al. *Natural fibers plastic composites for automotive applications*. in *SPE Automotive Composites Conference and Exposition, Troy, MI, CD-ROM Proceedings*. 2008.

61. Sanadi, A.R., D.F. Caulfield, and R.E. Jacobson, *Agro-fiber thermoplastic composites.* Paper and composites from agro-based resources, 1997. **377**: p. 401.

62. Heidi, P., et al., *The Influence of Biocomposite Processing and Composition on Natural Fiber Length, Dispersion and Orientation.* Journal of Materials Science and Engineering A: Structural Materials: Properties, Microstructure and Processing, 2011. **1**(2): p. 190-198.

63. Kabir, M., et al., *Chemical treatments on plant-based natural fibre reinforced polymer composites: An overview.* Composites Part B: Engineering, 2012.

64. Beckermann, G. and K.L. Pickering, *Engineering and evaluation of hemp fibre reinforced polypropylene composites: fibre treatment and matrix modification.* Composites Part A: Applied Science and Manufacturing, 2008. **39**(6): p. 979-988.

65. Chen, P., et al., *Influence of fiber wettability on the interfacial adhesion of continuous fiber-reinforced PPESK composite.* Journal of applied polymer science, 2006. **102**(3): p. 2544-2551.

66. Fuentes, C., et al., *Wetting behaviour and surface properties of technical bamboo fibres.* Colloids and Surfaces A: Physicochemical and Engineering Aspects, 2011. **380**(1): p. 89-99.

67. Aranberri-Askargorta, I., T. Lampke, and A. Bismarck, *Wetting behavior of flax fibers as reinforcement for polypropylene.* Journal of colloid and interface science, 2003. **263**(2): p. 580-589.

68. Wu, X.F. and Y.A. Dzenis, *Droplet on a fiber: geometrical shape and contact angle.* Acta mechanica, 2006. **185**(3): p. 215-225.

69. Bénard, Q., M. Fois, and M. Grisel, *Roughness and fibre reinforcement effect onto wettability of composite surfaces.* Applied surface science, 2007. **253**(10): p. 4753-4758.

70. Sinha, E. and S. Panigrahi, *Effect of plasma treatment on structure, wettability of jute fiber and flexural strength of its composite.* Journal of Composite Materials, 2009. **43**(17): p. 1791-1802.

71. Liu, Z.T., et al., *Adjustable wettability of methyl methacrylate modified ramie fiber.* Journal of applied polymer science, 2008. **109**(5): p. 2888-2894.

72. Chow, C., X. Xing, and R. Li, *Moisture absorption studies of sisal fibre reinforced polypropylene composites.* Composites Science and Technology, 2007. **67**(2): p. 306-313.

73. Chen, H., M. Miao, and X. Ding, *Influence of moisture absorption on the interfacial strength of bamboo/vinyl ester composites.* Composites Part A: Applied Science and Manufacturing, 2009. **40**(12): p. 2013-2019.

74. Joseph, P., et al., *Environmental effects on the degradation behaviour of sisal fibre reinforced polypropylene composites.* Composites Science and Technology, 2002. **62**(10): p. 1357-1372.

75. Ashori, A. and S. Sheshmani, *Hybrid composites made from recycled materials: moisture absorption and thickness swelling behavior.* Bioresource technology, 2010. **101**(12): p. 4717-4720.

76. Dhakal, H., Z. Zhang, and M. Richardson, *Effect of water absorption on the mechanical properties of hemp fibre reinforced unsaturated polyester composites.* Composites Science and Technology, 2007. **67**(7): p. 1674-1683.

77. Rowell, R.M., *Chemical modification of agro-resources for property enhancement.* Paper and composites from agro-based resources, 1997: p. 351-375.

78. Taj, S., M.A. Munawar, and S. Khan, *Natural fiber-reinforced polymer composites.* Proceedings-Pakistan Academy of Sciences, 2007. **44**(2): p. 129.

79. Holbery, J. and D. Houston, *Natural-fiber-reinforced polymer composites in automotive applications.* JOM Journal of the Minerals, Metals and Materials Society, 2006. **58**(11): p. 80-86.

80. Callister, W.D. and D.G. Rethwisch, *Materials science and engineering: an introduction*. Vol. 7. 2007: Wiley New York.

81. Pickering, K.L., M. Institute of Materials, and Mining, *Properties and Performance of Natural Fibre Composites*. 2008: CRC Press.

82. Madhavan Nampoothiri, K., N.R. Nair, and R.P. John, *An overview of the recent developments in polylactide (PLA) research.* Bioresource technology, 2010. **101**(22): p. 8493-8501.

83. Avinc, O. and A. Khoddami, *Overview of Poly (lactic acid)(PLA) Fibre.* Fibre Chemistry, 2009. **41**(6): p. 391-401.

84. Henton, D.E., et al., *Polylactic acid technology.* Natural Fibers, Biopolymers, and Biocomposites. Taylor & Francis, Boca Raton, FL, pp. 527Ã577, 2005.

85. Pandiyaraj, K.N., et al., *Adhesive properties of polypropylene (PP) and polyethylene terephthalate (PET) film surfaces treated by DC glow discharge plasma.* Vacuum, 2008. **83**(2): p. 332-339.

86. Yu, T., Y. Li, and J. Ren, *Preparation and properties of short natural fiber reinforced poly (lactic acid) composites.* Transactions of Nonferrous Metals Society of China, 2009. **19**: p. s651-s655.

87. Amor, I.B., et al., *Effect of Palm Tree Fiber Orientation on Electrical Properties of Palm Tree Fiber-reinforced Polyester Composites.* Journal of Composite Materials, 2010. **44**(13): p. 1553-1568.

88. Herrera-Franco, P.J. and A. Valadez-Gonzalez, *A study of the mechanical properties of short natural-fiber reinforced composites.* Composites Part B: Engineering, 2005. **36**(8): p. 597-608.

89. Norman, D.A. and R.E. Robertson, *The effect of fiber orientation on the toughening of short fiber-reinforced polymers.* Journal of applied polymer science, 2003. **90**(10): p. 2740-2751.

90. Brahim, S.B. and R.B. Cheikh, *Influence of fibre orientation and volume fraction on the tensile properties of unidirectional Alfa-polyester composite.* Composites Science and Technology, 2007. **67**(1): p. 140-147.

91. Baghaei, B., et al., *Novel aligned hemp fibre reinforcement for structural biocomposites: Porosity, water absorption, mechanical performances and viscoelastic behaviour.* Composites Part A: Applied Science and Manufacturing, 2014. **61**: p. 1-12.

92. Garkhail, S., R. Heijenrath, and T. Peijs, *Mechanical properties of natural-fibre-mat-reinforced thermoplastics based on flax fibres and polypropylene.* Applied Composite Materials, 2000. **7**(5-6): p. 351-372.

93. Miao, M. and M. Shan, *Highly aligned flax/polypropylene nonwoven preforms for thermoplastic composites.* Composites Science and Technology, 2011. **71**(15): p. 1713-1718.

94. Matthews, F. and R. Rawlings, *Composite materials: engineering and science*. 1999: Woodhead Publishing.

95. Huber, T. and J. Müssig, *Fibre matrix adhesion of natural fibres cotton, flax and hemp in polymeric matrices analyzed with the single fibre fragmentation test.* Composite Interfaces, 2008. **15**(2-3): p. 335-349.

96. Sun, Z.-Y., H.-S. Han, and G.-C. Dai, *Mechanical properties of injection-molded natural fiber-reinforced polypropylene composites: formulation and compounding processes.* Journal of Reinforced Plastics and Composites, 2010. **29**(5): p. 637-650.

97. Joffe, R., J. Andersons, and L. Wallström, *Interfacial shear strength of flax fiber/thermoset polymers estimated by fiber fragmentation tests.* Journal of materials Science, 2005. **40**(9): p. 2721-2722.

98. Vallejos, M., et al., *Micromechanics of hemp strands in polypropylene composites.* Composites Science and Technology, 2012. **72**(10): p. 1209-1213.

99. Harris, B., *Engineering composite materials*. 1986: Institute of metals London.

100. Roe, P. and M.P. Ansell, *Jute-reinforced polyester composites.* Journal of materials Science, 1985. **20**(11): p. 4015-4020.

101. Madsen, B., et al., *Hemp yarn reinforced composites–I. Yarn characteristics.* Composites Part A: Applied Science and Manufacturing, 2007. **38**(10): p. 2194-2203.

102. Madsen, B., P. Hoffmeyer, and H. Lilholt, *Hemp yarn reinforced composites–II. Tensile properties.* Composites Part A: Applied Science and Manufacturing, 2007. **38**(10): p. 2204-2215.

103. Gassan, J. and V.S. Gutowski, *Effects of corona discharge and UV treatment on the properties of jute-fibre epoxy composites.* Composites Science and Technology, 2000. **60**(15): p. 2857-2863.

104. Ragoubi, M., et al., *Impact of corona treated hemp fibres onto mechanical properties of polypropylene composites made thereof.* Industrial Crops and Products, 2010. **31**(2): p. 344-349.

105. Ragoubi, M., et al., *Effect of corona discharge treatment on mechanical and thermal properties of composites based on miscanthus fibres and polylactic acid or polypropylene matrix.* Composites Part A: Applied Science and Manufacturing, 2012. **43**(4): p. 675-685.

106. Seki, Y., et al. *The Influence of Oxygen Plasma Treatment of Jute Fibers on Mechanical Properties of Jute Fiber reinforced Thermoplastic Composites*. 2009.

107. Cao, Y., S. Sakamoto, and K. Goda, *Effects of heat and alkali treatments on mechanical properties of kenaf fibers, in 16th international conference on composite materials*, in *16th*

International Conference On Composite Materials. 2007: Kyoto Japan.

108. Grozdanov, A., et al. *Thermal Stability of Differently Treated Natural Fiber Reinforcements For Composites*. in *ICOSECS-International Conference of the Chemical Societies of the South-East European Countries*. 2009.

109. Islam, M., K. Pickering, and N. Foreman, *Influence of alkali treatment on the interfacial and physico-mechanical properties of industrial hemp fibre reinforced polylactic acid composites.* Composites Part A: Applied Science and Manufacturing, 2010. **41**(5): p. 596-603.

110. Meon, M.S., et al., *Improving tensile properties of kenaf fibers treated with sodium hydroxide.* Procedia Engineering, 2012. **41**: p. 1587-1592.

111. Ouajai, S. and R. Shanks, *Composition, structure and thermal degradation of hemp cellulose after chemical treatments.* Polymer degradation and stability, 2005. **89**(2): p. 327-335.

112. Goda, K., et al., *Improvement of plant based natural fibers for toughening green composites—Effect of load application during mercerization of ramie fibers.* Composites Part A: Applied Science and Manufacturing, 2006. **37**(12): p. 2213-2220.

113. Ibrahim, N.A. and K.A. Hadithon, *Effect of fiber treatment on mechanical properties of kenaf fiber-ecoflex composites.* Journal of Reinforced Plastics and Composites, 2010. **29**(14): p. 2192-2198.

114. Kabir, M., et al., *Mechanical properties of chemically-treated hemp fibre reinforced sandwich composites.* Composites Part B: Engineering, 2011.

115. Bledzki, A., et al., *The effects of acetylation on properties of flax fibre and its polypropylene composites.* Express Polym Lett, 2008. **2**(6): p. 413-22.

116. Khalil, H., et al., *The effect of acetylation on interfacial shear strength between plant fibres and various matrices.* European Polymer Journal, 2001. **37**(5): p. 1037-1045.

117. Tserki, V., et al., *A study of the effect of acetylation and propionylation surface treatments on natural fibres.* Composites Part A: Applied Science and Manufacturing, 2005. **36**(8): p. 1110-1118.

118. Hill, C.A.S., H. Khalil, and M.D. Hale, *A study of the potential of acetylation to improve the properties of plant fibres.* Industrial Crops and Products, 1998. **8**(1): p. 53-63.

119. Chun, K.S., S. Husseinsyah, and H. Osman, *Mechanical and thermal properties of coconut shell powder filled polylactic acid*

biocomposites: effects of the filler content and silane coupling agent. Journal of Polymer Research, 2012. **19**(5): p. 1-8.

120. Xie, Y., et al., *Silane coupling agents used for natural fiber/polymer composites: A review.* Composites Part A: Applied Science and Manufacturing, 2010. **41**(7): p. 806-819.

121. Kabir, M., et al. *Effects of natural fibre surface on composite properties: A review*. in *Proceedings of the 1st International Postgraduate Conference on Engineering, Designing and Developing the Built Environment for Sustainable Wellbeing (eddBE2011)*. 2011. Queensland University of Technology.

122. Rachini, A., et al., *Chemical modification of hemp fibers by silane coupling agents.* Journal of applied polymer science, 2012.

123. Zou, H., et al., *Effect of fiber surface treatments on the properties of short sisal fiber/poly (lactic acid) biocomposites.* Polymer Composites, 2012. **33**(10): p. 1659-1666.

124. Valadez-Gonzalez, A., et al., *Chemical modification of henequen fibers with an organosilane coupling agent.* Composites Part B: Engineering, 1999. **30**(3): p. 321-331.

125. Lee, B.-H., et al., *Bio-composites of kenaf fibers in polylactide: Role of improved interfacial adhesion in the carding process.* Composites Science and Technology, 2009. **69**(15): p. 2573-2579.

126. Huda, M.S., et al., *Effect of fiber surface-treatments on the properties of laminated biocomposites from poly (lactic acid)(PLA) and kenaf fibers.* Composites Science and Technology, 2008. **68**(2): p. 424-432.

127. Sarasini, F., et al., *Effect of fiber surface treatments on thermo-mechanical behavior of poly (lactic acid)/phormium tenax composites.* Journal of Polymers and the Environment, 2013. **21**(3): p. 881-891.

128. Rytlewski, P., et al., *Assessment of dicumyl peroxide ability to improve adhesion between polylactide and flax or hemp fibres.* Composite Interfaces, 2014. **21**(8): p. 671-683.

129. Kaushik, V.K., A. Kumar, and S. Kalia, *Effect of mercerization and benzoyl peroxide treatment on morphology, thermal stability and crystallinity of sisal fibers.* International Journal of Textile Science, 2012. **1**(6): p. 101-105.

130. Sreekala, M., et al., *Oil palm fibre reinforced phenol formaldehyde composites: influence of fibre surface modifications on the mechanical performance.* Applied Composite Materials, 2000. **7**(5-6): p. 295-329.

131. Wang, B., et al., *Pre-treatment of flax fibers for use in rotationally molded biocomposites.* Journal of Reinforced Plastics and Composites, 2007. **26**(5): p. 447-463.

132. Lei, Y., et al., *Influence of nanoclay on properties of HDPE/wood composites.* Journal of applied polymer science, 2007. **106**(6): p. 3958-3966.

133. Lu, T., et al., *Effects of modifications of bamboo cellulose fibers on the improved mechanical properties of cellulose reinforced poly (lactic acid) composites.* Composites Part B: Engineering, 2014. **62**: p. 191-197.

134. Wong, S., R.A. Shanks, and A. Hodzic, *Mechanical Behavior and Fracture Toughness of Poly (L-lactic acid)-Natural Fiber Composites Modified with Hyperbranched Polymers.* Macromolecular Materials and Engineering, 2004. **289**(5): p. 447-456.

135. Zhang, W., Y. Zhang, and Y. Chen, *Modified brittle poly (lactic acid) by biodegradable hyperbranched poly (ester amide).* Iranian Polymer Journal, 2008. **17**(12): p. 891-898.

136. Park, S.-D., M. Todo, and K. Arakawa, *Effect of annealing on the fracture toughness of poly (lactic acid).* Journal of materials Science, 2004. **39**(3): p. 1113-1116.

137. Nyambo, C., M. Misra, and A.K. Mohanty, *Toughening of brittle poly (lactide) with hyperbranched poly (ester-amide) and isocyanate-terminated prepolymer of polybutadiene.* Journal of materials Science, 2012: p. 1-11.

138. Bhardwaj, R. and A.K. Mohanty, *Modification of brittle polylactide by novel hyperbranched polymer-based nanostructures.* Biomacromolecules, 2007. **8**(8): p. 2476-2484.

139. Pickering, K., *Properties and performance of natural-fibre composites*. 2008: Woodhead Publishing.

140. Saheb, D.N. and J. Jog, *Natural fiber polymer composites: a review*. Advances in polymer technology, 1999. **18**(4): p. 351-363.

141. Fung, C.-P., *Fibre orientation of fibre-reinforced PBT composites in injection moulding.* Plastics, rubber and composites, 2004. **33**(4): p. 170-176.

142. Shokri, P. and N. Bhatnagar, *Effect of packing pressure on fiber orientation in injection molding of fiber-reinforced thermoplastics.* Polymer Composites, 2007. **28**(2): p. 214-223.

143. Silva, C.A., et al., *Fiber orientation in injection molding with rotating flow.* Polymer Engineering & Science, 2008. **48**(2): p. 395-404.

144. Brooks, R., *Injection molding based techniques.* Comprehensive Composite Materials, A. Kelly and C. Zweben, Editors, 2000.

145. Ho, M., et al., *Critical factors on manufacturing processes of natural fibre composites.* Composites Part B: Engineering, 2011.

146. Kaczmar, J., J. Pach, and C. Burgstaller, *The chemically treated hemp fibres to reinforce polymers.* Polimery, 2011. **56**(11-12): p. 817-822.

147. Luyt, A., T. Mokhothu, and B. Guduri, *Kenaf-fiber-reinforced copolyester biocomposites.* Wiley Online Library, 2011.

148. Beg, M.D.H., *The improvement of interfacial bonding, weathering and recycling of wood fibre reinforced polypropylene composites*. 2007, The University of Waikato.

149. Montgomery, D.C., G.C. Runger, and N.F. Hubele, *Engineering statistics*. 2009: John Wiley & Sons.

150. D, A., *Standard test method for tensile strength and Young's Modulus for high-modulus single-filament materials*. 1989.

151. Weibull, W., *A statistical distribution function of wide applicability.* Journal of applied mechanics, 1951. **18**(3): p. 293-297.

152. Zafeiropoulos, N. and C. Baillie, *A study of the effect of surface treatments on the tensile strength of flax fibres: Part II. Application of Weibull statistics.* Composites Part A: Applied Science and Manufacturing, 2007. **38**(2): p. 629-638.

153. Biagiotti, J., et al., *A systematic investigation on the influence of the chemical treatment of natural fibers on the properties of their polymer matrix composites.* Polymer Composites, 2004. **25**(5): p. 470-479.

154. Mwaikambo, L.Y. and M.P. Ansell, *Chemical modification of hemp, sisal, jute, and kapok fibers by alkalization.* Journal of applied polymer science, 2002. **84**(12): p. 2222-2234.

155. Roncero, M.B., et al., *The effect of xylanase on lignocellulosic components during the bleaching of wood pulps.* Bioresource technology, 2005. **96**(1): p. 21-30.

156. Le Troedec, M., et al., *Influence of various chemical treatments on the composition and structure of hemp fibres.* Composites Part A: Applied Science and Manufacturing, 2008. **39**(3): p. 514-522.

157. Ouajai, S. and R.A. Shanks, *Morphology and structure of hemp fibre after bioscouring.* Macromolecular bioscience, 2005. **5**(2): p. 124-134.

158. Islam, M.S., K.L. Pickering, and N.J. Foreman, *Influence of alkali fiber treatment and fiber processing on the mechanical properties of hemp/epoxy composites.* Journal of applied polymer science, 2011. **119**(6): p. 3696-3707.

159. Sawpan, M.A., K.L. Pickering, and A. Fernyhough, *Effect of various chemical treatments on the fibre structure and tensile properties of industrial hemp fibres.* Composites Part A: Applied Science and Manufacturing, 2011. **42**(8): p. 888-895.

160. Bismarck, A., et al., *Surface characterization of flax, hemp and cellulose fibers; surface properties and the water uptake behavior.* Polymer Composites, 2002. **23**(5): p. 872-894.

161. Rai, A. and C. Jha, *Natural fibre composites and its potential as building materials.* Express Textile, 2004. **25**.

162. Wang, H., et al., *Removing pectin and lignin during chemical processing of hemp for textile applications.* Textile Research Journal, 2003. **73**(8): p. 664-669.

163. Roy, A., et al., *Improvement in mechanical properties of jute fibres through mild alkali treatment as demonstrated by utilisation of the Weibull distribution model.* Bioresource technology, 2012. **107**: p. 222-228.

164. Doan, T.-T.-L., S.-L. Gao, and E. Mäder, *Jute/polypropylene composites I. Effect of matrix modification.* Composites Science and Technology, 2006. **66**(7): p. 952-963.

165. Joffe, R., J. Andersons, and L. Wallström, *Strength and adhesion characteristics of elementary flax fibres with different surface treatments.* Composites Part A: Applied Science and Manufacturing, 2003. **34**(7): p. 603-612.

166. Xia, Z., et al., *Study on the breaking strength of jute fibres using modified Weibull distribution.* Composites Part A: Applied Science and Manufacturing, 2009. **40**(1): p. 54-59.

167. Oraji, R., *The effect of plasma treatment on flax fibres*. 2008, University of Saskatchewan.

168. Wang, B., M. Sain, and K. Oksman, *Study of structural morphology of hemp fiber from the micro to the nanoscale.* Applied Composite Materials, 2007. **14**(2): p. 89-103.

169. Shih, Y.-F. and C.-C. Huang, *Polylactic acid (PLA)/banana fiber (BF) biodegradable green composites.* Journal of Polymer Research, 2011. **18**(6): p. 2335-2340.

170. Gañán, P. and I. Mondragon, *Surface modification of fique fibers. Effect on their physico-mechanical properties.* Polymer Composites, 2002. **23**(3): p. 383-394.

171. Kelly, A. and W. Tyson, *Tensile properties of fibre-reinforced metals: copper/tungsten and copper/molybdenum*. Journal of the Mechanics and Physics of Solids, 1965. **13**(6): p. 329-350.

172. Thomason, J., *Micromechanical parameters from macromechanical measurements on glass reinforced polyamide 6, 6.* Composites Science and Technology, 2001. **61**(14): p. 2007-2016.

173. Thomason, J., *The influence of fibre length and concentration on the properties of glass fibre reinforced polypropylene. 6. The properties of injection moulded long fibre PP at high fibre*

content. Composites Part A: Applied Science and Manufacturing, 2005. **36**(7): p. 995-1003.

174. Li, Y., Y.-W. Mai, and L. Ye, *Sisal fibre and its composites: a review of recent developments.* Composites Science and Technology, 2000. **60**(11): p. 2037-2055.

175. Kalaprasad, G., et al., *Theoretical modelling of tensile properties of short sisal fibre-reinforced low-density polyethylene composites.* Journal of materials Science, 1997. **32**(16): p. 4261-4267.

176. Fuchs, C., et al., *Application of Halpin–Tsai equation to microfibril reinforced polypropylene/poly (ethylene terephthalate) composites.* Composite Interfaces, 2006. **13**(4-6): p. 331-344.

177. Halpin, J.C., *Effects of Environmental Factors on Composite Materials*. 1969, DTIC Document.

178. Facca, A.G., M.T. Kortschot, and N. Yan, *Predicting the elastic modulus of natural fibre reinforced thermoplastics.* Composites Part A: Applied Science and Manufacturing, 2006. **37**(10): p. 1660-1671.

179. Alhuthali, A. and I.M. Low, *Mechanical properties of cellulose fibre reinforced vinyl-ester composites in wet conditions.* Journal of materials Science, 2013. **48**(18): p. 6331-6340.

180. Ku, H., et al., *A review on the tensile properties of natural fiber reinforced polymer composites.* Composites Part B: Engineering, 2011. **42**(4): p. 856-873.

181. Tucker III, C.L. and E. Liang, *Stiffness predictions for unidirectional short-fiber composites: review and evaluation.* Composites Science and Technology, 1999. **59**(5): p. 655-671.

182. Landel, R.F. and L.E. Nielsen, *Mechanical properties of polymers and composites*. 1993: CRC Press.

183. Fu, S.-Y., B. Lauke, and Y.-W. Mai, *Science and engineering of short fibre reinforced polymer composites*. 2009: Elsevier.

184. Thomason, J., et al., *Influence of fibre length and concentration on the properties of glass fibre-reinforced polypropylene: Part 3. Strength and strain at failure.* Composites Part A: Applied Science and Manufacturing, 1996. **27**(11): p. 1075-1084.

185. Hull, D. and T. Clyne, *An introduction to composite materials*. 1996: Cambridge Univ Pr.

186. Piggott, M.R., *Load bearing fibre composites*. 2002: Springer Science & Business Media.

187. Cox, H., *The elasticity and strength of paper and other fibrous materials.* British journal of applied physics, 1952. **3**(3): p. 72.

188. Krenchel, H., *Fibre reinforcement - theoretical and practical investigation of the elasticity and strength of fibre-reinforced materials* 1964, Alademisk forlag: Copenhagen.

189. Sanadi, A. and M. Piggott, *Interfacial effects in carbon-epoxies.* Journal of materials Science, 1985. **20**(2): p. 421-430.

190. Thomason, J. and M. Vlug, *Influence of fibre length and concentration on the properties of glass fibre-reinforced polypropylene: 1. Tensile and flexural modulus.* Composites Part A: Applied Science and Manufacturing, 1996. **27**(6): p. 477-484.

191. Bader, M. and W. Bowyer, *An improved method of production for high strength fibre-reinforced thermoplastics.* Composites, 1973. **4**(4): p. 150-156.

192. Bowyer, W. and M. Bader, *On the re-inforcement of thermoplastics by imperfectly aligned discontinuous fibres.* Journal of materials Science, 1972. **7**(11): p. 1315-1321.

193. Fu, S.-Y., et al., *Tensile properties of short-glass-fiber-and short-carbon-fiber-reinforced polypropylene composites.* Composites Part A: Applied Science and Manufacturing, 2000. **31**(10): p. 1117-1125.

194. Aziz, S.H. and M.P. Ansell, *The effect of alkalization and fibre alignment on the mechanical and thermal properties of kenaf and hemp bast fibre composites: Part 1–polyester resin matrix.* Composites Science and Technology, 2004. **64**(9): p. 1219-1230.

195. Serrano, A., et al., *Estimation of the interfacial shears strength, orientation factor and mean equivalent intrinsic tensile strength in old newspaper fiber/polypropylene composites.* Composites Part B: Engineering, 2013. **50**: p. 232-238.

196. Bos, H.L., J. Müssig, and M.J. van den Oever, *Mechanical properties of short-flax-fibre reinforced compounds.* Composites Part A: Applied Science and Manufacturing, 2006. **37**(10): p. 1591-1604.

197. Sui, G., et al., *The effect of fiber inclusions in toughened plastics–Part II: determination of micromechanical parameters.* Composites Science and Technology, 2005. **65**(2): p. 221-229.

198. López, J., et al., *PP composites based on mechanical pulp, deinked newspaper and jute strands: a comparative study.* Composites Part B: Engineering, 2012. **43**(8): p. 3453-3461.

199. Lafranche, E., et al., *Prediction of injection-moulded flax fibre reinforced polypropylene tensile properties through a micro-morphology analysis.* Journal of Composite Materials, 2013: p. 0021998313514875.

200. Fu, S.-Y. and B. Lauke, *Effects of fiber length and fiber orientation distributions on the tensile strength of short-fiber-*

reinforced polymers. Composites Science and Technology, 1996. **56**(10): p. 1179-1190.

201. Kabir, M., et al., *Mechanical properties of chemically-treated hemp fibre reinforced sandwich composites.* Composites Part B: Engineering, 2012. **43**(2): p. 159-169.

202. Fischer, G., *Characterization of Fiber-Reinforced Cement Composites by their Tensile Stress-Strain Behavior and Quantification of Crack Formation.* proceedings of BEFIB, 2004: p. 20-2.

203. Graupner, N., *Improvement of the mechanical properties of biodegradable hemp fiber reinforced poly (lactic acid)(PLA) composites by the admixture of man-made cellulose fibers.* Journal of Composite Materials, 2009.

204. Hu, R. and J.-K. Lim, *Fabrication and mechanical properties of completely biodegradable hemp fiber reinforced polylactic acid composites.* Journal of Composite Materials, 2007. **41**(13): p. 1655-1669.

205. Mathew, L. and R. Joseph, *Mechanical properties of short-isora-fiber-reinforced natural rubber composites: Effects of fiber length, orientation, and loading; alkali treatment; and bonding agent.* Journal of applied polymer science, 2007. **103**(3): p. 1640-1650.

206. Oksman, K., M. Skrifvars, and J.F. Selin, *Natural fibres as reinforcement in polylactic acid (PLA) composites.* Composites Science and Technology, 2003. **63**(9): p. 1317-1324.

207. Agari, Y., et al., *Preparation and properties of the biodegradable graded blend of poly (L-lactic acid) and poly (ethylene oxide).* Journal of Polymer Science Part B: Polymer Physics, 2007. **45**(21): p. 2972-2981.

208. Baghaei, B., M. Skrifvars, and L. Berglin, *Manufacture and characterisation of thermoplastic composites made from PLA/hemp co-wrapped hybrid yarn prepregs.* Composites Part A: Applied Science and Manufacturing, 2013. **50**: p. 93-101.

209. Baghaei, B., et al., *Mechanical and thermal characterization of compression moulded polylactic acid natural fiber composites reinforced with hemp and lyocell fibers.* Journal of applied polymer science, 2014. **131**(15).

210. Du, Y., et al., *Fabrication and characterization of fully biodegradable natural fiber-reinforced poly (lactic acid) composites.* Composites Part B: Engineering, 2014. **56**: p. 717-723.

211. Hu, R. and J.K. Lim, *Fabrication and mechanical properties of completely biodegradable hemp fiber reinforced polylactic acid*

composites. Journal of Composite Materials, 2007. **41**(13): p. 1655-1669.

212. Masirek, R., et al., *Composites of poly (L-lactide) with hemp fibers: Morphology and thermal and mechanical properties.* Journal of applied polymer science, 2007. **105**(1): p. 255-268.

213. Plackett, D., et al., *Biodegradable composites based on L-polylactide and jute fibres.* Composites Science and Technology, 2003. **63**(9): p. 1287-1296.

214. Sawpan, M.A., K.L. Pickering, and A. Fernyhough, *Improvement of mechanical performance of industrial hemp fibre reinforced polylactide biocomposites.* Composites Part A: Applied Science and Manufacturing, 2011. **42**(3): p. 310-319.

215. Krishnaprasad, R., et al., *Mechanical and thermal properties of bamboo microfibril reinforced polyhydroxybutyrate biocomposites.* Journal of Polymers and the Environment, 2009. **17**(2): p. 109-114.

216. Madsen, B. and H. Lilholt, *Physical and mechanical properties of unidirectional plant fibre composites—an evaluation of the influence of porosity.* Composites Science and Technology, 2003. **63**(9): p. 1265-1272.

217. Shah, D.U., et al., *Determining the minimum, critical and maximum fibre content for twisted yarn reinforced plant fibre composites.* Composites Science and Technology, 2012. **72**(15): p. 1909-1917.

218. Ghosh, R., et al., *Effect of fibre volume fraction on the tensile strength of Banana fibre reinforced vinyl ester resin composites.* Int J Adv Eng Sci Technol, 2011. **4**(1): p. 89-91.

219. Sawpan, M.A., K.L. Pickering, and A. Fernyhough, *Analysis of mechanical properties of hemp fibre reinforced unsaturated polyester composites.* Journal of Composite Materials, 2013. **47**(12): p. 1513-1525.

220. Thomason, J., *The influence of fibre length and concentration on the properties of glass fibre reinforced polypropylene: 7. Interface strength and fibre strain in injection moulded long fibre PP at high fibre content.* Composites Part A: Applied Science and Manufacturing, 2007. **38**(1): p. 210-216.

221. Pickering, K., et al., *The effect of silane coupling agents on radiata pine fibre for use in thermoplastic matrix composites.* Composites Part A: Applied Science and Manufacturing, 2003. **34**(10): p. 915-926.

222. Bax, B. and J. Müssig, *Impact and tensile properties of PLA/Cordenka and PLA/flax composites.* Composites Science and Technology, 2008. **68**(7): p. 1601-1607.

223. Prajer, M. and M.P. Ansell. *Interfacial micromechanics in PLA/sisal fibre composites*. in *Proceedings of the 11th International Conference on Non-Convertional Materials and Technologies*. 2009.

224. Sawpan, M.A., K.L. Pickering, and A. Fernyhough, *Effect of fibre treatments on interfacial shear strength of hemp fibre reinforced polylactide and unsaturated polyester composites.* Composites Part A: Applied Science and Manufacturing, 2011. **42**(9): p. 1189-1196.

225. Torres, F. and M. Cubillas, *Study of the interfacial properties of natural fibre reinforced polyethylene.* Polymer Testing, 2005. **24**(6): p. 694-698.

226. Zafeiropoulos, N.E., *On the use of single fibre composites testing to characterise the interface in natural fibre composites.* Composite Interfaces, 2007. **14**(7-9): p. 807-820.

227. Krishnan, K.A., R. Anjana, and K. George, *Effect of alkali-resistant glass fiber on polypropylene/polystyrene blends: Modeling and characterization.* Polymer Composites, 2014.

228. Venkateshwaran, N. and A. ElayaPerumal, *Modeling and evaluation of tensile properties of randomly oriented banana/epoxy composite.* Journal of Reinforced Plastics and Composites, 2011: p. 0731684411430559.

229. Indira, K., J. Parameswaranpillai, and S. Thomas, *Mechanical properties and failure topography of banana fiber PF macrocomposites fabricated by RTM and CM techniques.* ISRN Polymer Science, 2013. **2013**.

230. Sreenivasan, V., et al., *Mechanical properties of randomly oriented short Sansevieria cylindrica fibre/polyester composites.* Materials & Design, 2011. **32**(4): p. 2444-2455.

231. Krenchel, H., *Fibre reinforcement*. 1964: Aademisk forlag.

232. Taha, I. and Y.F. Abdin, *Modeling of strength and stiffness of short randomly oriented glass fiber—polypropylene composites.* Journal of Composite Materials, 2011. **45**(17): p. 1805-1821.

233. Van den Oever, M., H. Bos, and M. Van Kemenade, *Influence of the physical structure of flax fibres on the mechanical properties of flax fibre reinforced polypropylene composites.* Applied Composite Materials, 2000. **7**(5-6): p. 387-402.

234. Piggott, M.R., *Short fibre polymer composites: a fracture-based theory of fibre reinforcement.* Journal of Composite Materials, 1994. **28**(7): p. 588-606.

235. Sreekumar, P., et al., *A comparative study on mechanical properties of sisal-leaf fibre-reinforced polyester composites*

prepared by resin transfer and compression moulding techniques. Composites Science and Technology, 2007. **67**(3): p. 453-461.

236. Vilaseca, F., et al., *Biocomposites from abaca strands and polypropylene. Part I: Evaluation of the tensile properties.* Bioresource technology, 2010. **101**(1): p. 387-395.

237. Taha, I., A. El-Sabbagh, and G. Ziegmann, *Modelling of strength and stiffness behaviour of natural fibre reinforced polypropylene composites.* Polymers & Polymer Composites, 2008. **16**(5): p. 295.

238. Du, Y., et al., *Kenaf bast fiber bundle-reinforced unsaturated polyester composites. IV: effects of fiber loadings and aspect ratios on composite tensile properties.* Forest Products Journal, 2010. **60**(7): p. 582-591.

239. Kalia, S., B. Kaith, and I. Kaur, *Pretreatments of natural fibers and their application as reinforcing material in polymer composites—A review.* Polymer Engineering & Science, 2009. **49**(7): p. 1253-1272.

240. John, M.J., et al., *Effect of chemical modification on properties of hybrid fiber biocomposites.* Composites Part A: Applied Science and Manufacturing, 2008. **39**(2): p. 352-363.

241. Bledzki, A. and A. Jaszkiewicz, *Mechanical performance of biocomposites based on PLA and PHBV reinforced with natural fibres–A comparative study to PP.* Composites Science and Technology, 2010. **70**(12): p. 1687-1696.

242. Bhattacharya, A., J.W. Rawlins, and P. Ray, *Polymer grafting and crosslinking*. 2009: Wiley Online Library.

243. Jacob, M., S. Thomas, and K. Varughese, *Novel woven sisal fabric reinforced natural rubber composites: tensile and swelling characteristics.* Journal of Composite Materials, 2006. **40**(16): p. 1471-1485.

244. Goriparthi, B.K., K. Suman, and N.M. Rao, *Effect of fiber surface treatments on mechanical and abrasive wear performance of polylactide/jute composites.* Composites Part A: Applied Science and Manufacturing, 2012. **43**(10): p. 1800-1808.

245. Choi, H.Y. and J.S. Lee, *Effects of surface treatment of ramie fibers in a ramie/poly (lactic acid) composite.* Fibers and Polymers, 2012. **13**(2): p. 217-223.

246. Razak, N.I.A., et al., *The influence of chemical surface modification of kenaf fiber using hydrogen peroxide on the mechanical properties of biodegradable kenaf fiber/poly (lactic acid) composites.* Molecules, 2014. **19**(3): p. 2957-2968.

247. Pickering, K.L., S.R. Khimi, and S. Ilanko, *The effect of silane coupling agent on iron sand for use in magnetorheological elastomers Part 1: Surface chemical modification and*

characterization. Composites Part A: Applied Science and Manufacturing, 2015. **68**: p. 377-386.

248. Kim, J.T. and A.N. Netravali, *Mercerization of sisal fibers: Effect of tension on mechanical properties of sisal fiber and fiber-reinforced composites.* Composites Part A: Applied Science and Manufacturing, 2010. **41**(9): p. 1245-1252.

249. Kang, J.T., S.H. Park, and S.H. Kim, *Improvement in the adhesion of bamboo fiber reinforced polylactide composites.* Journal of Composite Materials, 2013: p. 0021998313501013.

250. Yu, T., N. Jiang, and Y. Li, *Study on short ramie fiber/poly (lactic acid) composites compatibilized by maleic anhydride.* Composites Part A: Applied Science and Manufacturing, 2014. **64**: p. 139-146.

251. Gunning, M.A., et al., *Improvement in mechanical properties of grafted polylactic acid composite fibers via hot melt extrusion.* Polymer Composites, 2014. **35**(9): p. 1792-1797.

252. Ansari, N.M., *Influence of Maleic anhydride on mechanical properties and morphology of Hydroxyapatite/Poly-(lactic acid) composites.* Regenerative Research, 2012. **1**(2): p. 32-38.

253. Kim, H.-S., et al., *Enhanced interfacial adhesion, mechanical, and thermal properties of natural flour-filled biodegradable polymer bio-composites.* Journal of thermal analysis and calorimetry, 2010. **104**(1): p. 331-338.

254. Avella, M., et al., *Poly (lactic acid)-based biocomposites reinforced with kenaf fibers.* Journal of applied polymer science, 2008. **108**(6): p. 3542-3551.

255. Tabi, T., et al., *Crystalline structure of annealed polylactic acid and its relation to processing.* Express Polym Lett, 2010. **4**(10): p. 659-668.

256. Afaghi-Khatibi, A. and Y.-W. Mai, *Characterisation of fibre/matrix interfacial degradation under cyclic fatigue loading using dynamic mechanical analysis.* Composites Part A: Applied Science and Manufacturing, 2002. **33**(11): p. 1585-1592.

257. Song, Y., et al., *Mechanical properties of poly (lactic acid)/hemp fiber composites prepared with a novel method.* Journal of Polymers and the Environment, 2013. **21**(4): p. 1117-1127.

258. Yu, T., et al., *Effect of fiber surface-treatments on the properties of poly (lactic acid)/ramie composites.* Composites Part A: Applied Science and Manufacturing, 2010. **41**(4): p. 499-505.

259. Hwang, S.W., et al., *Grafting of maleic anhydride on poly (L-lactic acid). Effects on physical and mechanical properties.* Polymer Testing, 2012. **31**(2): p. 333-344.

260. Muenprasat, D., S. Suttireungwong, and C. Tongpin, *Functionalization of Poly (lactic acid) with maleic anhydride for biomedical application.* Journal of Metals, Materials and Minerals, 2010. **20**(3): p. 189-192.

261. Taib, R.M., et al., *Properties of kenaf fiber/polylactic acid biocomposites plasticized with polyethylene glycol.* Polymer Composites, 2010. **31**(7): p. 1213-1222.

262. Harmaen, A., et al., *Effect of triacetin on tensile properties of oil palm empty fruit bunch fiber-reinforced polylactic acid composites.* Polymer-Plastics Technology and Engineering, 2013. **52**(4): p. 400-406.

263. Lin, Y., et al., *Study of hydrogen-bonded blend of polylactide with biodegradable hyperbranched poly (ester amide).* Macromolecules, 2007. **40**(17): p. 6257-6267.

264. Abdelwahab, M.A., et al., *Thermal, mechanical and morphological characterization of plasticized PLA–PHB blends.* Polymer degradation and stability, 2012. **97**(9): p. 1822-1828.

265. Alam, A.M., et al., *Structures and performances of simultaneous ultrasound and alkali treated oil palm empty fruit bunch fiber reinforced poly (lactic acid) composites.* Composites Part A: Applied Science and Manufacturing, 2012. **43**(11): p. 1921-1929.